Identification of a novel TetR-family transcription regulator, PsrA and its involvement in *Legionella pneumophila* virulence

by

Palak Patel

A Thesis submitted to the Faculty of Graduate Studies of

The University of Manitoba

In partial fulfillment of the requirements of the degree of

MASTER OF SCIENCE

Department of Microbiology

University of Manitoba

Winnipeg

Abstract

Legionella pneumophila, an intracellular pathogen of protozoa, is well known for its dimorphic life cycle that alternates between the vegetative replicative form (RF) and cyst-like form (CLF). Studies have showed that CLFs are metabolically dormant and resistant to the effects of antibiotics, detergents and heat. *L. pneumophila* thrives in natural and man-made aquatic habitats that range from lakes to cooling towers. It is believed that upon inhalation of aerosols containing CLFs by humans, *L. pneumophila* opportunistically infects alveolar macrophages, eventually causing a typical pneumonia known as the Legionnaires' disease or legionellosis. To this date several virulence factors including LpRpoS, LpIHF, and the Dot/Icm secretion system have been found to be required for the survival of *L. pneumophila* in macrophage and protozoa. In *Pseudomonas* species, a TetR-family regulator PsPsrA has been found to regulate the expression of RpoS and type III secretion system by responding to the changes in fatty acid levels in surroundings. In *L. pneumophila,* stringent response is initiated when fatty acid biosynthesis is inhibited leading to excess amount of short chain fatty acids and accumulation of guanosine tetraphosphate (ppGpp). Here we have identified and characterised Lpg1967, an orthologue of PsPsrA in *L. pneumophila*. PsrA (Lpg1967) was found to regulate previously known virulence factors such non-coding RNAs, RsmY/Z, RpoS and LpIHF in *L. pneumophila.* Moreover, PsrA was also found to control expression of the Dot/Icm secretion system components and flagella. In addition, the *ΔpsrA* mutant strain was unable to establish *Legionella*-containing vacuole and thus displayed a severe growth defect in the U937 derived macrophage cell line. Thus, PsrA was found to play an important role in controlling the regulatory cascade governing virulence in *L. pneumophila.*

Acknowledgements

I would like to thank my supervisor, Dr. Brassinga for all the support and guidance. I appreciate the time you spent with me as well as the valuable information you offered. I would also like to thank my committee members, Dr. Hausner and Dr. McKenna for insightful comments, hard questions and keeping my project on track.

Thank you to Levin lab for the use of microplate reader and other department members for experimental assistance.

I would also like to thank Jennifer Tanner, Jackie Hellinga and Aniel Moya-Torres for their help with experiments, and emotional support.

This work was supported by Faculty of graduate studies and Natural Sciences and Engineering Research Council of Canada (NSERC).

TABLE OF CONTENTS

List of Tables

List of Figures

List of copyrighted material for which permission was obtained

Section	Reference	Licence ID
Figure 1.1	Hoffman, P., Friedman, H., & Bendinelli, M. (2007). *Legionella pneumophila: Pathogenesis and Immunity*. (P. Hoffman, Ed.) (Vol. 54, pp. 1–207). Boston, MA: Springer US. doi:10.1007/978-0-387-70896-6	3402611098308
Figure 1.2	Magnusson, L. U., Farewell, A., & Nyström, T. (2005). ppGpp: a global regulator in Escherichia coli. *Trends in Microbiology*, *13*(5), 236–42. doi:10.1016/j.tim.2005.03.008	3402611098308
Figure 1.4	Isberg, R. R., O'Connor, T. J., & Heidtman, M. (2009). The Legionella pneumophila replication vacuole: making a cosy niche inside host cells. *Nature Reviews. Microbiology*, *7*(1), 13–24. doi:10.1038/nrmicro1967	3400890995438
Figure 3.14A,B,C	Pitre, C. a J., Tanner, J. R., Patel, P., & Brassinga, A. K. C. (2013). Regulatory control of temporally expressed integration host factor (IHF) in Legionella pneumophila. *Microbiology (Reading, England)*, *159*(Pt 3), 475–92. doi:10.1099/mic.0.062117-0	3401741137231
Figure 3.15A	Pitre, C. a J., Tanner, J. R., Patel, P., & Brassinga, A. K. C. (2013). Regulatory control of temporally expressed integration host factor (IHF) in Legionella pneumophila. *Microbiology (Reading, England)*, *159*(Pt 3), 475–92. doi:10.1099/mic.0.062117-0	3401741137231
Figure 5.2 A,B	Pitre, C. a J., Tanner, J. R., Patel, P., & Brassinga, A. K. C. (2013). Regulatory control of temporally expressed integration host factor (IHF) in Legionella pneumophila. *Microbiology (Reading, England)*, *159*(Pt 3), 475–92. doi:10.1099/mic.0.062117-0	3401741137231
Figure 5.3 A,B	Pitre, C. a J., Tanner, J. R., Patel, P., & Brassinga, A. K. C. (2013). Regulatory control of temporally expressed integration host factor (IHF) in Legionella pneumophila. *Microbiology (Reading, England)*, *159*(Pt 3), 475–92. doi:10.1099/mic.0.062117-0	3401741137231
Figure 5.4A	Pitre, C. a J., Tanner, J. R., Patel, P., & Brassinga, A. K. C. (2013). Regulatory control of temporally expressed integration host factor (IHF) in Legionella pneumophila. *Microbiology (Reading, England)*, *159*(Pt 3), 475–92. doi:10.1099/mic.0.062117-0	3401741137231
Figure 5.5A	Pitre, C. a J., Tanner, J. R., Patel, P., & Brassinga, A. K. C. (2013). Regulatory control of temporally expressed integration host factor (IHF) in Legionella pneumophila. *Microbiology (Reading, England)*, *159*(Pt 3), 475–92. doi:10.1099/mic.0.062117-0	3401741137231

List of Abbreviations

°C	degrees Celsius
A	adenine
A. castellanii	*Acanthamoeba castellanii*
Amp	ampicillin
APS	ammonium persulfate
B. abortus	*Brucella abortus*
BaIHF	IHF protein from *B. abortus*
BCV	*Brucella*-containing vacuole
BCYE	buffered charcoal yeast extract
BLAST	Basic Local Alignment Search Tool
BLAST	Basic Local Alignment Search Tool
bp	base pair
BSA	bovine serum albumin
BYE	buffered yeast extract
C	cytosine
$CaCl_2$	calcium chloride
CFU	colony forming unit
CIP	calf intestinal alkaline phosphatise
CIP	calf intestinal alkaline phosphatase
CLF	cyst-like form
Cm	chloramphenicol

CO_2	carbon dioxide
DAPI	4',6-diamidino-2-phenylindole
DBD	DNA-binding domain
dH2O	distilled water
DMSO	dimethyl sulfoxide
DNA	deoxyribonucleic acid
dNTP	deoxyribonucleotide triphosphate
DTT	dithiothreitol
E. coli	*Escherichia coli*
EcIHF	IHF protein from *E. coli*
EcRpoS	RpoS protein from *E. coli*
EDTA	ethylenediaminetetraacetic acid
Em	emission
EMSA	electrophoretic mobility shift assay
ER	Endoplasmic reticulum
EtOH	ethanol
Ex	excitation
Fe	iron
g	gram
G	guanine
Gent	gentamicin
GFP	green fluorescent protein
HCl	hydrochloric acid

HeLa	Henrietta Lacks
HEPES	N-2-hydroxyethylpiperazine-N-2-ethane sulfonic acid
HIFBS	heat inactivated Fetal bovine serum
Hr	hour
HTH	helix-turn-helix
IHF	integration host factor
IPTG	Isopropyl-β-D-galactoside
kb	kilo base pair
KCl	potassium chloride
kDa	kiloDalton
KO	knockout
KOH	potassium hydroxide
kV	kilo volts
L	litre
L. pneumophila	*Legionella pneumophila*
LB	Luria-Bertani
LCFA	long-chain fatty acid
LCV	*Legionella*-containing vacuole
LpIHF	IHF protein from *L. pneumophila*
LpIHF	IHF protein from *L. pneumophila*
PsrA	protein product from *lpg1967*
LPS	Lipopolysaccharide
MCS	multiple cloning site

mg	milligram
$MgCl_2$	magnesium chloride
min	minute
mL	millilitre
mm	millimeter
mM	millimolar
MnCl2	magnesium chloride
MOI	Multiplicity of infection
MOPS	4-morpholinepropanesulfonic acid
mRNA	messenger ribonucleic acid
NaCl	sodium chloride
ncRNA	noncoding ribonucleic acid
NEB	New England Biolabs
ng	nanogram
Ni-NTA	nickel-nitrilotriacetic acid
nm	nano meter
OD	optical density
ori	origin of replication
P. aeruginosa	*Pseudomonas aeruginosa*
P. fluorescens	*Pseudomonas fluorescens*
P. syringae	*Pseudomonas syringae*
PAGE	polyacrylamide gel electrophoresis
PaRpoS	RpoS protein from *P. aeruginosa*

PCR	polymerase chain reaction
PF	primer forward (5‟)
PHBA	poly-B-hydroxybutyrate
PLA	phospholipase A
PMA	phorbol 12-myristate 13-acetate
pmol	picamol
PMSF	Phenylmethanesulfonyl fluoride
poly(dI-dC)	Poly(deoxyinosinic-deoxycytidylic) acid
ppGpp	guanosine 3‟,5‟-bispyrophosphate
PR	primer reverse (3‟)
PsIHF	IHF protein from *Pseudomonas* species
PsPsrA	PsrA from *Pseudomonas* spp.
RbCl2	rubidium chloride
Rbs	ribosome binding site
RF	replicative form
RFU	relative fluorescence units
RFU	Relative fluorescence unit
RNA	ribonucleic acid
RNase	ribonuclease
rpm	revolutions per minute
RPMI media	Roswell Park Memorial Institute medium
RT	room temperature
s	second

S. enterica	*Salmonella enterica* servovar Typhimurium
SDS	sodium dodecyl sulfate
SeIHF	IHF protein from *S. enterica*
SeRpoS	RpoS protein from *S. enterica*
spp.	Species
T	thymine
T4SS	type four secretion system
TAE	tris base, acetic acid, EDTA buffer
Taq	*Thermus aquaticus* polymerase enzyme
TE	tris base, EDTA buffer
Thy	thymidine
TTSS	type three secretion system
V	volts
V. cholerae	*Vibrio cholerae*
VcIHF	IHF protein from *V. cholerae*
VcRpoS	RpoS protein from *V. cholerae*
α	alpha
β	beta
Δ	inactivation of gene
µg	microgram
µL	microlitre
µm	micrometer
µM	micromolar

Chapter 1: Introduction

1.1 General characteristics of *Legionella pneumophila*

Legionella pneumophila is a Gram-negative bacterium that is able to evade the immune system and infect alveolar macrophages resulting in the atypical pneumonia known as Legionnaires' disease (Isberg *et al.*, 2009). This infection most commonly occurs in immunocompromised or elderly individuals via inhalation of aerosolized water contaminated with *L. pneumophila* (Isberg *et al.*, 2009). *L. pneumophila* was first recognised as a human pathogen in 1976 and since then, over 50 different species of *Legionella* have been identified with at least 24 of them being pathogenic to humans (Newton *et al*., 2010).

L. pneumophila is a well-adapted pathogenic bacterium that can survive in water as a free living parasite and replicate in its natural host, *Acanthamoeba castellanii* for protection from the harsh environment. It is believed that the interaction between *L. pneumophila* and protozoa have equipped this bacterium with virulence factors that enables them to infect alveolar macrophages through a similar infection mechanism (Swanson and Hammer, 2000). In this kind of aquatic habitat, *L. pneumophila* exhibits a dimorphic life cycle that alternates between the vegetative replicative form (Figure 1.1A) and cyst-like form (CLF) (Figure 1.1B). The CLFs possess unique morphological characteristics that include thickened cell walls, multilayer membrane laminations, and poly-β-hydroxybutyrate (PBHA) inclusions (Figure 1.1B) (Faulkner and Garduno, 2002).

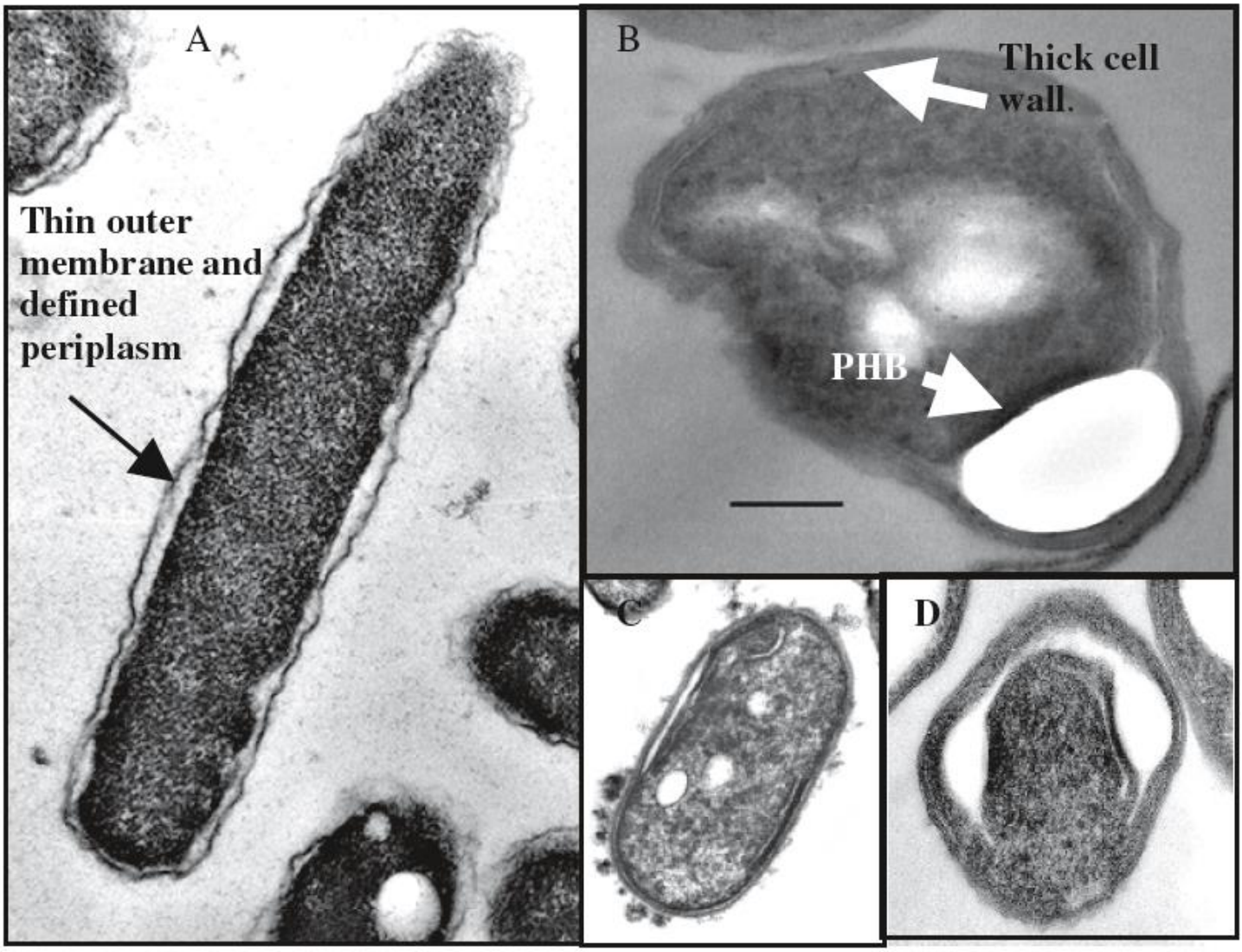

Figure 1.1: Morphological differences between different forms of *L. pneumophila.* A) Replicative form with a typical Gram-negative rod shaped morphology, B-D) cyst-like from (CLF) of *L. pneumophila* with multilayer membrane laminations and poly-β-hydroxybutyrate (PBHA) inclusion (arrows). Image adapted from (Hoffman *et al.*, 2007).

Studies have demonstrated that CLFs are metabolically dormant and resistant to the effects of antibiotics, detergents and heat. Moreover, CLFs have been shown to be hyper-infectious as determined by cell-based models (Garduño, 2007). Thus, *L. pneumophila* and related species can be transmitted from contaminated environment to humans; however, studies have suggested that *L. pneumophila* cannot be transmitted from person to person due to immaturity of the CLFs (Newton *et al*., 2010).

1.2 Stringent response and intracellular life cycle of *Legionella pneumophila*

L. pneumophila resides and replicates in a vacuole (i.e. LCV) made from the components of endocytic pathway. It is well known that changes in the nutrient conditions can trigger the transformation of the virulent form of *L. pneumophila* (CLF) (Isberg *et al.*, 2009). However, the exact stimulus responsible for this transformation is still unknown. Since *L. pneumophila* uses amino acids as a carbon source, it was hypothesized that the change in the amino acids supply is one of the key stimuli that initiate the transformation from replicative from to CLFs (Jules and Buchrieser, 2007). For instance, *L. pneumophila* uses PhtA transporter protein to acquire threonine, an essential amino acid. Studies have shown that loss of PhtA results in inability to replicate in minimum media and premature transformation to CLFs in rich media (Sauer *et al.*, 2005). Thus, vacuolar pathogens like *L. pneumophila* use phagosomal transporter (Pht) proteins to assess the changes in amino acids in the surroundings. After the detecting the nutrient stress, *L. pneumophila* activates several cellular and physiological changes known as stringent response to cope with the stress.

Upon the activation of the stringent response, inhibition of the protein and nucleic acid synthesis, protein degradation, growth inhibition, elevated amino acid synthesis and transport are initiated (Jules and Buchrieser, 2007). The main cause behind the whole stringent response is the uncharged tRNAs buildup in the A site of the 50S ribosome. The accumulation of uncharged tRNAs activate the ribosome associated protein RelA leading to the production of alarmone called guanosine tetra phosphate (ppGpp) (Figure 1.2) (Zusman *et al.*, 2002). ppGpp binds to the β and β' subunits of RNA polymerase and drives up the expression of the virulence genes. Thus, when the amino acids supplies are low, RelA protein is activated and the ppGpp effector molecules guides the RNA polymerase to express the virulent genes and supress the genes involved in replication (Figure 1.2) (Zusman *et al.*, 2002; Magnusson *et al.*, 2005a). In addition, there are many other cues that can trigger the stringent response in *L. pneumophila*. Another enzyme called SpoT assesses the surroundings for nutrient stress using two distinct enzymatic activities (Magnusson *et al.*, 2005a). In nutrient rich environment, SpoT exhibits hydrolase activity by degrading guanosine tetra phosphate (ppGpp) in cytosol (Figure 1.2) (Dalebroux *et al.*, 2009). Conversely, SpoT displays ppGpp synthase activity in the time of nutrient stress such as fatty acid starvation to initiate the stringent response (Figure 1.2) (Dalebroux *et al.*, 2009). However, not much is known about the proteins involved in this whole surveillance system, but it seems that *L. pneumophila* uses SpoT to recognise any disturbances in the fatty acid biosynthesis.

During stringent response, several stress related genes were expressed including stationary sigma factor RpoS. In *L. pneumophila,* RpoS further expresses genes from *dot/icm* secretion system locus and other virulence factors required for motility, lysosome

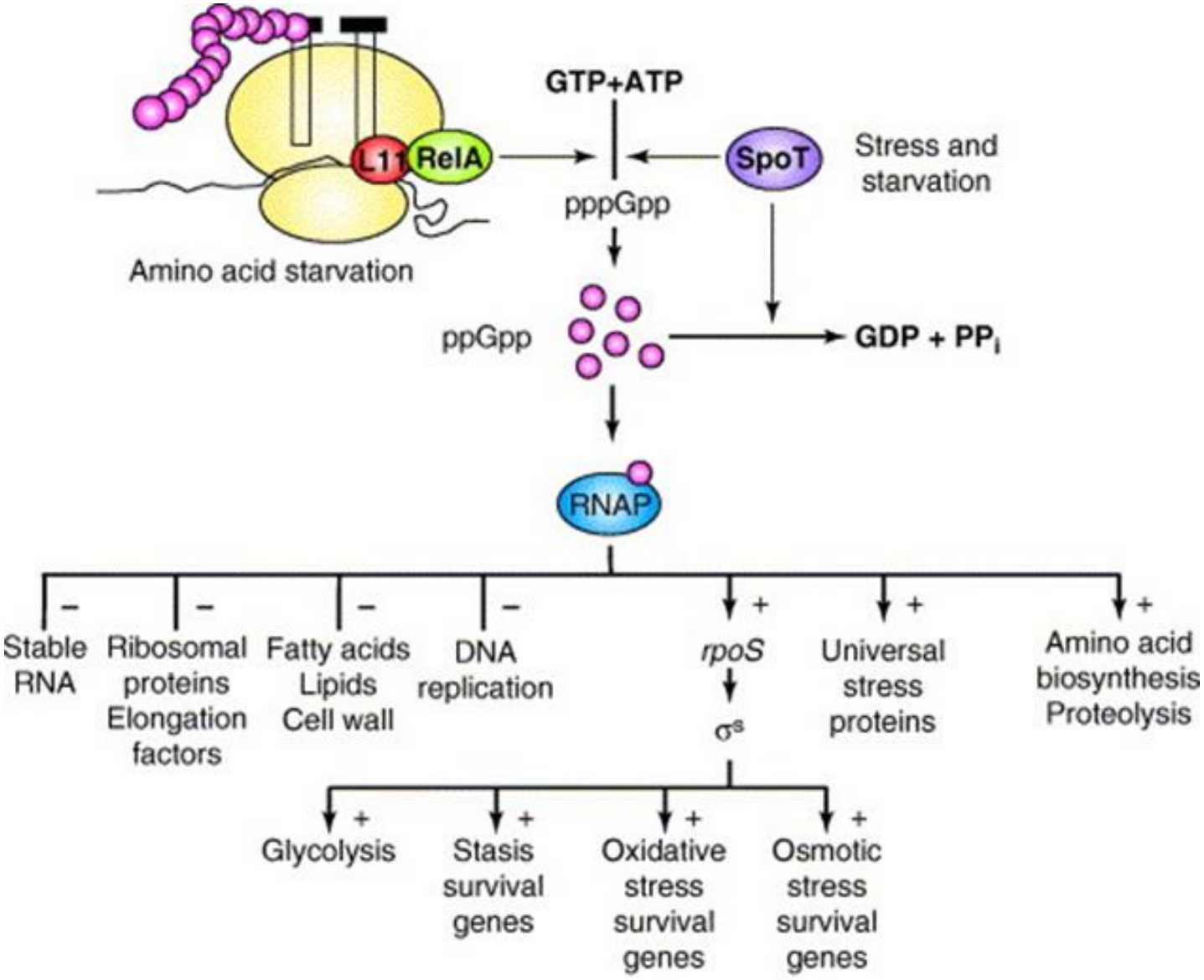

Figure 1.2: The stringent response. Effector molecule, ppGpp is produced by two parallel pathways involving RelA and SpoT enzymes. ppGpp binds to the RNA polymerase drives up the expression of genes associated with stress/starvation response while suppressing the growth-related genes. Figure adapted from Magnusson, Farewell, & Nyström, 2005.

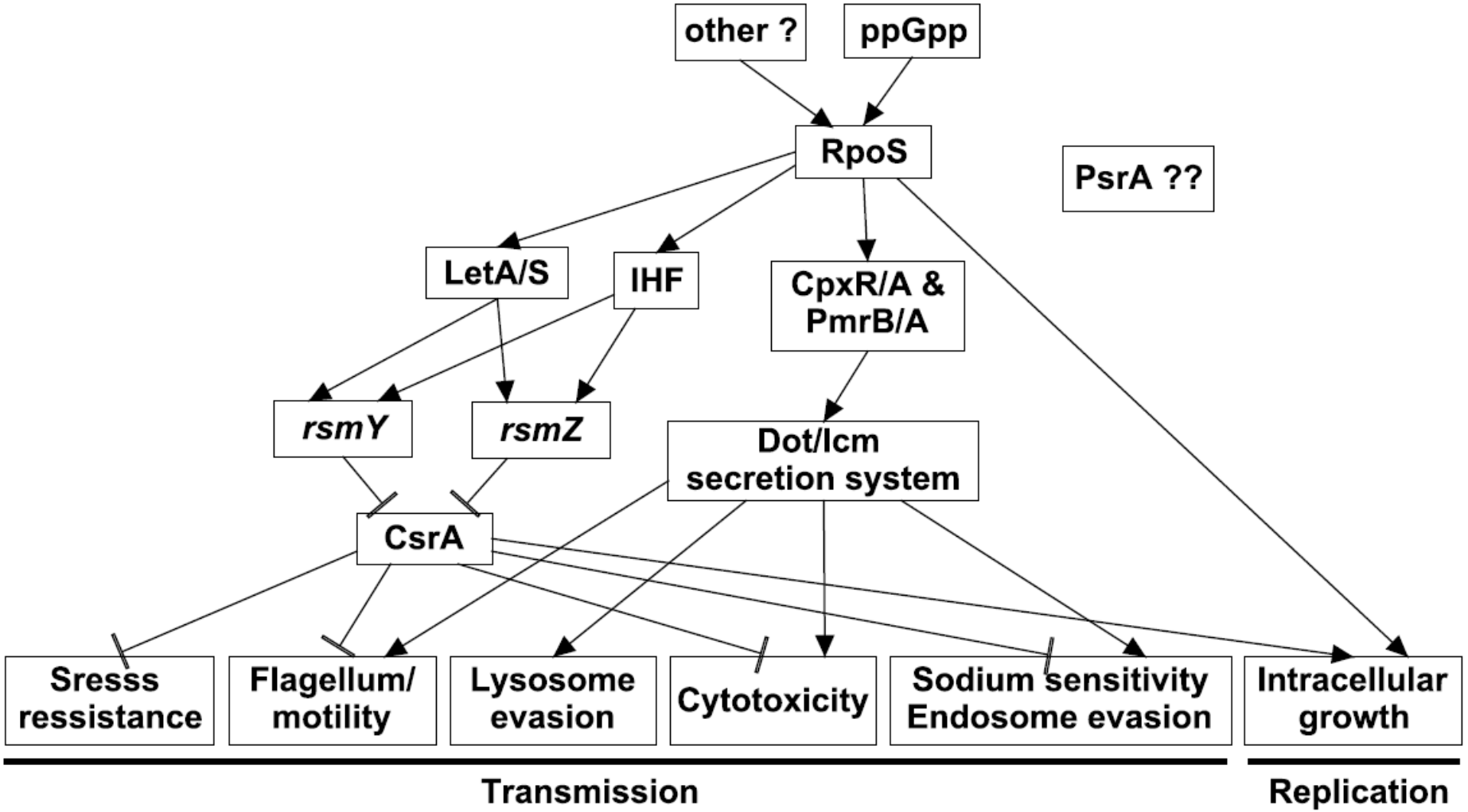

Figure 1.3: Regulatory cascade responsible for governing virulence in *L. pneumophila.* General overview outlining key regulators involved in the regulation of the virulence traits. However, the placement and role of PsrA in this pathway is yet to be determined. Figure modified and edited from (Hoffman *et al.*, 2007; Kozak *et al.*, 2010).

evasion, and intracellular growth (Figure 1.2 and 1.3) (Hovel-Miner *et al.*, 2009). Normally macrophage degrade the non-pathogenic bacteria through lysosomal-mediated degradation pathway; however, *L. pneumophila* escape the degradation with help of well evolved virulence system (Figure 1.4) (Jesús *et al.*, 2013). When alveolar macrophages encounter CLFs, phagocytosis of these infectious forms of *L. pneumophila* occurs and a *Legionella*-containing vacuole (LCV) is formed (Figure 1.4B). *L. pneumophila* escapes lysosome-mediated bacterial degradation pathway and avoids the fusion with the lysosomal network by secreting virulence effectors protein from the Dot/Icm secretion system (Figure 1.4B). Moreover, *L. pneumophila* also prevents the acidification of LCVs and replicates within this vacuoles (Isberg *et al.*, 2009). Because of this unique virulence strategy, *L. pneumophila* is responsible for the majority of Legionnaires' disease cases worldwide and poses a public health risk due to its unpredictable nature of explosive point outbreaks (Fields *et al.*, 2002).

The key regulatory controls of the entire virulence cascade are shown in Figure 1.3. It seems that RpoS acts as a master regulator that is responsible for regulating various different pathways ultimately leading to the successful infection and intracellular growth (Hovel-Miner *et al.*, 2009). Interestingly, LetA/LetS two component system has been reported to be a crucial component regulating the differentiation from replicative phase to transmissive phase. Studies have shown that LetA response regulator is required for intracellular growth within protozoa making LetA a crucial virulence factor for *L. pneumophila* (Lynch *et al*., 2003).

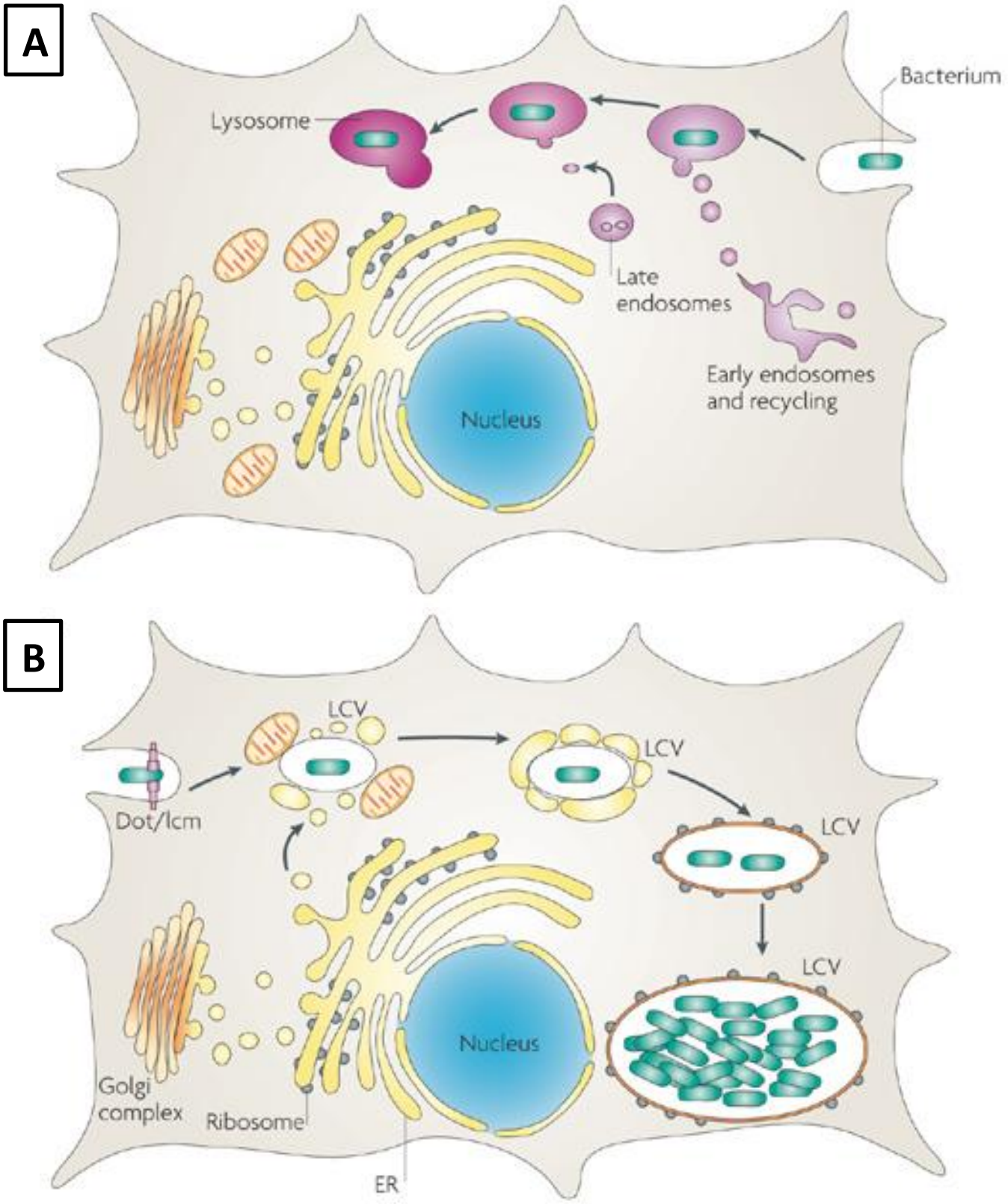

Figure 1.4: Intracellular life cycle of *L. pneumophila* within macrophages. A) The default lysosome-mediated bacterial degradation pathway. When the macrophage engulfs the non-pathogen, the phagosome starts to acquire the endosome characteristics ultimately leading to the lysosome formation. B) Lysosomal evasion by *L. pneumophila.* By expressing Dot/Icm secretion system and effector proteins, *L. pneumophila* circumvents the lysosome mediated degradation and establishes replicative niche known as *Legionella* containing vacuole (LCV). Figure adapted from Isberg, O'Connor, & Heidtman, 2009.

1.3 LetA/LetS two component system

A key physical feature of the cyst-like forms (CLFs) is the flagellum composed of flagellar protein encoded by *flaA* gene. To identify the regulatory components responsible for the expression of virulence traits, Hammer and colleagues (2002) used a *flaAgfp* reporter strain to screen for mutants with defective expression of the reporter which ultimately led to the discovery of *letA,* a *gacA* homologue from GacA/GacS two component system of *P. fluorescens.* In *L. pneumophila*, the LetA/LetS two component system induces expression of several virulent traits and genetic studies have suggested that the CsrA represses the expression of all the virulence traits induced by LetA/LetS two component system (Hammer *et al.*, 2002; Molofsky and Swanson, 2003). This system is a part of the protein family that employs a kinase receptor on the cell membrane to evaluate the surrounding environment for nutrient stress signals (Hammer *et al.*, 2002). After the activation of the LetS kinase receptor, series of phosphorylation events take place which ends up activating the response regulator, LetA (Hammer *et al.*, 2002).

In vitro analysis of post exponential culture of the insertion *letA* mutant strain showed defects in osmotic and acid stress resistance, motility and sodium sensitivity (Hammer *et al*., 2002; Lynch *et al*., 2003). In addition, macrophage infection studies with *letA* mutant have reported impaired cytotoxicity and bacterial viability. Since *A. castellanii* is a natural host of *Legionella* species, the protozoa studies have demonstrated that wild-type *L. pneumophila* successfully infected and replicated within these protozoa. However, the Δ*letA* mutant had a deficiency in infecting and replicating within protozoa signifying the role of LetA in cell cycle progression and virulence (Lynch *et al*., 2003). Moreover, LetA

does not play a role in maintaining the integrity of the replicative vacuole within protozoa (Molmeret *et al*., 2007). Taken together, LetA regulates several key virulence factors that are required for infection and replication in protozoa. Furthermore, it was determined that LetA positively regulates the expression of *dotA*, a crucial component of the Dot/Icm Type IV secretion system (Lynch *et al*., 2003). Thus, without the LetA protein, *L. pneumophila* is halted in its replicative growth phase and therefore is unable to transition into the CLFs.

In *P. fluorescens,* GacA negatively regulates the expression of the stationary sigma factor 38 (PsRpoS) (Whistler *et al.*, 1998). *In vitro* studies have well characterised the regulatory role of LetA in *L. pneumophila* virulence. LetA positively regulates the expression of *rpoS* during the transition from exponential to stationary phase and is therefore required for full expression of *rpoS* in *L. pneumophila* (Lynch *et al*., 2003). RpoS is a sigma factor that is known to regulate the genes associated with morphogenesis and virulence in *L. pneumophila* (Newton *et al*., 2010). A significant drop in *hfq* transcripts in the Δ*letA* mutant strain background was observed suggesting a possible regulation by LetA. Hfq is a chaperone protein which is expressed during the exponential phase to stabilize CsrA and a ferric uptake regulator (McNealy and Forsbach-Birk, 2005).

Upon activation, the response regulator LetA recognizes the TNAGAAATTTCTNA palindromic sequence located upstream of the RsmY and RsmZ non-coding RNAs and mediates the expression of these ncRNAs (Figure 1.3) (Sahr *et al*., 2009). *In vitro* studies have shown that RsmY and RsmZ non coding RNAs have high binding affinity for CsrA (Sahr *et al.*, 2009). Moreover, CsrA is known to sequester the mRNA transcripts associated with virulence traits and the interaction of CsrA with RsmY and RsmZ releases the

sequestered transcripts making them available for translation (Figure 1.3) (Molofsky and Swanson, 2003; Sahr *et al.*, 2009). The functional role of these non-coding RNAs was further verified by *in vivo* studies using *ΔrsmYrsmZ* knockouts and overexpression strains of RsmY and RsmZ (Sahr *et al.*, 2009). Recently, it was reported that LetA negatively regulates the expression of integration host factor (IHF, encoded by *ihfα* and *ihfβ*). Using a GFP reporter system, LetA was shown to repress the transcription of the *ihfα* and *ihfβ* genes during lag and post exponential growth phases (Pitre *et al*., 2013). In addition, it has been reported that LetA is involved in the production of lipases and proteases that contribute to bacterial pathogenesis. For instance, phospholipase A (PLA) is capable of destroying the surfactant which is an essential lipoprotein present on the surface of alveoli for lung stability. Thus, the destruction of the alveolar surfactant layer in lungs aids in the establishment of severe pneumonia (Flieger *et al.*, 2000). PLA activity (encoded by *plaC)* is present during the late log and early stationary phase in *L. pneumophila* (Banerji *et al.*, 2005). *In vitro* enzymatic assays on *L. pneumophila* JR32 *ΔletA* mutants and wildtype controls showed a significant reduction in the PLA activity indicating a strong LetA role as an activator. These results were further conformed by gene expression analysis of *plaC* in *ΔletA* mutants and wildtype controls (Broich *et al*., 2006).

Overall, extensive research has been done to further elucidate the role of LetA in the whole *L. pneumophila* virulence cascade. LetA regulator is one of the key players in the virulence regulatory network since it has been known to be required for infectivity & intracellular growth in *A. castellanii* and regulates several major virulence traits. However, recently it was found that IHF is also required for intracellular growth in protozoa and is also involved in cyst-biogenesis in *L. pneumophila*.

1.4 Integration Host Factor

Integration host factor (IHF) is a heterodimeric protein comprised of alpha and beta subunits. It is highly conserved in many bacteria and is known to be involved in cell differentiation and virulence by acting as a transcription regulator (Arvizu-Gómez *et al*., 2011; Aviv & Giladi, 1994; Mangan *et al*., 2006; Morash *et al*., 2009). In *E. coli*, IHF protein recognises consensus sequence WATCAANNNNTTR and is involved in DNA bending. Because of the DNA bending action, it is believed that IHF could be controlling the expression of genes by inhibiting or promoting the interaction of other regulators or protein with DNA (Aviv and Giladi, 1994). In *Vibrio cholerae,* IHF controls the expression of *tcpA* (encodes toxin-coregulated pilus) and *ctx* (cholera toxin) as determined by mutants studies of *ihfα* and *ihfβ* genes which make up VcIHF (Stonehouse *et al.*, 2008). According to the EMSA and DNaseI footprint studies, VcIHF directly binds to the *tcpA* promoter region but not the *ctx* promoter. Since these two genes are key virulence factors, it can be argued that VcIHF is tightly associated with virulence in *V. cholerae* (Stonehouse *et al.*, 2008). Similarly, in *Salmonella enterica* serovar Typhimurium, IHF (SeIHF) is also involved in the virulence. Studies have shown that SeIHF is required to express the type III secretion system (TTSS) and the effector proteins which are essential for invasion and survival within macrophages (Mangan *et al.*, 2006). Moreover, SeIHF levels were elevated during the stationary phase based on the gene expression profiles (Mangan *et al.*, 2006). Similar results were also found with *P. syringae* where studies have shown effects of PsIHF in the virulence (Arvizu-Gómez *et al.*, 2011).

There are several protein factors known to be involved in the expression of *L. pneumophila* virulence traits. The regulatory control of the cyst biogenesis is not well understood. Studies in other bacteria have shown that the temporal expression of integrated host factor (IHF) is involved in the virulence gene expression and in *E. coli,* IHF protein seems to influence regulatory process like transcription and replication by DNA bending (Goosen and Putte, 1995). In *E. coli,* IHF protein consists of an alpha subunit encoded by *himA* and a beta subunit encoded by *himD.* Moreover, homologues of these subunits have been found to be encoded by distantly located *ihfα* and *ihfβ* in *L. pneumophila* (Morash *et al.*, 2009). Single deletion Lp02Δ*ihfα* and, Lp02Δ*ihfβ* strains as well as Lp02*ihf* double deletion mutants were unable to grow in *A. castellanii*. Complementation studies of these proteins restored the infectivity; however, constitutive expression of IHF in Lp02 resulted in a growth defect (Morash *et al.*, 2009). Thus, it seems that the inappropriate expression of *L. pneumophila* IHF (LpIHF) in early exponential phase interferes with processes involved in developmental cycle. Moreover, these effects were not present in infection studies with HeLa cells (Morash *et al.*, 2009). In addition, MagA has been identified as a post exponential marker for *L. pneumophila* and GFP reporter expression assays were carried out in Lp02 and Lp02*ihf* mutant background to further evaluate the regulation of *magA.* The GFP assays showed a substantial reduction in GFP expression during late and post exponential phases proposing the role of LpIHF as an activator of *magA.* Electrophoretic mobility shift assays further showed a gel shift in the presence of LpIHF further confirming its regulatory role (Morash *et al.*, 2009). Thus, this study was the first one to report the integral role of LpIHF in the transformation from replicative form to cyst-like form. Recently, using the GFP reporter expression assays it was found that LpIHF

positively regulates the expression of the non-coding RNAs, RsmY and RsmZ (Figure 1.3). These results were also confirmed by qPCR and in *ΔletA* background (positive control) (Pitre *et al*., 2013). Moreover, *in vitro* GFP kinetic assays further showed RpoS as a positive regulator and LetA as a repressor of *ihfα and ihfβ* genes (Figure 1.3). In addition, *in vitro* IHF binding assays showed functional IHF binding sites on *ihfα* and *ihfβ* further indicating the auto regulatory role of IHF possibly through a DNA bending mechanism (Pitre *et al*., 2013).

To sum up, IHF protein seems to be one of the key regulators involved in cyst-biogenesis, however not much is known about the targeted genes or the exact role of IHF in the whole virulence cascade.

1.5 Stationary sigma factor 38 (RpoS)

It is well known that during the transition between the replicative and virulent phases, complete different sets of genes are turned on and off (Chatterji & Ojha, 2001; Srivatsan & Wang, 2008). For many years, researchers have been trying to find the exact mechanism responsible for the changes in the gene expressions during the replicative and virulent phases. Several key proteins and transcription regulators have been identified to be crucial for the transformation during the stressful environment. To cope with the changing environment, several genes are tightly regulated in response to this drastic change (Brüggemann *et al.*, 2006). The mechanism behind this switch between the gene expressions is well understood through the studies in *L. pneumophila* and various other organisms.

RpoS is a highly conserved sigma factor which is responsible for expressing stationary phase characteristics and traits in Gram-negative bacteria. RpoS replaces the vegetative sigma factor RpoD during the stationary phase or under stress conditions to redirect the RNA polymerase to express genes associated with virulence and stress response (Figure 1.3) (Bachman & Swanson, 2004; Hovel-Miner *et al*., 2009). RpoS is also known to regulate the genes involved in general stress response in several bacteria including *E. coli*, *Vibrio cholerae,* and *Salmonella* and *Yersinia* species. In *E. coli,* genes associated with osmo- and acid tolerance, oxidative stress resistance and high temperature have been identified to be regulated by RpoS (Hales and Shuman, 1999; Battesti *et al.*, 2011).

E. coli RpoS (EcRpoS) regulates variety of genes associated with various stress conditions including heat shock, low pH, osmotic and oxidative stress. During the stationary phase or stress conditions, EcRpoS expression is increased by 5-10 fold and is also involved in overall morphological changes that takes places during stationary phase (Hengge-Aronis, 2002). Moreover, a significant drop in *himA* and *himD* expression was detected in *ΔrpoS* mutant showing that EcRpoS controls the EcIHF expression since *himA* and *himD* encode alpha and beta subunits of EcIHF respectively (Aviv and Giladi, 1994).

In *V. cholerae*, RpoS (VcRpoS) drives the expression of more than 25 genes associated with stress response during stationary phase. In addition, VcRpoS is a key regulator during the osmotic stress, oxidative stress and starvation (Yildiz and Schoolnik, 1998). Similar results were reported with respect to RpoS function in *Salmonella enteric* serovar Typhimurium where SeRpoS was involved in stress response and virulence

(Nickerson and Curtiss, 1997). In *P. aeruginosa*, RpoS levels rose at significantly high levels during the transition to stationary phase. Interestingly, in *P. aeruginosa* RpoS seems to have a more extensive role in virulence than in stress conditions (Suh *et al.*, 1999). The *ΔrpoS* mutant of *P. aeruginosa* had defective motility and 50% reduction in exotoxin A production. The mutant was also sensitive to osmotic and oxidative stress (Suh *et al.*, 1999).

Likewise, *L. pneumophila* employs the alternative sigma factor RpoS (LpRpoS) to express the genes associated with sodium sensitivity, flagellin expression, replicative niche formation and lysosome evasion (Figure 1.3) (Bachman and Swanson, 2004). In addition several other alternative sigma factors are known to regulate the expression of complete different sets of genes crucial for the development of transmissive traits in CLFs (Magnusson *et al.*, 2005a; Brüggemann *et al.*, 2006; Srivatsan and Wang, 2008). The *E. coli rpoS* homologue was found in *L. pneumophila* by functional complementation studies and during the stationary phase, LpRpoS levels were elevated like in *E. coli*. Further analysis of the *rpoS* insertion mutant of *L. pneumophila* showed that the mutant strain does not have any dramatic effect on the growth in broth cultures (Hales and Shuman, 1999). To further assess the role of RpoS in *L. pneumophila* stress response, the mutant strain was grown in under various stress conditions involving pH 3, 10mM H_2O_2, or 5M sodium chloride. The *rpoS* mutants were more sensitive during the log phase compared to stationary phase. These results suggested that LpRpoS is not required for growth phase dependent stress response unlike in *E. coli* (Bachman & Swanson, 2001; Hales & Shuman, 1999).

Further *in vivo* infection studies on macrophage-like cell line HL-60 showed that the LpRpoS is not required for replication within macrophage and is able to kill the

macrophage just like wild type strain JR32. These infection studies were further extended to *A. castellanii*. The mutant strain was unable to replicate within the protozoa showing a possible involvement of LpRpoS in the regulation of the genes associated with the survival within protozoa (Hales and Shuman, 1999). LpRpoS is also involved in the expression of *flaA* gene and has minor effect on the gene expression from Dot/Icm secretion system (Zusman *et al.*, 2002; Heuner and Steinert, 2003). In addition, CpxR/CpxA and PmrB/PmrA two component systems are known to be the direct regulators of Dot/Icm system and effector proteins and by regulating these two component systems LpRpoS exerts its indirect effect on the genes associated with Dot/Icm system (Kozak *et al.*, 2010). Moreover, *ΔrpoS* mutant causes a drastic decline in the *csrA*, *letE*, *fliA*, and *flaA* transcripts suggesting a possible role in the regulation of these genes. LpRpoS was also found to be responsible for cytotoxicity, infectivity and motility (Figure 1.3) (Bachman & Swanson, 2004; Hales & Shuman, 1999). Interestingly, CsrA also represses the expression of LpRpoS by binding to the *rpoS* transcripts as determined by luciferase assays (Forsbach-Birk *et al*., 2004). As mentioned above, LetA was reported to be the activator of Hfq protein however studies have shown that LpRpoS acts as a positive regulator for *hfq* genes and other effector genes including *ylfA, ylfB* and *vipA* (Mcnealy *et al*., 2005; Rasis & Segal, 2009). Recently it was found that LpRpoS also positively regulates the expression of *ihfα* and *ihfβ* gene (Figure 1.3) (Pitre *et al*., 2013). Because of its deep association with the virulence system, the removal of *rpoS* results severe intracellular growth defect possibly from multiple virulence pathways being affected in *L. pneumophila*.

Thus, LpRpoS is a stationary sigma factor which is expressed at post exponential phase. LpRpoS has been documented to be associated with initiating the whole

stress/virulence response and is a central part of regulatory system controlling transmissive traits.

1.6 The Dot/Icm secretion system

As stated above, *L. pneumophila* is able to escape the default endosomal-lysosomal degradation pathway. Moreover, it also forms a replicative vacuole redirecting the endocytic vacuoles originating from the rough ER (Isberg *et al.*, 2009). It is well known that the Dot/Icm secretion system, categorised as a type IV secretion system is required for the formation of replicative niche and the evasion of the lysosome-mediated degradation. Approximately 26 genes are known to be involved to make the whole Dot/Icm secretion complex which *L. pneumophila* uses to transfer effector proteins across the cell membrane into the host cell (Isberg *et al.*, 2009). Several of these effector proteins are known to be involved in modulating host cell processes like apoptosis, vesicle trafficking, and autophagy (Isberg *et al*., 2009; Newton *et al* , 2010). Lynch *et al*., 2003 carried out several experiments using *ΔletA* mutant to investigate the role of LetA in *dot/icm* gene expression. A significant drop in the *dotA* gene expression was reported indicating a possible regulation by LetA. Other studies have shown that the regulatory proteins like RelA, and LpRpoS also regulate the expression of few dot/icm genes indirectly (Lynch *et al*., 2003; Zusman *et al*., 2002). The study involving nine *icm* translation fusions showed that most of the fusion constructs had similar expression in *L. pneumophila* and *E. coli*. However, the *icmR:lacZ* fusion construct had very high expression levels in *L. pneumophila* and very low expression in *E. coli* (Gal-Mor & Segal, 2003). This suggests that there is another regulator

involved in the regulation of this gene in *L. pneumophila* which is not present or has different function in *E. coli*.

This unknown factor was identified as CpxR through the genetic screens and CpxR/CpxA two component system is known to directly regulate the expression of these genes (Zusman *et al.*, 2002; Gal-Mor and Segal, 2003). CpxA is a sensor kinase which upon recognition of a stimulus causes the auto phosphorylation of its conserved histidine residue. In addition, the activated CpxA further phosphorylates the aspartate residue on the CpxR, the cytosolic response regulator. To further identify the other *dot*/*icm* genes, Altman & Segal (2008) introduced a deletion in the *cpxR* gene and monitored the expression levels of the dot/icm components. Thus, they reported that the CpxR regulates *icmR, lvgA, icmV, icmW-icmX* and *icmV-dotA* transcriptional units and 11 other *dot*/*icm* genes. Even though, it seems like CpxR is a key component of this regulatory system, Δ*cpxA* and *ΔcpxR* mutants showed no effect on the intracellular growth in *A. castellanii* and HL-60-derived human macrophages and they replicated similarly as wild type (Gal-Mor and Segal, 2003). Moreover, PmrA/PmrB two component system is also known to regulate several of the Dot/Icm system and effector proteins and genomic studies and EMSAs studies have supported their involvement (Zusman *et al.*, 2007). Mutant studies involving PmrA/PmrB two component system showed that *ΔpmrA* mutant was unable to grow within *A. castellanii* and had a partial growth defect in HL-60-derived human macrophages (Figure 1.3) (Zusman *et al.*, 2007). Thus, the PmrA/PmrB two component system seems to be the primary system responsible for regulation of *dot/icm* genes.

Overall, the *dot/icm* secretion system is an essential component for the intracellular survival of *L. pneumophila* in macrophages and protozoa. In addition, it is also responsible for translocating the effector proteins to the host cell. However, it is very likely that the *dot/icm* system is regulated by other unknown regulator proteins since not much is known about its mode of regulation.

1.7 PsrA

PsrA*, Pseudomonas* sigma regulator A, was identified as a key regulator of *rpoS* in *Pseudomonas putida*. Homology search identified PsrA as a TetR family regulator with a helix-turn-helix motif at the N-terminus of the polypeptide chain (Kojic and Venturi, 2001). The *ΔpsrA* mutant showed a 90% reduction in *rpoS* expression at the stationary phase in *P. putida* and these results were also confirmed in *P. aeruginosa* (Kojic and Venturi, 2001). The mutant was also sensitive to the high temperature and osmotic changes as expected since RpoS is known to regulate genes during the these stress conditions (Kojic and Venturi, 2001). Moreover, it was also found that PsrA inhibits its own synthesis showing a negative auto regulation. Thus PsrA acts as an activator of *rpoS* and repressor of *psrA* in *Pseudomonas* species (Kojic and Venturi, 2001). It was found that PsrA binds to the C/GAAAC N_{2-4} GTTTG/C consensus palindromic sequence in *P. putida.* Both *psrA* and *rpoS* promoter regions have similar palindromic sequences which was verified by EMSAs and DNaseI footprints (Kojic *et al.*, 2002). In addition, PsrA was found to negatively regulate the expression of the two key quorum sensing genes *phzI* and *phzR* in *P. chlororaphis* PCL1391. Moreover, PsrA is also known to directly regulate several housekeeping genes which

encode proteins such as acyl CoA dehydrogenase, electron transfer flavoprotein β-subunit and electron transfer flavoprotein-ubiquinone oxidoreductase (Kojic *et al*., 2005).

Studies have also shown that PsrA is a key component tied up in the virulence in *P. aeruginosa*. PsrA also directly binds to the *exsCEBA* operon region which is known to make up components of type III secretion system and the *exoS* effector protein. The *ΔpsrA* mutant showed a drastic decrease in the secretion of the effector proteins and was also less resistant to the phagocyte like PLB-985 cells (Shen *et al*., 2006). In *P. aeruginosa,* microarray analysis showed that type III secretion system components, effectors proteins, adhesion and motility genes were dysregulated in Δ*psrA* mutant indicating a complex role of PsrA in virulence (Gooderham *et al*,, 2008). PsrA gene expression was induced in response to the antimicrobial peptides in *P. aeruginosa.* No effects were found in swimming or the twitching motility; however the swarming motility was significantly impaired in Δ*psrA* mutant. In addition, biofilm formation was also affected in Δ*psrA* mutants and the outer membrane was found to be more permeable to the antimicrobial peptides in Δ*psrA* mutants compared to the wildtype (Gooderham *et al.*, 2008).

Moreover, the function of PsrA is influenced by long-chain fatty acid (LCFA) levels in the environment where accumulation of the LCFAs prevents PsrA from binding DNA (Kang *et al.*, 2009). Interestingly, *psrA* expression was induced by the long chain fatty acid (LCFAs) which was proved by β- galactosidase activity assay however. Since PsrA is negatively autoregulated, in the presence of LCFAs PsrA is unable to bind to DNA and thus cannot regulate *psrA* leading to its enhanced expression (Kang *et al.*, 2009). Moreover, PsrA is also been reported to regulate the β-oxidative enzymes which are involved in fatty

acid degradation in *P. aeruginosa* (Kang *et al.*, 2008). Similarly in *Azotobacter vinelandii,* PsrA has been found to directly regulate the *rpoS* expression and the *ΔpsrA* mutant also showed a defect in cyst biogenesis indicating a significant role in virulence (Cocotl-Yañez and Sampieri, 2011).

In *L. pneumophila*, stringent response is also initiated when the bacteria senses the inhibition of fatty acid biosynthesis, excess amount of short chain fatty acids and accumulation of guanosine tetraphosphate (ppGpp) (Edwards *et al.*, 2009). However in *L. pneumophila*, it is not known about any sensor proteins like PsrA that responds to changes in fatty acid levels to initiate the virulence response.

1.8 Study aims

The objectives are: (I) to identify the orthologue of *psrA* in *Legionella pneumophila* and determine its possible involvement in virulence as observed in *Pseudomonas* species and (II) identify its potential gene targets associated with virulent traits in *L. pneumophila.*

Chapter 2: Materials and Methods

2.1 Bacterial strains and plasmids

All the strains used in this study are listed in Table 2.1. For cloning purposes, *E. coli* DH5α and *E. coli* DH5αλpir cells were used where applicable. *Escherichia coli* BL21 CodonPlus RIL™ strain was used for recombinant protein purification.

pET16b expression vector (Novagen, Madison, WI) was used to clone in and express the recombinant protein (Table 2.2). pBlueScriptKS(-) high copy number plasmid was used in cloning for di-deoxy sequencing experiments (Table 2.2). pBH6119 promoter less GFP vector was used in cloning for the purpose of GFP assays (Figure 2.1, Table 2.2). The GFP assays were done in the strains that were derived from *L. pneumophila* Lp02. To create unmarked in-frame deletion mutants, pSR47S suicide plasmid (Merriam *et al.*, 1997) was used in the allelic exchange mutagenesis (Table 2.2). pJB908 vector was used in complement studies (Table 2.2).

All the restriction enzymes were received from New England Biolabs (Whitby, Ontario). Chemicals, reagents, antibiotics and other lab materials were obtained from sigma-Aldrich Canada (Oakville, Ontario), GE Healthcare (Baie d‟Urfe, Quebec), Fisher Scientific Canada (Ottawa, Ontario), Bio-Rad Canada (Mississauga, Ontario) and VWR International (Mississauga, Ontario).

Table 2.1: Catalogue of bacterial strains used in this study.

Strain	Genotype or Strain description	Source (Reference)
Escherichia coli		
BL21 (DE3) CodonPlus™RIL	B F^- *ompT hsdS*(r_B^- m_B^-) *dcm*$^+$ Tet^r *gal* λ(DE3) *endA* Hte [*argU ileY leuW* Camr]	Stratagene
BL21 PsrA	pET16b::psrA in BL21 (DE3) CodonPlusTMRIL; Cm^R and Amp^R	This study
DH5α	F‟ *endA1 hsdR17(rk- mk-) supE44 thi-1 recA1 gyrA (Nalr) relA1 Δ(lacZYA-argF)U169 deoR* (ϕ80dlacΔ(lacZ)M15)	New England Biolabs
DH5α pBH6119	Amp^R; Thymidine producing	M. Swanson (Hammer *et al.*, 2002)
DH5α Z1	*E. coli* DH5α pBH6119::*rsmZ* P1	This study
DH5α Z2	*E. coli* DH5α pBH6119::*rsmZ* P2	This study
DH5α Z3	*E. coli* DH5α pBH6119::rsmZ P3	This study
DH5α psrA	*E. coli* DH5α pBH6119::psrA prom	This study
DH5α rpoS	*E. coli* DH5α pBH6119::rpoS prom	This study
DH5α psrA compl	*E.coli* DH5α pJB908::psrA	This study
KS rsmZ	*E.coli* DH5α pBluescrpt:*rsmZ* P1	This study
DH5α psrA	*E. coli* DH5α pBH6119::*psrA*	This study

DH5α rpoS	*E. coli* DH5α pBH6119::*rpoS*	This study
DH5α letA compl	*E.coli* DH5α pJB908::*letA*	This study
DH5α rpoS compl	*E.coli* DH5α pJB908::*rpoS*	This study
DH5α ihfα compl	*E.coli* DH5α pJB908::*ihfα*	This study
DH5α ihfβ compl	*E.coli* DH5α pJB908::*ihfβ*	This study
KS letA	*E. coli* DH5α pBlueScript KS(-)::*letA*	This study
KS ihfα	*E. coli* DH5α pBlueScript KS(-)::*ihfα*	This study
KS letA/rpoS	*E. coli* DH5α pBlueScript KS(-)::*letArpoS*	This study
KS ihfα/ihfβ	*E. coli* DH5α pBlueScript KS(-)::*ihfαihfβ*	This study
KS rsmY	*E.coli* DH5α pBluescrpt:rsmYP1	This study
KS rsmZ	*E.coli* DH5α pBluescrpt:rsmZP1	This study
DUET IhfαIhfβ	*E. coli* DH5α pETDUET::IHFα::IHFβ; (C-term His on IHFA with RBS)	This study
BL21 DUET IhfαIhfβ	pETDUET::IHFα::IHFβ; (C-term His on IHFA with RBS) in BL21	This study
DH5αλpir	K-12 F^- φ80*lacZ*ΔM15 *endA recAhsdR17 (rm- mK+) supE44 thi-1 gyrA96 relA1 Δ(lacZYA-argF)* U169 *λpir*	M. Swanson (Carlson *et al.*, 2010)
DH5αλpir psrA	pSR47S::psrA *sacB* Kan^R into DH5αλpir	This study
DH5αλpir ihfα	pSR47S::*ihfα sacB* Kan^R into DH5αλpir	This study

DH5αλpir ihfβ	pSR47S::*ihfβ sacB* Kan^R into DH5αλpir	This study
DH5αλpir letA	pSR47S::*letA sacB* Kan^R into DH5αλpir	This study
DH5αλpir rpoS	pSR47S::*rpoS sacB* Kan^R into DH5αλpir	This study
Legionella pneumophila		
Lp02	StrR, Thy$^-$, HsdR- derivative of Philadelphia-1 strain	M. Swanson (Berger and Isberg, 1993)
Lp02-pBH6119	*L. pneumophila* Lp02 pBH6119	C. Pitre (Pitre *et al*., 2013)
Z1	*L. pneumophila* Lp02 pBH6119::*rsmZ* P1 – GFP assay	This study
Z2	*L. pneumophila* Lp02 pBH6119::*rsmZ* P2 – GFP assay	This study
Z3	*L. pneumophila* Lp02 pBH6119::*rsmZ* P3 – GFP assay	This study
Lp02 *Δihfαihfβ*	*L. pneumophila* Lp02 *ihfα*::gent^R, *ihf* ::kan^R	A.K. Brassinga (Morash *et al.*, 2009)
pBH6119-Δihf	Lp02 *Δihfαihfβ* pBH6119	C. Pitre (Pitre *et al*., 2013)
Z1-Δihf	Lp02 *Δihfαihfβ* pBH6119::*rsmZ* P1	This study
Z2-Δihf	Lp02 *Δihfαihfβ* pBH6119::*rsmZ* P2	This study
Z3-Δihf	Lp02 *Δihfαihfβ* pBH6119::*rsmZ* P3	This study
Lp02 ΔletA	*L. pneumophila* Lp02 *letA*::kan^R	M. Swanson (Hammer *et al.*, 2002)
pBH6119-ΔletA	Lp02 *letA*::kan^R pBH6119	C. Pitre (Pitre *et al*., 2013)

Z1-ΔletA	Lp02 *letA*::kan^R pBH6119::*rsmZ* P1 – GFP assay	This study
Z2-ΔletA	Lp02 *letA*::kan^R pBH6119::*rsmZ* P2 – GFP assay	This study
Z3-ΔletA	Lp02 *letA*::kan^R pBH6119::*rsmZ* P3 – GFP assay	This study
ΔpsrA (lpg1967)	*L. pneumophila* Lp02 *ΔpsrA*	This study
ΔpsrA compl	*L. pneumophila* Lp02 *ΔpsrA* pJB908::psrA	This study
pBH6119-ΔpsrA	Lp02 *ΔpsrA* pBH6119	This study
Z1-ΔpsrA	Lp02 *ΔpsrA* pBH6119::*rsmZ* P1 – GFP assay	This study
Z2-ΔpsrA	Lp02 *ΔpsrA* pBH6119::*rsmZ* P2 – GFP assay	This study
Z3-ΔpsrA	Lp02 *ΔpsrA* pBH6119::*rsmZ* P3 – GFP assay	This study
Y1-ΔpsrA	Lp02 *ΔpsrA* pBH6119::*rsmY* P1 – GFP assay	This study
Y2-ΔpsrA	Lp02 *ΔpsrA* pBH6119::*rsmY* P2 – GFP assay	This study
Y3-ΔpsrA	Lp02 *ΔpsrA* pBH6119::*rsmY* P3 – GFP assay	This study
α1-ΔpsrA	Lp02 *ΔpsrA* pBH6119::*ihfα* P1 – GFP assay	This study
β1-ΔpsrA	Lp02 *ΔpsrA* pBH6119::*ihfβ* P1 – GFP assay	This study
IcmR-ΔpsrA	Lp02 *ΔpsrA* pBH6119::*icmR* – GFP assay	This study
OxyR-ΔpsrA	Lp02 *ΔpsrA* pBH6119::*oxyR* – GFP assay	This study
PsrA-WT	*L. pneumophila* Lp02 pBH6119::*psrA* – GFP assay	This study

PsrA-ΔpsrA	Lp02 *ΔpsrA* pBH6119::*psrA*– GFP assay	This study
FlaA-WT	*L. pneumophila* Lp02 pBH6119::*flaA* – GFP assay	This study
FlaA-ΔpsrA	Lp02 *ΔpsrA* pBH6119::*flaA*– GFP assay	This study
DotD-WT	*L. pneumophila* Lp02 pBH6119::*dotD*– GFP assay	This study
DotD-ΔpsrA	Lp02 *ΔpsrA* pBH6119::*dotD*– GFP assay	This study
IcmV-WT	*L. pneumophila* Lp02 pBH6119::*icmV*– GFP assay	This study
IcmV-ΔpsrA	Lp02 *ΔpsrA* pBH6119::*icmV*– GFP assay	This study
IcmT-WT	*L. pneumophila* Lp02 pBH6119::*icmT*– GFP assay	This study
IcmT-ΔpsrA	Lp02 *ΔpsrA* pBH6119::*icmT*– GFP assay	This study
Lp02 *Δihfα*	Lp02 *Δihfα* (clean unmarked in-frame deletion)	This study
Lp02 *Δihfβ*	Lp02 *Δihfβ* (clean unmarked in-frame deletion)	This study
Lp02 *ΔrpoS*	Lp02 *ΔrpoS* (clean unmarked in-frame deletion)	This study
Lp02 *Δihfαihfβ* (DKO)	Lp02 *Δihfαihfβ* (clean unmarked in-frame deletions)	This study
Lp02 *ΔihfAihfBletA* (TKO)	Lp02 *ΔihfAihfBletA* (clean unmarked in-frame deletions)	This study
Lp02 *ΔrpoSletA* (DKO)	Lp02 *ΔrpoSletA* (clean unmarked in-frame deletions)	This study
Lp02 *ΔihfAihfBletArpoS* (QKO)	Lp02 *ΔihfAihfBletArpoS* (clean unmarked in-frame deletions)	This study
Lp02 *ΔihfAihfBletApsrA*	Lp02 *ΔihfAihfBletApsrA* (clean unmarked in-frame deletions)	This study

(QKO)		
Lp02 *ΔletA*	Lp02 *ΔletA* (clean unmarked in-frame deletion)	This study
Lp02 *ΔihfAihfBrpoS* (TKO)	Lp02 *ΔihfAihfBrpoS* (clean unmarked in-frame deletions)	This study
ΔletA α1	Lp02 *letA*::kan^R pBH6119::ihfα P1	This study
ΔletA α2	Lp02 *letA*::kan^R pBH6119::ihfα P2	This study
ΔletA α3	Lp02 *letA*::kan^R pBH6119::ihfα P3	This study
ΔletA α4	Lp02 *letA*::kan^R pBH6119::ihfα P4	This study
ΔletA α5	Lp02 *letA*::kan^R pBH6119::ihfα P5	This study
ΔletA α6	Lp02 *letA*::kan^R pBH6119::ihfα P6	This study
ΔletA α7	Lp02 *letA*::kan^R pBH6119::ihfα P7	This study
ΔletA α8	Lp02 *letA*::kan^R pBH6119::ihfα P8	This study
ΔletA β1	Lp02 *letA*::kan^R pBH6119::ihfβ P1	This study
ΔletA β2	Lp02 *letA*::kan^R pBH6119::ihfβ P2	This study
ΔletA β3	Lp02 *letA*::kan^R pBH6119::ihfβ P3	This study
ΔletA β4	Lp02 *letA*::kan^R pBH6119::ihfβ P4	This study
ΔletA β5	Lp02 *letA*::kan^R pBH6119::ihfβ P5	This study
ΔletA β6	Lp02 *letA*::kan^R pBH6119::ihfβ P6	This study
ΔletA β7	Lp02 *letA*::kan^R pBH6119::ihfβ P7	This study

ΔrpoSletA α1	Lp02 *ΔrpoSletA* pBH6119::ihfα P1	This study
ΔrpoSletA α2	Lp02 *ΔrpoSletA* pBH6119::ihfα P2	This study
ΔrpoSletA α3	Lp02 *ΔrpoSletA* pBH6119::ihfα P3	This study
ΔrpoSletA α4	Lp02 *ΔrpoSletA* pBH6119::ihfα P4	This study
ΔrpoSletA α5	Lp02 *ΔrpoSletA* pBH6119::ihfα P5	This study
ΔrpoSletA α6	Lp02 *ΔrpoSletA* pBH6119::ihfα P6	This study
ΔrpoSletA α7	Lp02 *ΔrpoSletA* pBH6119::ihfα P7	This study
ΔrpoSletA α8	Lp02 *ΔrpoSletA* pBH6119::ihfα P8	This study
ΔrpoSletA β1	Lp02 *ΔrpoSletA* pBH6119::ihfβ P1	This study
ΔrpoSletA β2	Lp02 *ΔrpoSletA* pBH6119::ihfβ P2	This study
ΔrpoSletA β3	Lp02 *ΔrpoSletA* pBH6119::ihfβ P3	This study
ΔrpoSletA β4	Lp02 *ΔrpoSletA* pBH6119::ihfβ P4	This study
ΔrpoSletA β5	Lp02 *ΔrpoSletA* pBH6119::ihfβ P5	This study
ΔrpoSletA β6	Lp02 *ΔrpoSletA* pBH6119::ihfβ P6	This study
ΔrpoSletA β7	Lp02 *ΔrpoSletA* pBH6119::ihfβ P7	This study

Table 2.2: Catalogue of plasmids used in this study.

Plasmid	Description	Source (Reference)
pBH6119	RSF1010 ori, promoterless gfpmut3 tdΔi (Amp^R)	M. Swanson
pBHα1	pBH6119::ihfα P1 in BamHI and XbaI	C. Pitre (Pitre *et al.*, 2013)
pBHβ1	pBH6119::ihfβ P1 in BamHI and XbaI	C. Pitre (Pitre *et al.*, 2013)
pBHY1	pBH6119::rsmY P1 in BamHI and XbaI	C. Pitre (Pitre *et al.*, 2013)
pBHY2	pBH6119::rsmY P2 in BamHI and XbaI	C. Pitre (Pitre *et al.*, 2013)
pBHY3	pBH6119::rsmY P3 in BamHI and XbaI	C. Pitre (Pitre *et al.*, 2013)
pBHZ1	pBH6119::rsmZ P1 in BamHI and XbaI	This study
pBHZ2	pBH6119::rsmZ P2 in BamHI and XbaI	This study
pBHZ3	pBH6119::rsmZ P3 in BamHI and XbaI	This study
pBHIcmR	pBH6119::icmR in BamHI and XbaI	J.R.Tanner
pKSIcmR (seq)	pBlueScript KS::icmR	A.K. Brassinga
pBHOxyR	pBH6119::oxyR in BamHI and XbaI	J.R.Tanner
pJB908OxyR (seq)	pJB908::oxyR in BamHI and XbaI	J.R.Tanner
pBHPsrA	pBH6119::psrA in BamHI and XbaI	This study

pBHRpoS	pBH6119::rpoS in BamHI and XbaI	This study
pBHFlaA	pBH6119::flaA in BamHI and XbaI	M. Swanson (Hammer and Swanson, 1999)
pBHDotD	pBH6119::dotD	M. Morash
pBHIcmT	pBH6119::icmT	M. Morash
pBHIcmV	pBH6119::icmV in BamHI and EcoRI	A.K. Brassinga
pSR47S::PsrA	pSR47S::3' and 5' psrA flanking regions in SalI and SacI	This study
pET16b	N-terminal 10-histidine-tagged fusion protein expression vector; CmR, AmpR	Novagene
pET16b::PsrA	Expression vector; Cm^R, Amp^R	This study
pBluescript KS(-)	Cloning vector; Amp^R	Stratagene
pKS::rsmZ	pBluescript KS(-)::*rsmZ* promoter region	This study
pETDuet-1	Dual expression vector; Amp^R	Novagen
pET29b	Expression vector, Kan^R	Novagen
α1	pBH6119::ihfα P1 in BamHI and XbaI	C. Pitre (Pitre *et al.*, 2013)
α2	pBH6119::ihfα P2 in BamHI and XbaI	C. Pitre (Pitre *et al.*, 2013)

α3	pBH6119::ihfα P3 in BamHI and XbaI	C. Pitre (Pitre *et al.*, 2013)
α4	pBH6119::ihfα P4 in BamHI and XbaI	C. Pitre (Pitre *et al.*, 2013)
α5	pBH6119::ihfα P5 in BamHI and XbaI	C. Pitre (Pitre *et al.*, 2013)
α6	pBH6119::ihfα P6 in BamHI and XbaI	C. Pitre (Pitre *et al.*, 2013)
α7	pBH6119::ihfα P7 in BamHI and XbaI	C. Pitre (Pitre *et al.*, 2013)
α8	pBH6119::ihfα P8 in BamHI and XbaI	C. Pitre (Pitre *et al.*, 2013)
β1	pBH6119::ihfβ P1 in BamHI and XbaI	C. Pitre (Pitre *et al.*, 2013)
β2	pBH6119::ihfβ P2 in BamHI and XbaI	C. Pitre (Pitre *et al.*, 2013)
β3	pBH6119::ihfβ P3 in BamHI and XbaI	C. Pitre (Pitre *et al.*, 2013)
β4	pBH6119::ihfβ P4 in BamHI and XbaI	C. Pitre (Pitre *et al.*, 2013)
β5	pBH6119::ihfβ P5 in BamHI and XbaI	C. Pitre (Pitre *et al.*, 2013)
β6	pBH6119::ihfβ P6 in BamHI and XbaI	C. Pitre (Pitre *et al.*, 2013)
β7	pBH6119::ihfβ P7 in BamHI and XbaI	C. Pitre (Pitre *et al.*, 2013)
Y1	pBH6119::rsmY P1 in Bam HI and XbaI	C. Pitre (Pitre *et al.*, 2013)
Y2	pBH6119::rsmY P2 in Bam HI and XbaI	C. Pitre (Pitre *et al.*, 2013)
Y3	pBH6119::rsmY P3 in Bam HI and XbaI	C. Pitre (Pitre *et al.*, 2013)

ihfα KO	pSR47S::5' and 3' ihfα flanking regions in SalI and SacI	This study
ihfβ KO	pSR47S::5' and 3' ihfβ flanking regions in SalI and SacI	This study
letA KO	pSR47S::5' and 3' letA flanking regions in SalI and SacI	This study
rpoS KO	pSR47S::5' and 3' rpoS flanking regions in SalI and SacI	This study
pETDuet IHF	pETDuet-1::*ihfα::ihfβ* expression vector, Amp^R	This study

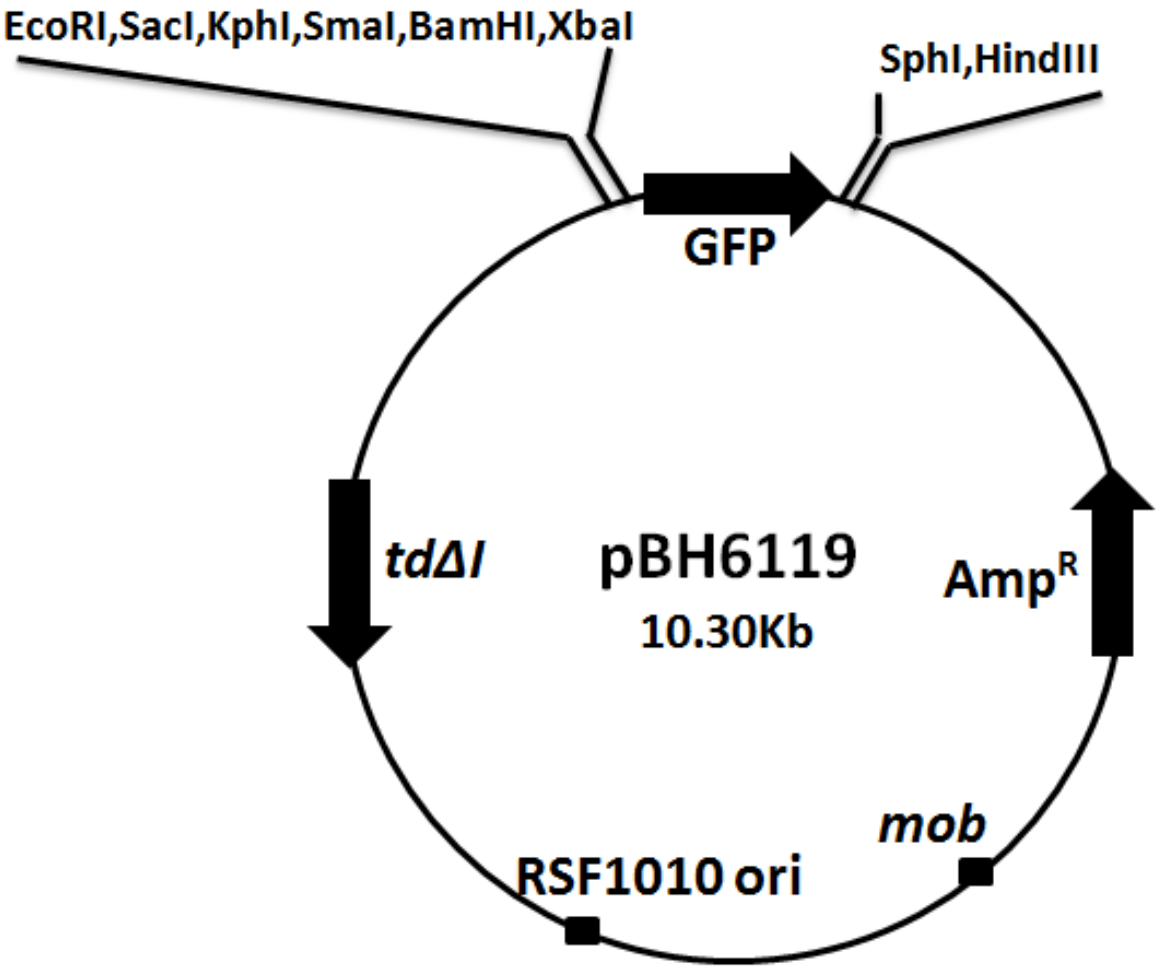

Figure 2.1: Genetic map of pBH6119 promoterless vector

2.2 Culture conditions:

2.2.1 *E. coli* culture conditions

Luria-Burtani (LB) agar (10 g Tryptone, 5 g Yeast extract, 10 g NaCl, 15 g agar per liter) media was used for all the *E. coli* cultures. The LB broth (same recipe except agar) liquid media was used to culture the *E. coli* strains. Strains were struck out on the LB agar plates containing appropriate antibiotics and were incubated overnight at 37^0C. For overnight cultures, an isolated colony was inoculated in 3mL LB broth with appropriate antibiotics and was incubated at 37^0C for overnight with aeration.

Following antibiotics were added to media at indicated final concentrations when needed: kanamycin (40µg/mL), ampicillin (100µg/mL), and chloramphenicol (20µg/mL). Isopropyl-β-D-galactoside (IPTG from Sigma-Aldrich) was added to final concentration of 1mM where indicated. 40µL of X-Gal solution (20mg/mL from Sigma-Aldrich) was added to the media where indicated.

2.2.2 *L. pneumophila* culture conditions

Buffered Charcoal Yeast Extract (BCYE) (10g Bacto Yeast Extract, 1g α-Ketogluatric acid, 1g ACES, 1.5g Activated Charcoal, 15g Agar per 1L) was used to culture *Legionella pneumophila*. BYE broth (same recipe minus charcoal and agar) was used. The pH of both media was adjusted to 6.6 – 6.7 using 6M KOH before autoclaving. The media was cooled to 55^0C after autoclaving and was supplemented with 0.4g L-Cysteine and 1mL 25% Fe-pyrophosphate.

L-cysteine was freshly prepared by dissolving 0.5g in 5mL of water and the pH was adjusted to 6.6-6.7 using 6M KOH. The solution was filter sterilized via 0.2µm syringe membrane filtration. 25% Fe-pyrophosphate solution was prepared by dissolving 10g of Fe-pyrophosphate in 40mL of water which was then filter sterilized. 25% Fe-pyrophosphate solution was covered in aluminum foil and stored at 4^0C.

Strains were struck on BCYE plate with appropriate antibiotics and were incubated at humid 37^0C + 5% CO_2. Following antibiotics were added to media at indicated final concentrations when needed: kanamycin (25µg/mL), and thymidine (100µg/mL).

2.3 *L. pneumophila* genome extraction

Two loops of Lp02 were collected from a 48 – 72 h grown *L. pneumophila* Lp02 plate and was resuspended into 440 µL of TE (pH 8) in a microfuge tube using vortex. After that 50µL of 10mg/mL Proteinase K (in 50mM Tris-HCl pH 8.0, 1mM $CaCl_2$), and 10µL of 10% SDS were added to the microfuge tube and the culture tube was incubated at 37^0C with gentle rocking for about 2hr. 50 µL of 10M ammonium acetate and an equal volume of phenol/chloroform/isoamyl alcohol (25:24:1) was added to the sample tube. The sample was vortexed and then centrifuged at 13,000 rpm for 10min at room temperature (RT). The aqueous layer was extracted two more times with an equal volume of phenol/chloroform/isoamyl alcohol and was precipitated in 100% ethanol in a sterile microfuge tube. The sample was centrifuged at 4^0C for 30 min at 13,000 rpm. The pelleted DNA was washed with 70% ethanol for 5 min and was air dried. The pellet was resuspended in 100µL of TE + RNAse (100µg/mL).

2.4 Molecular cloning

2.4.1 PCR

Taq polymerase (NEB) was used in gradient and colony PCR using the following reaction volumes: 40-60ng of *L. pneumophila* Lp02 genomic DNA or 1µL of colony supernatant for colony PCR, 0.5 µL of dNTPs (10 mM), 2.5 µL of 10x of Thermo Pol buffer, 0.1 µM forward primer, 0.1 µM reverse primer, 0.125µL Taq Polymerase and nuclease-free grade water in total reaction volume of 25µL. Following cycling conditions were used in PCR thermal cycler: Initial denaturation at 94°C for 3 min, denaturation at 94°C for 30 s, annealing (for temperature see Table 2.3) for 30 seconds, extension at 72° (for time see Table 2.3) for 25 cycles and final extension at 72° for 5 min. Gradient PCR was performed to determine the ideal annealing temperature for each primer set using the following sets of annealing temperatures: 50°C, 51.5°C, 53.9°C, 57.5°C, 62.2°C, 66.0°C, 68.5°C, 70°C.

For cloning purposes, Q5® High-Fidelity DNA Polymerase was used in the following 50µL reaction volume: For Phusion reactions 100ng of *L. pneumophila* Lp02 DNA, 4µL of dNTPs (10mM), 1.5µL of DMSO, 10µL of 5x Phusion HF buffer, 0.1µM forward primer and 0.1µM reverse primers (Table 2.3), 0.25µL Phusion polymerase, and nuclease-free water. For Q5 reactions: 100ng of *L. pneumophila* Lp02 DNA, 4µL of dNTPs (10 mM), 10µL of 5x Q5 buffer, 0.1µM forward primer and 0.1µM reverse primers (Table 2.3), 0.5µL Q5® polymerase, and nuclease-free water. Following cycling conditions were used: Initial denaturation at 98^0C for 30 seconds then denaturation at 98°C for 30s, annealing (for temperature see Table 2.3) for 30s, extension at 72°C (for time see Table 2.3) for 35 cycles and final extension at 72° for 5 min.

Table 2.3: Description of the PCR conditions of all the primers used in this study

Amplicon Name	Primers (5'-->3' direction)	Annealing Temp. (°C)	Extension Time (Taq/Q5)	Extension Temp. (°C)	Length (bp)
α1 (*ihfα* P1)	PF:GCGATAggatccGCCAGTCAGCTCAGATTGTGA PR:GCGATAtctagaGCTTAGTGCGTTCACGATC	70	30s/20s	72	469
β1 (*ihfβ* P1)	PF:GCGATAggatccCAAGTACCTTATTCGGTGCA PR:GCGATAtctagaTCAATGAGTTCGGATTTAATC	57.5	30s/20s	72	460
Y1 (*rsmY* P1)	PF:GCGATAggatccCTCGATGTATTTTCTGGTGG PR:GCGATAtctagaGGTCCCTTAGTTGACTTCCT	62.5	30s/20s	72	210
Z1 (*rsmZ* P1)	PF:GCGATAggatccCCCCGCTACATTTCATCGTA PR:GCGATAtctagaGCACGACTCATATCCATATA	53.9	30s/20	72	316
Z2 (*rsmZ* P2)	PF:GCGATAggatccCAAGCAGCATATTGCTCTAA PR:GCGATAtctagaGCACGACTCATATCCATATA	51.5	30s/20s	72	268
Z3 (*rsmZ* P3)	PF:GCGATAggatccCCTGACAATAATTCTTACA PR:GCGATAtctagaGCACGACTCATATCCATATA	50	30s/20s	72	172
psrA 5'	PF:GCGATAgtcgacGTTCACTTGCAAATACCACTA PR:GCGATAggatccTTACTTATATTCATAGGCATA	53.9	60s/30s	72	898

psrA 3’	PF:GCGATAggatccAATAAAGTGATTTTTTTTAAC PR:GCGATAgagctcGTTTACAGCATGTCCTGTATCA	53.9	60s/30s	72	911
PsrA (for protein expression)	PF: GCGATAcatatgAATATAAGTAATACGA PR: GCGATActcgagTCACTTTATTGTTTGATCAAT	51.5	30s/20s	72	561
psrA (seq 1)	GCGTATTAAAAAATATTGT	-	-	-	-
psrA (seq 2)	TACGCCATTTTCCCAGCT	-	-	-	-
psrA (seq 3)	TGATATGCTCCAATCAAGCT	-	-	-	-
psrA (seq 4)	GAGCATATCAGAATAATCTGAT	-	-	-	-
psrA (int)	PF:TAATGAATGAGCAGTCCACC PR:TTTTGCCTTGACTTTACTCA	57.5	20s/10s	60	757/220
psrA complement	PF:GCGATAgagctcTACATATATTACCTCCCGT PR:GCGATAggtaccTCACTTTATTGTTTGATCAA	53.9	45s/25s	72	787
psrA (GFP assay)	PF:GCGATAggatccTGATAGACGCTGCATCTCCT PR:GCGATAtctagaTGAAACTAAAGGCGTTATATCCG	62.2	30s/20s	72	488
IcmR	PF:GCGATAggatccGTGTTCCTTGTGTTTGGGTTA PR:GCGATAtctagaCGTGCACTGTCATCAGTAT	62.2	30s/20s	72	339

OxyR	PF:GCGATAggatccGCCGATAAATTGTTCAAA PR:GCGATAtctagaCTTTACATCTGCCAGGATGAC	62.2	30s/20s	72	291
IcmR (KB)	PF:GCGATAggatccTATGACGGATGTTATG PR:GCGATAgaattcAGTTACATCAGGTTCA	57.5	30s/20s	72	289
rpoS (GFP assay)	PF:GCGATAggatccCAGCTTATAATGTACGTTCTTC PR:GCGATAtctagaTCAGACCATTCCTCTTCTTT	62.2	30s/20s	72	533
GFP (seq)	PR: GTAAGTAGCATCACCTTCA	-	-	-	-
ihfα 5’	PF:GCGATAgtcgacGCTATGACAAGTTACAAGCT PR:GCGATAggatccGCGTTCACGATCATTCCCTCA	53.9	60s/30s	72	981
ihfα 3’	PF:GCGATAggatccAGGAAAGTAGTTTGTTGTCTC PR:GCGATAgagctcCTGTATGATGATGATACAT	53.9	60s/30s	72	902
ihfβ 5’	PF:GCGATAgtcgacCAGGATAATACTGTGCTTGA PR:GCGATAggatccTCGGATTTAATCATATACTCA	53.9	60s/30s	72	995
ihfβ 3’	PF:GCGATAggatccTAAAGATTAAATTTTATTTTT PR:GCGATAgagctcTACAAGCCTCTCAAGTACTAGC	51.5	60s/30s	72	991
ihfα (screening)	PF:GCTATGACACTACAAGACGA PR:AAAATTCTTCTCCACCGGAA	53.9	20s	60	505/229

ihfβ (screening)	PF:ACCCGTGTTTCAAGATACAA PR:AGAGGCTAATGAGGTTTGTG	53.9	20s	60	519/231
rpoS 5’	PF:GCGATAgtcgacGACATGACTCATTATAAGCTA PR:GCGATAggatccTCATCATCTTGCATTGTATCA	53.9	60s/30s	72	930
rpoS 3’	PF:GCGATAggatccTTTGTTTTGATTTAACCAGTT PR:GCGATAgagctcGAGATTCATCTGCATACTGA	53.9	60s/30s	72	925
letA 5’	PF:GCGATAgtcgacTTATTAGCAGAAAAATATTT PR:GCGATAgcggccgcAATACTTTAATCAAATAATGC	53.9	45s/25s	72	678
letA 3’	PF:GCGATAgcggccgcAGATGATTAGATGTTAATTTC PR:GCGATAgagctcTTCTTCGAAATTTAATTG	53.9	45s/25s	72	708
rpoS (screening)	PF:AAATTAGAAGAGCAGGGGTG PR:CTATCGACATCCCAGTAGG	53.9	25s	72	340
letA (screening)	PF:GTAAGACAGCTGGACTTG PR:ACATATAGAACGGTGCCTTC	57.5	25s	72	891/255
ihfα S1	GTTTTCTGTTGATTCAGTA	-	-	-	-
ihfα S2	CCCGATACTAATTTTCAT	-	-	-	-

ihfα S3	CTCATCATGCGCTTCACC	-	-	-	-
ihfα S4	GATGATTGAATAAATTCAA	-	-	-	-
ihfβ S1	GCACTTGACCGGCCTGAA	-	-	-	-
ihfβ S2	AGTGCGAGAAAACCAAAA	-	-	-	-
ihfβ S3	TATCTGAGGCGACCTTAAT	-	-	-	-
ihfβ S4	ATAAATCAACGGTTAGAA	-	-	-	-
rpoS S1	GTTAGAAACACCGGGTATT	-	-	-	-
rpoS S2	TAACTTGGACTTTGTTATT	-	-	-	-
rpoS S3	TCTTCCTCTGGTTGGCTAT	-	-	-	-
rpoS S4	AAGAACGTACATTATAAGCT	-	-	-	-
letA S1	CCTATCCTGGGGTAGCTGCTG	-	-	-	-
letA S2	TAGGGGCCAAAAAAATTA	-	-	-	-
letA S3	AAAGGGCTTAGAGCATAC	-	-	-	-
letA S4	GCCCTTTAGGCGTTTTAAT	-	-	-	-

ihfα (pDUET)	PF:GCGATAtctagaAATAATTTTGTTTAACTTTAAGAAGGAGATATACCATGATCGTGAACGCACTAAGCAA PR:GCGATAgcggccgcCTAGTGGTGATGATGGTGATGCTTTCCTATTTTTTCAATT	53.9	30s/20s	72

2.4.2 Agarose gel electrophoresis

Gel electrophoresis was performed to verify the results from PCR, ethanol precipitation, plasmid extraction, PCR clean-up and gel extraction. 1xTAE (40mM Tris acetate, 20mM acetic acid, 1mM EDTA) was used to prepared 1% w/v (for constructs ≥ 1kb) or 2% w/v (for constructs <1kb) agarose gel supplemented with 0.5mg/mL ethidium bromide. Then the gel was loaded with 1kb or 100bp ladder (New England Biolabs, NEB) and the samples was run on a gel electrophoresis machine in 1x TAE buffer under 100V for about 30 min. The bands were visualised on the Alphaimager™ 2200.

2.4.3 Cloning DNA fragment into plasmid

Using appropriate primer sets (Table 2.3), DNA insert was amplified using Q5® polymerase and was cleaned using the Qiagen gel extraction kit (Qiagen, Valencia, CA) according to the manufactures instructions. The purified product was then subjected to double digestion using appropriate restriction enzymes (Table 2.4) in a total volume of 50µL volume. The following recipe was used to setup the double digests: 10 µL of PCR amplicon, 5 µL of 10x BSA, 5 µL of appropriate 10x buffer (NEB), 2 µL of each restriction enzyme, and nuclease-free grade water. The digest was performed at 37^0C for 2-3 hours and was cleaned using the Qiagen gel extraction kit.

The vectors used for in the plasmid construction were also digested in a similar manner as the DNA inserts (Table 2.4). After the digest the sample was treated with 10µL of calf intestinal alkaline phosphatase (CIP) and incubated at 37^0 for an hour. The sample was cleaned using the Qiagen gel extraction kit and 5µL of insert and vector samples were ran on an agarose gel.

Table 2.4: List of restriction enzymes that were used to digest amplicons and vectors for plasmid construction in this study

Amplicon or Vector	Restriction Enzymes (FP/RP)
Z1 – Z3	BamHI/XbaI
psrA 5’	Sall/BamHI
psrA 3’	BamHI/SacI
letA 5’	Sall/NotI
letA 3’	NotI/SacI
rpoS 5’	Sall/BamHI
rpoS 3’	BamHI/SacI
pSR47S for 5’ cloning	Sall/BamHI
pSR47S for 3’ cloning	BamHI/SacI
PsrA (protein purification)	Ndel/XhoI
pET16B	Ndel/XhoI
psrA complement	Sacl/KpnI
pBH908	Sacl/KpnI
psrA (GFP assay)	BamHI/XbaI
rpoS (GFP assay)	BamHI/XbaI
pBH6119	BamHI/XbaI

Both digested amplicon and vector were ligated using T4 DNA ligase (NEB) in the following reaction in total volume of 10µL: 7µL amplicon, 1 µL vector, 1 µL 10x T4 DNA ligase buffer and 1 µL of T4 DNA ligase. The ligation sample was incubated at room temperature for 2 hours or overnight at 16^0C. After the incubation the sample was transformed into rubidium chloride competent *E. coli* DH5α cells. However, in the suicide plasmid construction the ligated sample was transformed in *E. coli* DH5α λpir cells.

2.5 *E. coli* transformations

2.5.1 Preparation of rubidium chloride competent *E. coli* DH5α cells

E. coli DH5α cells were grown on LB agar plates and a single colony was inoculated in 3mL LB broth and incubated overnight at 37^0C. The overnight culture was subcultured into 500mL LB broth and incubated at 37^0C. Once the OD_{600} reached 0.5, the culture was kept on ice for 5 min and was centrifuged at 3700 rpm at 4^0C for 20 min. The supernatant was discarded and the cells were resuspended in 200mL of TFB I (30mM Potassium acetate, 100mM $RbCl_2$, 10mM $CaCl_2$, 50mM MnCl2, 0.0225% glycerol in dH2O, pH to 5.8 with 0.2M acetic acid) and were kept on ice for 5 more min. The cells were then centrifuged again at 3700 rpm at 4^0C for 15 min and the supernatant was discarded. The cells were resuspended in TFB II (10mM MOPS, 75mM CaCl2, 0.0563% glycerol in dH2O, pH to 6.5 with 1M KOH, sterilized via membrane filtration) and were kept on ice for 15 min. 200µL aliquots were made in sterile microfuge tubes which were flash frozen and stored at -80^0C.

2.5.2 Heat shock Transformation

For the transformation, 10 µL of ligation sample was added to the 100µL of thawed rubidium chloride competent cells. The sample was incubated on ice for 1 hour and then

heat shocked by incubating it at 42^{0}C for 90 sec. After the heat shock the sample was resuspended in 500µL of LB broth. The sample was further incubated for one hour at 37^{0}C with aeration. About 25-100 µL sample was spread on LB agar plates containing appropriate antibiotics which were later incubated overnight at 37^{0}C.

2.5.3 Colony PCR to verify the constructed plasmid in *E. coli*

After transformation, about 40 colonies were picked and struck out on a new appropriate LB agar plate. The plate was incubated at 37^{0}C overnight. Next day, 5 colonies were resuspended into a PCR tube 50µL and same was done for the remaining colonies. The samples were lysed at 95^{0}C for 10 min in thermocycler and centrifuged at 13000 rpm for 1 minute at RT. The supernatant was treated as a template DNA in multi colony PCR using appropriate primer set and extension times (Table 2.3). The samples were run on 1% agarose gel and colony set with a desired band was picked for single colony PCR. Another set of colony lysates were prepared but this time only one colony was included in one PCR tube. Taq PCR was performed and colony carrying the desired plasmid was inoculated in 3mL LB broth. 900µL of the culture and 100µL of sterile DMSO was added to the cryogenic tubes and the stocks were kept at -80^{0}C. The remaining culture was then applied in plasmid DNA extraction using QIAprep Spin Miniprep Kit (Qiagen, Valencia, CA).

2.6 Transformation of *L. pneumophila*

2.6.1 *L. pneumophila* electrocompetent cells preparation

L. pneumophila was heavily struck out on BCYE plate containing appropriate antibiotics and supplements. It was grown for 48hrs at 37^{0}C + 5% CO_2. The cells were harvested using sterile disposable loops and resuspended in 40mL sterile cold water. The cells were centrifuged at 3700 rpm for 15 min at 4^{0}C. The supernatant was discarded and

the pellet was resuspended in 40mL of cold sterile water. The cells were centrifuged and washed two more times as described previously. After the washes the pellet was resuspended in 2mL of 15% glycerol and 100µL aliquots were prepared in 1.5mL eppendorf tubes which were stored at -80^{0}C.

2.6.2 Electroporation of *L. pneumophila* competent cells

The following steps were taken to achieve successful transformation of *L. pneumophila* cells. 5µL of desired plasmid was added to the 95µL thawed electrocompetent cells. The sample was mixed and loaded on the 1 mm-gap BioRad™ electroporation cuvette. The cuvette was placed in the BioRad MicroPulser™ Electroporator and was electroporated at 2.1kV. The electroporated cells were incubated in BYE broth for 2 hours at 37^{0}C. The recovered cells were plated on appropriate BCYE plates for 3-4 days at 37^{0}C + 5% CO_2.

2.7 GFP reporter assay

Promoter regions of targeted genes (200-500bp in length) were cloned into promoter less GFP reporter plasmid, pBH6119 (Figure 2.1) and were electroporated in appropriate *L. pneumophila* strains. *L. pneumophila* strains carrying GFP reporter plasmids (Table 2.2) were struck out on appropriate BCYE plate and incubated at 37^{0}C+CO_2 for 3 days. A loop full of each strain was resuspended in 3mL BYE broth and was subcultured into 10mL of BYE to adjust the OD_{600} to 0.2. 150µL of this culture was placed in 96-well black microclear plate (Greiner Bio-One), and the plate was incubated shaking (fast speed setting) at 37^{0}C in a BioTek Synergy™ 2 hybrid automated microplate reader. GFP fluorescence (Ex 485/20, Em 528/ 20) and OD600 readings were measured on an hourly basis for 24 hours. Relative

fluorescence unit (RFU) values were normalised by diving the GFP by OD_{600} and then subtracting the negative controls (Table 2.1).

2.8 *Legionella pneumophila* knockout construction

Once the knockout construct (pSR47S::psrA 3' &5') sequence was verified, the plasmid was electroporated in Lp02 electro competent cells. Approximately 1µg of the plasmid was added to 100µL of Lp02 competent cells and the sample was kept on ice for 10 min after gentle mixing. The sample was electroporated in BioRad MicroPulser™ Electroporator and then the cells were incubated in 1mL of BYE broth at 37^0C for 2 hours. Since the knockout plasmid backbone carries kanamycin resistance cassette, the transformed cells were plated on BCYE-thy/kan plates. The colonies were picked and struck out on BCYE-thy plate containing 5% sucrose. The grown colonies were then picked and streaked on both BCYE-thy and BCYE-thy/kan plates. The colonies that didn't grow on BCYE-thy/kan were used in colony PCR to screen to verify the knockouts using the psrA int primer set (Table 2.3).

Where indicated, BCYE plates where supplemented with 100µg/mL thymidine, and 25µg/mL kanamycin. All the streaked out plates were incubated at 37^0C for 3-5 days.

2.9 Protein purification

2.9.1 Growth and Protein induction

E. coli BL21 CodonPlus pET16b::psrA strain was cultured on LB plate containing ampicillin and chloramphenicol. Single colony was picked and was inoculated in 50mL of LB broth with appropriate antibiotics. The entire culture was used to subculture 1L of LB broth containing ampicillin and was incubated on a shaker at 37^0C until the OD_{600} of 0.6-0.7 was reached. The culture was induced with 1mM IPTG for 3-4 hours. The culture was centrifuged at 4^0C for 30 min at 6000rpm. The supernatant was discarded and the pellet

was resuspended in 40mL of 50mM Tris-pH8 and was centrifuged again at 3800 rpm for 20min at 4^0C. The supernatant was discarded and the pellet was stored at -80^0C.

2.9.2 Beads prep and French Press

2.5 mL of Qiagen Ni-NTA beads was transferred to sterile 15mL conical tube containing 10mL of sterile water. The tube was mixed well and was kept at 4^0C for about an hour to let the beads settle. The supernatant was discarded and the beads were washed again with 10mL of sterile water. After the beads were settled, they were resuspended in 5mL of binding buffer (5mM imidazole, 0.5M NaCl, 0.02M Tris, pH 8.0) and the tube was left at 4^0C for overnight.

The cell pellet from previous step was suspended in 20mL of binding buffer and following components were added to the tube: 200 ml each of Halt Protease Inhibitor Cocktail (Thermo Scientific) and 0.5M EDTA, pH 8.0. The cells were then lysed in a French Press (20K cell, American Instrument Company, Silver Spring, Md.) and the lysate was centrifuged at 12,000 rpm at 4^0C. The supernatant was kept on ice where the beads were added to the tube. The sample was kept at 4^0C with gentle rocking on the Orbitron Rotator II (Mandel Scientific, Guelph, Ontario) for 1 hour to allow the protein to bind the beads.

2.9.3 Gravity column and dialysis

The protein bead mixture was applied to the Pierce® Centrifuge Columns (GE Healthcare, Baie d‟Urfe, Quebec). The column was washed with wash buffer (0.5M NaCl, 0.02M Tris pH 8) with increasing amounts of imidazole (0mM, 10mM and 25mM). After washing the column, elution buffer (0.25M NaCl, 0.05M Tris pH8, 0.5mL of concentrated HCl, 250mM Imidazole, up to 100 mL H_2O) was applied to the column and the flow through was collected in 1.5mL aliquots. The elution fractions were ran on a 12% SDS gel (2mL

Resolving gel buffer [1.5M Tris, 0.4% SDS, pH 8.8], 12% polyacrylamide, 50µL 10% APS, 12µL Temed [BioRad, Mississauga, Ontario], up to 8 mL dH2O) at 120V for about 1½ h in 1x running buffer (0.025M Tris, 0.192M glycine, 0.1% SDS). The gel was then stained with Coomassie Brilliant Blue (BioRad) for 30 min and then destained for an hour in destaining solution I (50% Ethanol, 10% Acetic acid) and then in destaining solution II (5% Ethanol, 7% Acetic acid). Moreover, Bradford assay was also performed to verify the protein concentration where 10µL of elution sample and 10µL of Bradford Protein Assay Dye Reagent (Bio-Rad) were added to 80µL of water. The elution samples containing protein were then transferred to the dialysis tubing which was submerged in dialysis buffer 1 (0.02M Tris pH 8, 0.3M KCl, 77mg DTT, 0.4mM EDTA, 10% glycerol) for 4 hours. The dialysis was repeated with new buffer 1 for another 4-24hrs.

2.9.4 HiTrap Heparin HP column and centration

HiTrap Heparin HP column (GE Healthcare, Baie d‟Urfe, Quebec) was first washed with 10mL of buffer A (20mM Tris-HCl pH 8, 200mM 4M KCl). The protein sample was then loaded on the column and the column was washed again with 5mL of buffer A. 5mL of buffer A and 0.5mM DTT was applied to the column. Buffer A and Buffer B (20mM Tris-HCl pH 8, 1.5M 4M KCl) supplemented with 0.5mM DTT were added together and the column was washed with increasing KCl concentrations beginning at 200 mM KCl and increasing in 100mM increments to 1.5M KCl. The flow through was collected and the protein concentration was checked again through SDS-PAGE and Bradford assay. The samples containing protein were pooled together and the protein was concentrated in protein storage buffer (20mM Tris pH 7.9, 200mM KCl, 0.2mM EDTA, 30% glycerol) via centrifugation in a Amicon® Ultra 10K Centrifugal filter units (Millipore, Long Beach,

California). The sample was centrifuged at 4000 rpm at 4^0C until the protein started precipitating. The resulting concentrated protein was then stored at -20^0C.

2.9.5 Protein concentration analysis

The protein concentration was determined by using the standard curve of increasing Bovine BGG50 concentrations. 200µL of the Bio-Rad protein reagent was added to the standards and the total reaction volume was brought to 1mL. The standard curve was prepared with BGG50 concentrations at set points of 0, 2.5, 5, 10, 20 µg/µL. 100µL of 1 in 10 dilution was prepared for protein sample using protein dilution buffer (20 mM Tris pH 8, 10 mM MgCl2, 100 µM KCl, 10% glycerol 0.05 mg/mL BSA). The samples were further diluted by 1/500 and 1/250 and the final volume was brought to 800µL. 200µL of the Bio-Rad protein reagent was added to the samples and the A_{280} values were plotted on the standard curve to determine the protein concentration.

2.10 Radio-labelled Mobility Shift Assay (EMSA)

Radio-labelled probes were prepared in the following random-labelling reaction (volume: 50µL): 60-80ng of template DNA (Lp02 genome), 5µL 10x PCR buffer, 8µL (1.25mM dATP, 1.25mM dGTP, 1.25mM dTTP and 0.3125mM dCTP) 0.1µM forward primer, 0.1µM reverse primer, 0.5µL Taq polymerase and 5µL dCTP([α-^{32}P]- 3000Ci/mmol 10mCi/ml). Standard PCR protocol was performed and the samples were cleaned with Qiagen Nucleotide Exchange Kit (Qiagen, Valencia, CA). Each reaction contained appropriate amount of purified psrA protein and dH_2O up to the total volume of 10µL. Then 10µL of binding reaction mix (4µl of 50% glycerol, 3µl of salmon sperm DNA, radiolabeled amplicon totalling 1000 cpm per lane, 2µl of 10x binding mix (in 250µl - 25µl 100x BSA, 25µl 1M HEPES pH7.9, 62.5µl 4M KCl, 1µl EDTA pH 8.0, 10µl 0.5M DTT, 10µl 0.5M PMSF

and 116.5µl ddH2O)) was added to all the samples. The reactions were then incubated at room temperature for 30 min and 2µL of the 10x loading buffer (600 µL of 50% glycerol, 9.4 mL 5x TBE [500 mL solution containing 27 g Tris, 13.75 g Boric Acid, 0.01 M EDTA pH 8], 0.1 g bromophenol blue) was added. 6% polyacrylamide gels (in 40ml– 8ml 30% acrylamide (29% acrylamide, 1% bisacyrlamide), 29.7ml of ddH2O, 4ml 5x TBE buffer, 0.25ml 10% APS) were made and were pre-runned for 1hr at 20mA in 0.5x TBE buffer. The samples were loaded on the pre-runned gel and ran for 2.5hrs. The gel was then dried on a gel fryer at 80˚C and exposed on the Kodak phosphor screen for overnight. The screen was scanned using Molecular Imager PharosFX™ Plus System (BioRad).

2.11 DNaseI footprinting

Appropriate primers (Table 2.3) were used in a standard Q5® PCR to amplify the promoter region and amplified sample was cleaned using the Qiagen gel extraction kit. The cleaned amplicon was then digested with appropriate restriction enzyme to label top strand or the bottom strand for 3 hours. Then 10µL of CIP was added to the samples followed by one hour incubation at 37˚C. The samples were cleaned again using Qiagen gel extraction kit and the DNA sample was eluted from the column in 30µL of EB buffer. Next the amplicon was end labelled in the following reaction: 30µL eluted DNA, 4µL of ATP ([γ-^{32}P]- 3000Ci/mmol 10mCi/ml), 1µL of T4 poly nucleotide kinase (NEB), 5µL of 10x T4 Polynucleotide Kinase Reaction Buffer and 10µL of dH_2O. The sample was incubated at 37˚C for 1hr and then heat inactivated at 65˚C for 30 min in thermocycler. The samples were then cleaned using Qiagen Nucleotide Exchange Kit. Binding reaction were performed in the following reaction conditions: 10-20µg of the protein in 20µL was added to the 180µL of assay buffer (radiolabeled amplicon totalling 60,000 cpm per reaction, 20mM Tris

pH8, 5mM MgCl2, 1mM CaCl2, 100mM KCL, 4µg/mL poly(dI-dC), 0.05mg/mL bovine serum albumin (BSA) and 200mM DTT) and incubation was done for 30min at RT. 1µL of DNaseI (Sigma) was added to the 500µL of the protein dilution buffer (20mM Tris pH8, 10mM MgCl2, 100mM KCl, 50% glycerol, 0.05mg/mL BSA and 100mM DTT). The DNaseI was further diluted by adding 2µL of diluted DNaseI to 750µL protein dilution buffer. The incubated samples were then digested with DNaseI for 90sec and then the reaction was stop by adding the stop buffer (200 mM EDTA, pH 8.0; 5 M ammonium acetate; and 100 µg of salmon sperm DNA). The digest was performed in a similar manner for all remaining samples and then 200µL of phenol/chloroform/isoamyl alcohol was added and the tubes were centrifuged at 13,000 rpm for 30min. the aqueous layer was then transferred to a tube continuing 750µL of 100% ethanol and the samples were precipitated at -20^{0}C overnight. The tubes were centrifuged again next day at 4^{0}C for 30min at 13,000 rpm. The pelleted DNA was then washed with 70% ethanol and pellet was air dried. Dried pellet was resuspended in 20µL of formamide loading dye (80% deionized formamide, 10mM EDTA pH8, 1mg/mL bromophenol blue, 1mg/mL Xylene Cyanol FF).

To prepare 8% polyacrylamide sequencing gel, 36g urea was dissolved in 15mL of 5x TBE, and water up to 62.5mL. After the urea was dissolved completely, 450µL 10% APS and 12.5mL of 30% acrylamide (29% acrylamide, 1% bisacyrlamide) was added and the solution was degased for 15 min. Then 45µL of TEMED was added to the solution and sequencing gel was poured. Once the gel was ready it was pre-ran in 1x TBE buffer for about 30 min at 2000V at 45-50˚C. Once the gel was warm enough the samples were heated at 75˚C for 2min and then 10µL of the sample was loaded on the gel. Gel was ran for 2.5 -

3hrs and then dried for 1hr. The dried gel was exposed on Kodak phosphor screen. The image was developed using Molecular Imager PharosFX™ Plus System (BioRad).

The sequencing ladder was prepared using the Sequenase™ Quick Denature Plasmid Sequencing Kit (Affymetrix, Santa Clara, CA). The Glycol/heat denaturation protocol was followed as described by the manufacturer with 1:20 dilution of labelling mix. The sequencing ladder was run with footprint samples on the sequencing gel.

2.12 Cell culture

2.12.1 Maintenance of Cell Line

All work was completed in a sterile Biosafety cabinet unless otherwise stated. U937 cell line (isolated from the histiocytic lymphoma of a 37 year old male patient) were grown in RPMI media with 10% heat inactivated FBS (HIFBS). 1 mL of freezer stocks at passage 8 was thawed at 37^0C. This was centrifuged at 1000 rpm for 5 minutes at room temperature to pellet the cells and separate out the DMSO. The supernatant was removed from the pellet and 6mL of warm RPMI+10% HIFBS was added. These cells were moved into a T25mL flask. A media control of the RPMI+10% HIFBS was made by 5mL of media into a separate flask. These cells were allowed to grow at 37^0C+5% CO_2. When a layer of cells was visible, the cells were passed.

2.12.2 Passing of the Cell Line

When a monolayer of U937 cells was visible, 2.5mL of cells was taken from the flask, added to a 15mL conical tube and centrifuged at 1000 rpm for 5 minutes at room temperature. The supernatant was then remove and dumped into a 10% bleach waste bottle. The cells were resuspended in 1mL of warm RPMI+10% HIFBS. The amount of

media was measured and a corresponding amount of warm RPMI+10% HIFBS was added to bring the volume to 5mL. 20mL of warm RMPI+10% HIFBS was added to a T75mL flask. The 5mL of cell suspension was then added to the T75 ml flask and swirled to ensure proper mixing. A 5mL media control of the RMPI+10% HIFBS was also made. This allowed the cells to grow and provide a monolayer within three days.

2.12.3 Activation of the Cell Line

When a monolayer of U937 cells was visible, the entire contents of the flask was removed and placed into a 50 ml conical tube. The cells were then centrifuged for 5 minutes at 1000 rpm and at room temperature. The supernatant was then removed and dumped into a 10% bleach waste bottle. The cells were resuspended in 3mL of warm RPMI+10% HIFBS. The cells were then combined into one 50 ml conical tube. 15mL of warm RPMI+10% HIFBS was added to a corresponding number of 75mL flasks for either growth kinetics or Immunofluorescence (8 or 3 flasks respectively). 50ng/mL of phorbol 12-myristate 13-acetate (PMA) (1µg/µL PMA was dissolved in DMSO and further diluted in sterile water for final concentration of 0.1µg/µL) was added to the 20mL of cell suspension for differentiation of the cells. The cells were allowed to activate for at least 24 hours at 37^0C+5% CO_2 before being transferred to infection plates.

2.13 Intracellular growth kinetics

2.13.1 Transferring of Activated U937 cells to Infection Plates

After 24 hours of the activation process, cells were washed three times with warm RPMI+10% HIFBS. The cells were then scraped with cell scraper (Thermo Scientific Nunc Cell Scraper PE Blade PS Handle Sterile 32 cm2) to detach the macrophages. After the scrapping the cells were placed into one 75 ml flask. 10 µL of the cell sample was taken and

mixed with 10µL of trypan blue stain 0.4% (Life Technologies). 10µL of the cell and trypan blue sample was then placed on a hemocytometer and the four corners of the hemocytometer were counted for live cells. The average of the counts was taken then multiplied by a factor of 10^4 then by a dilution factor of 2. A cell count near 1 x 10^6 cells/mL was used for the infection. The cells were then moved to a 24 well infection plate where each well contained 1 x 10^6 cells. These cells were allowed to adhere to the sides and bottom of the wells for 24 hours at 37^0C+5% CO_2.

2.13.2 Infection of Activated U937 cells for growth kinetics

The U937 cells in the 24 well infection plates were washed three times with warm RPMI+10% HIFBS. The bacterial strains (Table 2.1) were grown overnight in 3mL cultures of BYE broth with appropriate supplements. The bacterial strains were then diluted by a factor of three and 1mL of this new dilution was taken and centrifuged at 13,000 rpm for 1 minute to pellet the cells. The supernatant was removed and the bacteria was resuspended in warm RPMI+10% HIFBS. This suspension was then measured at an OD of 600 to calculate the number of bacterial cells needed for the MOI of 2 in 10mL media volume. For the infection plate, the U937 cells were infected in duplicate with the bacteria suspension at MOI of 2. This was centrifuged at 1000 rpm for 5 minutes to help the bacteria to make contact with the cells. The plates were then incubated at 37^0C+5% CO_2 for 1 hour. After incubation the cells were then washed three times with warm RPMI+10% HIFBS. The cells were then incubated in RPMI+10% HIFBS with 100µg/mL gentamicin at 37^0C+5% CO_2 for 1hour after centrifuging at 1000 rpm for 5min. After the incubation the cells were washed three times with warm RPMI+10% HIFBS. This became time zero. All other time points (24,

48 and 72hr) were treated with warm RPMI+10% HIFBS and necessary supplements for bacterial growth, and placed in the incubator at 37^0C+5% CO_2 until the lysis process.

2.13.3 Lysis of Infected U937 cells for growth kinetics

The U937 cells were lysed with 1 ml of cold HyPure™ Molecular Biology Grade Water (Thermo Scientific) for 5 minutes with rigorous scraping. 100µL of the lysis suspension was serial diluted up to 10^{-5} in HyPure™ Molecular Biology Grade Water. The serial dilution was spotted in triplicate onto corresponding BCYE plates (with necessary nutrients for bacterial growth) with 10µL. The serial dilutions were incubated for 3 days at 37^0C+5% CO_2. The number of bacterial cells grown was counted via a stereomicroscope and the data was plotted on a graph.

2.14 Immunofluorescence studies

2.14.1 Transferring of Activated U937 cells for Immunofluorescence

After 24 hours of the activation process, cells were washed three times with warm RPMI+10% HIFBS. The cells were then scraped with cell scraper (Thermo Scientific Nunc Cell Scraper PE Blade PS Handle Sterile 32 cm2) to detach the macrophages. After the scrapping the cells were placed into one 75 ml flask. 10 µL of the cell sample was taken and mixed with 10µL of trypan blue stain 0.4% (Life Technologies). 10µL of the cell and trypan blue sample was then placed on a hemocytometer and the four corners of the hemocytometer were counted for live cells. The average of the counts was taken then multiplied by a factor of 10^4 then by a dilution factor of 2. Cell count near 1-5x10^5cells/mL was used for the infection. In the infection plate positively charged sterile coverslips (Fisher) were rinsed in sterile 1X PBS (1 in 10 dilution with dH_20 of 10X PBS (for 500mL: 40g NaCl, 1g KCl, 1g KH_2PO_4, 5.75g $NaHPO_4$)) and placed at the bottom of each well in the

infection plate. The cells were then moved to a 24 well infection plate with 1-5x10^5cells per wells. These cells were allowed to adhere to the coverslip at the bottom of the well for 24 hours at 37^0C+5% CO_2.

2.14.2 Infection of Activated U937 cells for Immunofluorescence

The U937 cells in the 24 well infection plates were washed three times with warm RPMI+10% HIFBS. The bacterial strains (Table 2.1) were grown overnight in 3mL cultures of BYE broth with appropriate supplements. The bacterial strains were then diluted by a factor of three and 1mL of this new dilution was taken and centrifuged at 13,000 rpm for 1 minute to pellet the cells. The supernatant was removed and the bacteria was resuspended in warm RPMI+10% HIFBS. This suspension was then measured at an OD of 600 to calculate the number of bacterial cells needed for the MOI of 2 in 10mL media volume. For the infection plate, the U937 cells were infected in duplicate with the bacteria suspension at MOI of 2. This was centrifuged at 1000 rpm for 5 minutes to help the bacteria to make contact with the cells. The plates were then incubated at 37^0C+5% CO_2 for 1 hour. After incubation the cells were then washed three times with warm RPMI+10% HIFBS. The cells were then incubated in RPMI+10% HIFBS with 100µg/mL gentamicin at 37^0C+5% CO_2 for 1hour after centrifuging at 1000 rpm for 5min. After the incubation the cells were washed three times with warm RPMI+10% HIFBS. This became time zero. At this point the cells were fixed by 4% of Paraformaldehyde (Thermo Scientific) in 1X PBS for 30 minutes with gentle shaking, then washed three times in sterile 1X PBS and placed at 4^0C until further processed. At other time points, the cells were treated the exactly the same.

2.14.3 Immunofluorescence Staining of Infected U937 cells

The fixed cells in 1x PBS were then treated with 0.1% TRITON® X-100 Detergent (Calbiochem) for 20 minutes at room temperature. The cells were then washed three times with 1x PBS. The cells were then treated with a blocking solution of 5% milk (for 20mL: 1g of skimmed milk powder in 1xPBS) for 1 hour with gentle shaking. The cells were washed again 3 times with 1X PBS. The primary anti-lp-1 (rabbit antibody applied at a dilution factor of 1 in 10,000) and anti-calnexin (mouse antibody applied at a dilution factor of 1 in 2500, Millipore) was applied in 5% milk. The cells were shaken constantly at room temperature for 1 hour and then washed with 1X PBS. Secondary antibodies were applied Donkey anti-rabbit IgG Antibody at 555 nm (1 in 2500, Alexa Fluor) and Donkey anti-mouse IgG Antibody at 488 (1 in 500, Alexa Fluor) and cell stain DAPI (1 in 200) in 5% milk for 1 hour with gentle shaking and covered in tin foil. The cells were then washed 3 times with 1X PBS. The coverslips were removed and mounted on the 3”x 1”x 1 mm microscope slide by a single drop of Immu-Mount (Shandon). Excess Immu-Mount was removed from the coverslips by 70% ethanol. The slides were stored at -20C until imaged by the LSM 700 confocal (Zeiss Canada, Toronto, ON).

Chapter 3: Results

3.1 Bioinformatics analysis

3.1.1 Identification of PsPsrA orthologue in *L. pneumophila*

As stated earlier, *Pseudomonas* PsrA (PsPsrA) responds to the changes in long-chain fatty acid (LCFA) levels in the environment and also regulates the expression of several virulence traits. However in *L. pneumophila*, it is not known if sensor proteins like PsPsrA respond to changes in fatty acid levels in the surroundings. So in order to identify the orthologue of *pspsrA* in *L. pneumophila,* BLAST analysis was performed with the BLAST: Basic Local Alignment Search Tool (Altschul *et al.*, 1997) using PsPsrA protein sequence from *P. fluorescens* A506. The alignment results showed a weak homology to the orthologue of PsPsrA, TetR-family transcription regulator (Lpg1967) with query coverage of only 24% (Table 3.1) on the amino acid level. Moreover, this alignment was solely based on the TetR-type helix-turn-helix (HTH) DNA-binding domain that lies within the first 64 amino acids of the peptide chain of encoded by *lpg1967*. Even with the 40% identity and 55% positives in the query coverage, UniProt analysis identified 68 residues with 50% homology in the HTH DNA-binding domain (Table 3.1) (Consortium, 2014). Orthologues of PsPsrA have also been identified in several *Pseudomonas* species and *A. vinelandii* with very good score values (>300) (Table 3.1).

Because of very low score and query coverage, Lpg1967 (PsrA) protein sequence was further analysed using InterProScan 5 (Jones *et al.*, 2014), an online protein prediction tool from The European Bioinformatics Institute. The TetR type DNA-binding HTH domain

Table 3.1: *P. fluorescens* A506 PsPsrA sequence was used in the BLAST search to identify potential orthologues in other bacteria.

Organism	E-Value	Query Coverage	Identities	Positives	Description	Score
L. pneumophila subsp. pneumophila str. Philadelphia 1	3e-04	24% (HTH domain)	40%	55%	DNA-binding HTH domain, TetR-type	40.0
L. pneumophila str. Corby	2e-04	24% (HTH domain)	40%	55%	DNA-binding HTH domain, TetR-type	40.0
P. fluorescens	7e-168	100%	98%	99%	DNA-binding HTH domain, TetR-type	468
P. aeruginosa PAO1	8e-143	97%	85%	93%	DNA-binding HTH domain, TetR-type	405
A.vinelandii DJ	1e-109	100%	69%	78%	DNA-binding HTH domain, TetR-type	316

was predicted in the region of 6-64 amino acids of the peptide chain correlating these results nicely with the BLAST results mentioned above. Moreover, the TetR-type C-terminal domain was deemed to be present within 81-187 amino acid region of the peptide chain. For further verification, secondary structure alignment was performed on the PRALINE server (Simossis and Heringa, 2005) using the *P. fluorescens* A506 PsPsrA and PsrA (Lpg1967) amino acid sequence. The predicted structure was then cross-referenced with the crystal structures of PsPsrA (Lunin *et al*., 2005) and PsrA (Michalska *et al*., 2013) proteins. Both proteins were found to form homodimers and are structurally similar in all 9 α-helices (Figure 3.1)(Lunin *et al*., 2005; Michalska *et al*., 2013). Taken together, the bioinformatic analyses indicate that PsrA is an orthologue of PsPsrA. Therefore, on this basis, PsrA was selected for further studies in *L. pneumophila*.

3.1.2 Bioinformatics pattern search using *Pseudomonas* PsrA binding site

In *Pseudomonas* species, PsPsrA is known to be involved in various different systems that include virulence, motility, and energy metabolism (Gooderham *et al*., 2008; Kojic *et al*., 2005; Shen *et al*., 2006). In *L. pneumophila*, non-coding RNAs, RsmY and RsmZ are key components of the virulence system, and regulatory proteins LetA and IHF have recently been identified to be involved in their regulation. In contrast, PsPsrA was found to directly regulate the expression of RsmZ in *P. fluorescens* (Humair *et al.*, 2010). Interestingly, PsPsrA was found not to be involved in RsmY expression. PsPsrA was determined to directly regulate the RpoS expression in a similar manner to that of RsmZ expression. Thus, to further identify additional targets of PsrA in *L. pneumophila*, it was assumed that since the HTH region and homodimer conformation was fairly conserved,

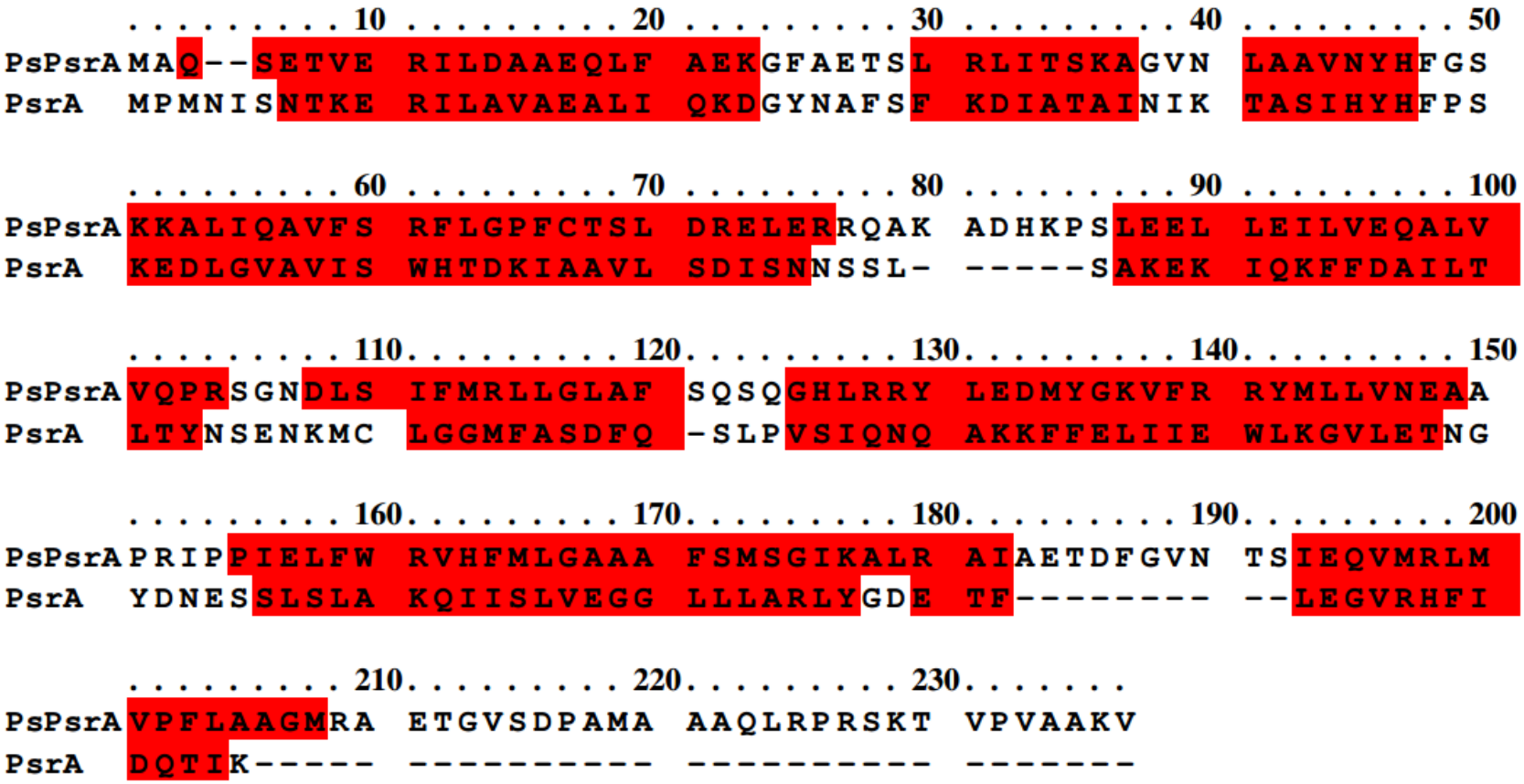

Figure 3.1: Secondary structural comparison of PsPsrA and PsrA. *P. fluorescens* A506 PsPsrA and PsrA (Lpg1967) amino acid sequences were used in the secondary structure alignment. The alignment was performed on the PRALINE server using DSSP (Kabsch & Sander, 1983) and PSIPRED (Jones, 1999) algorithms. α-helices are represented in red. The predicted structure was then cross-referenced with the crystal structures of PsPsrA and PsrA to further verification.

then the consensus DNA binding site sequence C/GAAACN$_{2-4}$GTTTG/C reported for *P. putida* PsPsrA (Kojic *et al.*, 2002) could be used in the bioinformatics pattern search using the Legiolist genome sequence database (*genolist.pasteur.fr/LegioList/)*. The pattern search identified multiple PsrA binding sites within the promoter region of several gene targets involved in virulence, cyst-biogenesis, the Dot/Icm secretion system and stress response (Table 3.2). Moreover, several genes encoding flagella apparatus, and energy metabolism proteins were also predicted to have multiple PsrA binding sites.

3.2 Δ*psrA* knockout construction

3.2.1 Creation of suicide vector for knockout studies

To create an unmarked in-frame deletion mutant of *psrA*, the pSR47S allelic exchange suicide vector was used to generate a plasmid construct carrying fused 5' & 3' flanking regions of *psrA.* The location of the primers used to amplify the 5' and 3' flanking regions are shown in Figure 3.2. The plasmid map of the pSR47S suicide vector is shown in Figure 3.3.

First, the *psrA* 3' primer set (Table 2.3) was assessed via gradient PCR to determine the optimum annealing temperature (see Materials and Methods). A representative photograph of a gradient PCR run on an agarose gel is shown in Figure 3.4. 53.9^{0}C was selected as the optimum annealing temperature based on the brightness and clarity of the band produced at this temperature. Once the annealing temperature was determined, Q5® high fidelity polymerase was used in a PCR reaction to amplify the DNA fragment (see Materials and Methods). Negative control showed the lack of DNA and the positive sample

Table 3.2: Legiolist pattern search results. *P. putida* PsPsrA binding site was used in pattern search to identify potential binding sites in *L. pneumophila*. Several genes were identified with multiple PsrA binding sites with 4 mismatches allowed.

Gene	Description	possible binding sites
ihfA (ihfα)	Integration host factor (IHF) alpha subunit	multiple
ihfB (hipB)	Integration host factor (IHF) beta subunit	multiple
rsmY	non-coding RNA	multiple
rsmZ	non-coding RNA	multiple
lpg1967 (psrA)	Transcriptional regulator, TetR family	multiple
rpoS	Stationary phase specific sigma factor, RpoS	multiple
oxyR(oxyR2)	hydrogen peroxide-inducible genes activator, OxyR	multiple
flaA (fliC)	flagellin	multiple
icmR	Component of Dot/Icm secretion system. Chaperone for IcmQ	multiple
icmT	Component of the Dot/Icm secretion system	multiple
icmV	Component of the Dot/Icm secretion system	multiple
icmW	Component of the Dot/Icm secretion system	multiple
dotA	Component of the Dot/Icm secretion system	multiple
dotD	Component of the Dot/Icm secretion system	multiple

lpg1967* (*psrA)

(-884)PF 5'

GTTCACTTGCAAATACCACTACGTTTTCCTCAACGAGGCTGGCTATGGTATTGAGAATGTCCTTTATCATT

TAATACTCTCTTACTCAATAGAATGGGCTTTGATTG……GAGCAGTCC

ACCACCTACTTCTATTTAGATAAACAAGTGTTATTTTAATTTGATATAGAAAACTATAAAAAGCTTGACAA

(+14)PR 5'

TCTATCTATGAATAGGTAGAATTTATGCCT**ATGAATATAAGTAA**TACGAAAGAACGGATATTAGCAGTT

GCGGAAGCATTGATCCAAAAAGACGGATATAACGCCTTTAGTTTCAAAGATATTGCAACAGCCATCAA

TATTAAAACTGCCAGCATCCATTATCATTTTCCTTCAAAAGAAGATCTTGGGTTGCCGTTATATCCTGGC

ATACCGATAAAATTGCTGCTGTGCTATCTGACATAAGCAATAATTCGTCGTTATCAGCCAAGGAAAAA

ATTCAAAAATTCTTTGATGCCATTTTAACACTCACCTACAACTCTGAAAACAAAATGTGCCTCGGCGGT

ATGTTCGCCTCTGATTTTCAATCATTACCCGTTTCAATTCAAAATCAGGCAAAAAAATTTTTTGAGCTTA

TCATCGAATGGCTTAAAGGAGTTCTTGAAACAAATGGATATGATAACGAATCCTCATTATCTCTTGCAA

AACAAATTATTTCATTGGTTGAAGGCGGATTATTATTAGCAAGATTATATGGAGATGAAACGTTCCTG

PF 3' (-9 from the stop codon (TGA))

GAAGGAGTTCGGCATTTTATTGATCAAAC**AATAAAGTGA**TTTTTTTTAACACCACAAACTATCTATCAGT

AGGTAGATTTTATGGGGAAATTTT……AACCAACATATGATCAATCAGGTAT

PR 3' (+904

TTATTGCTAGTTACACATATTGACCCACCTGGTAACTCCTGTGACTGGATCAGTAACCTT**TGATACAGGA**

from the stop codon (TGA))

CATGCTGTAAAC

Figure 3.2: Primer design and the in-frame *psrA* deletion strategy. *psrA* 5' forward and reverse primers were designed with SalI and BamHI, respectively. *psrA* 3' forward and reverse primers were designed with BamHI and SacI, respectively. The reasoning behind designing primers this way was to remove the gene completely while leaving behind few base pairs from the coding sequence so that the transcription of the neighbouring genes are not affected. Highlighted regions represent the primer sequences and the *psrA* coding sequence is shown in red.

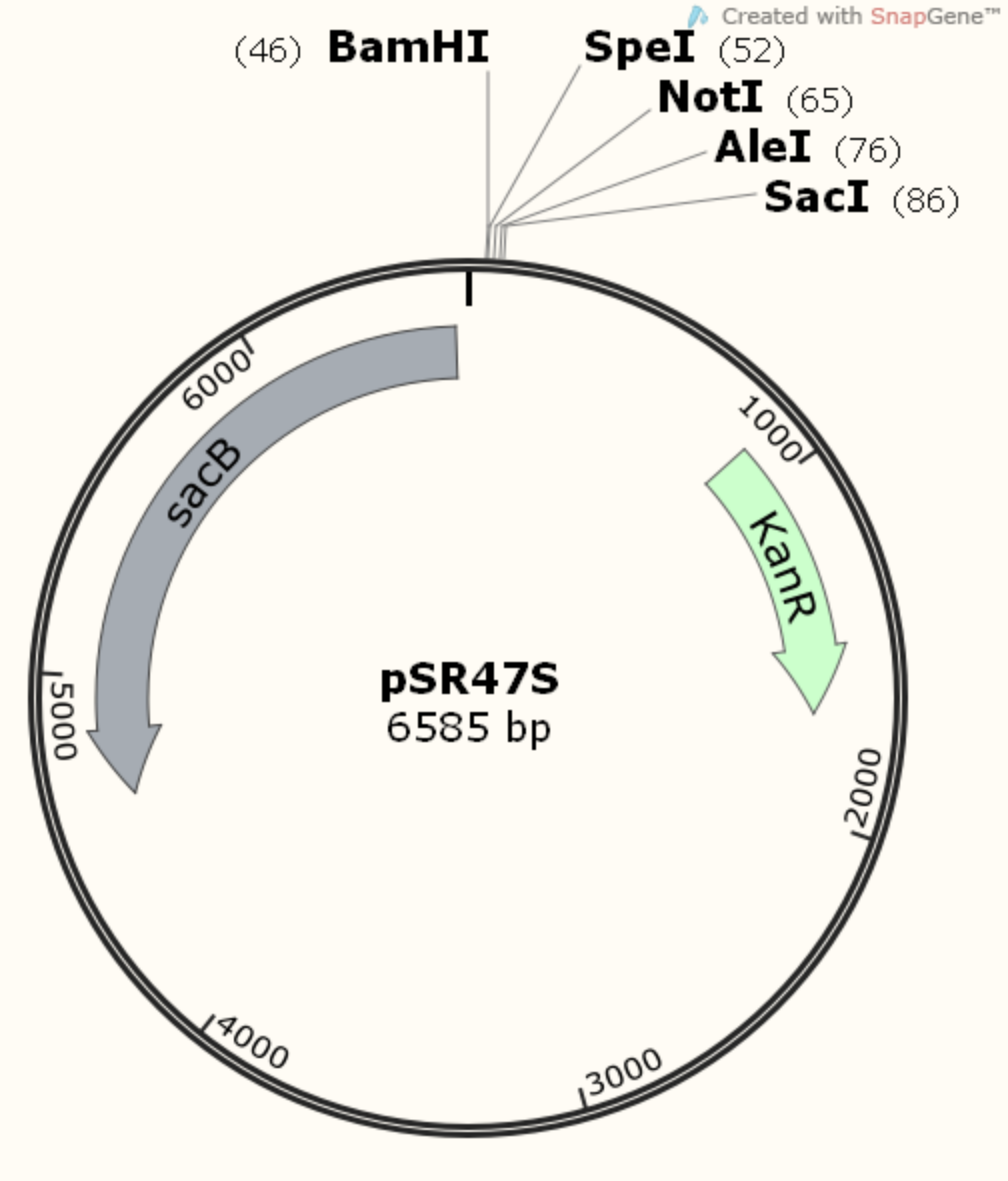

Figure 3.3: Genetic map of pSR47S suicide vector

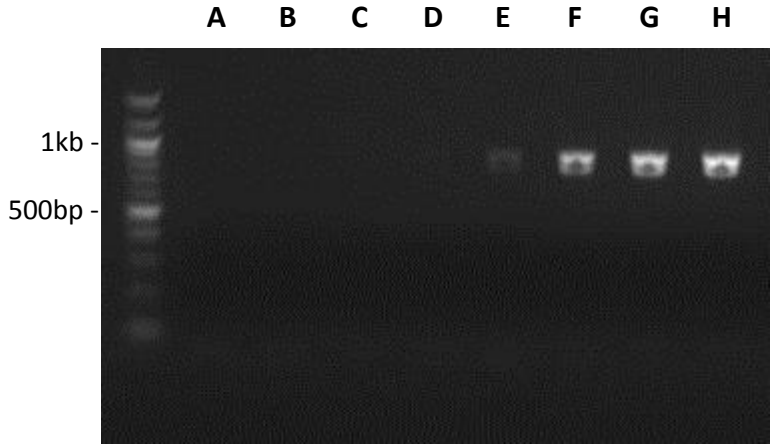

Figure 3.4: Gradient PCR of 3' *psrA*. 5µL of the PCR reactions were loaded on 1% agarose gel with 100bp DNA ladder and the gel electrophoresis was performed for 30 min at 100V. Letters A through H refer to specific temperature (A: 70°C, B: 68.5°C, C: 66.0°C, D: 62.2°C, E: 57°C, F: 53.5°C, G: 51.5°C, H: 50°C).

was verified by the presence of the expected size of a 911bp amplicon (Figure 3.5). The sample was cleaned up using the Qiagen Gel Extraction kit and was then digested with SalI and BamHI restriction enzymes (Table 2.4). The suicide vector pSR47S vector was miniprepped and was digested in a similar manner as the amplicon with SalI and BamHI restriction enzymes (Table 2.4). Unlike the amplicon, the digested pSR47S was further treated with calf-alkaline phosphatase (CIP) to prevent the re-ligation of the linearized vector. Both the digested vector and the *psrA* 3' insert were cleaned up with Qiagen Gel Extraction kit and the fragments ligated together to generate the pSR47S::psrA 3' construct for transformation into the competent *E. coli* DH5αλpir cells.

The transformed cells were screened for the pSR47S::psrA 3' construct using the *psrA* 3' primer set in multi-colony or single-colony PCR (see Materials and Methods). Figure 3.6 represents a typical colony PCR screening results on an agarose gel. Since colony#2 had a nice bright band with the expected size of 911bp, freezer stocks of this colony were made for future use and overnight cultures were also prepared for further cloning steps (Figure 3.6). The plasmid was extracted using the QIAprep Spin Miniprep Kit and the pSR47S::psrA 3' construct was verified again by PCR (see Methods and Materials).

Once the 3' flanking region of *psrA* was confirmed to be ligated into the pSR47S vector, similar steps were taken to insert the 5' flanking region in the pSR47S::psrA 3' construct. Annealing temperature was determined to be 53.9^0C through a gradient PCR for the *psrA* 5' primer set. The 5' flanking region was amplified using Q5® high fidelity polymerase after which the amplicon was digested with BamHI and SacI restriction enzymes. The pSR47S::psrA 3' construct was also digested with BamHI and SacI restriction

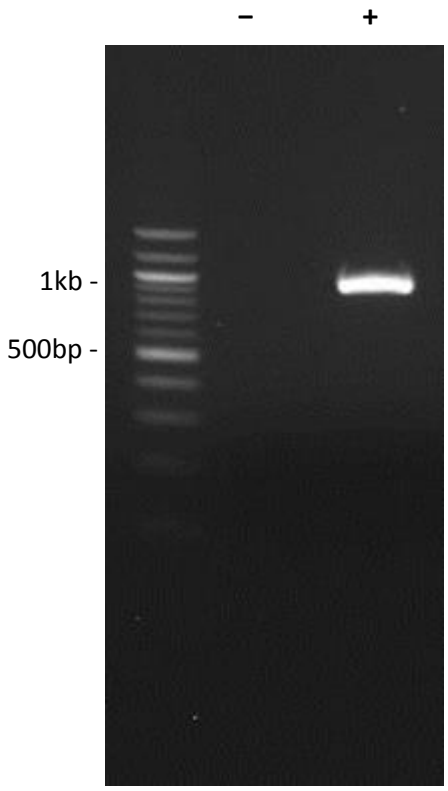

Figure 3.5: *psrA* 3' Q5® PCR. 5µL of the PCR reactions were loaded on 1% agarose gel with 100bp DNA ladder and the gel electrophoresis was performed for 30 min at 100V. Sign – and + represent negative control and the sample, respectively. Approximate size of *psrA* 3' flanking region is 911bp.

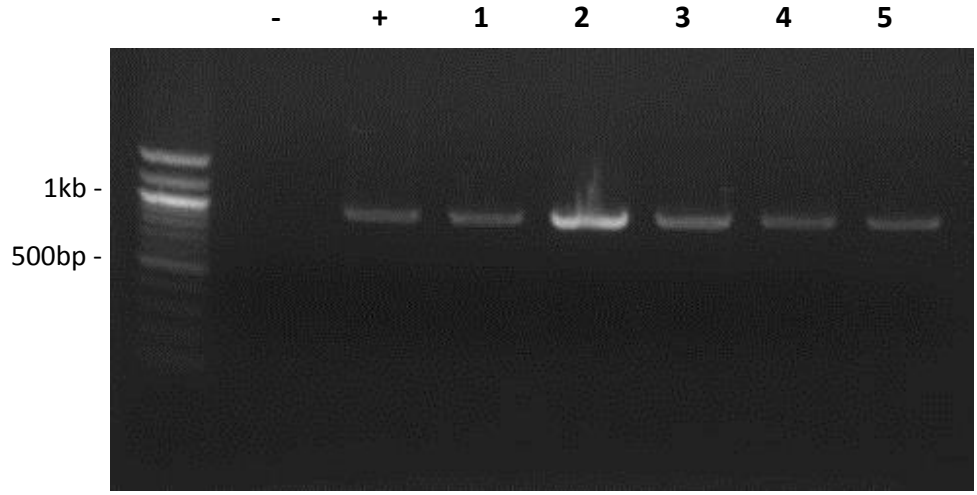

Figure 3.6: *psrA* 3' colony PCR. 5µL of the PCR reactions were loaded on 1% agarose gel with 100bp DNA ladder and the gel electrophoresis was performed for 30 min at 100V. Sign – and + represent negative control and positive controls. Numbers represent potential colonies.

enzymes. Both the digested vector and 5' fragments were ligated, transformed into the competent *E. coli* DH5αλpir cells and colony screen PCR was performed to identify the pSR47S::psrA 3'&5' construct. The final construct was miniprepped and verified by PCR and sequencing using the psrA sequencing primers (Figure 3.7 and Table 2.3).

3.2.2 Δ*psrA* knockout generation in *L. pneumophila*

The pSR47S::psrA 3'&5' plasmid construct was electroporated into electrocompetent *L. pneumophila* Lp02 cells and plated for kanamycin resistance (see Methods and Materials). After several rounds of selecting for kanamycin resistance and counter selecting for sucrose sensitivity, the potential Δ*psrA* knockout colonies were subjected to the colony PCR using the psrA int primer set (Table 2.3; see Methods and Materials) to detect the lack of *psrA* gene. The selected colonies were cultured and genome extraction was performed. Internal primers were designed to amplify the coding sequence of *psrA* and representative results are shown in Figure 3.8. As expected for a potential Δ*psrA* knockout colony, no amplification was resulted from this PCR confirming the absence of the coding sequence. For further verification of the Δ*psrA* knockout colony, 5' and 3' flanking primers were used to amplify the whole flanking region and coding region of *psrA.* A difference of about 600bp was observed in the mutant genome in comparison to the wild type Lp02 genome indicating the absence of the *psrA* gene (Figure 3.8). Thus, these data show that the coding region of *psrA* was successfully deleted and just to further verify the genotype of the mutant strain, the flanking regions were sequenced using the psrA sequencing primers (Table 2.3).

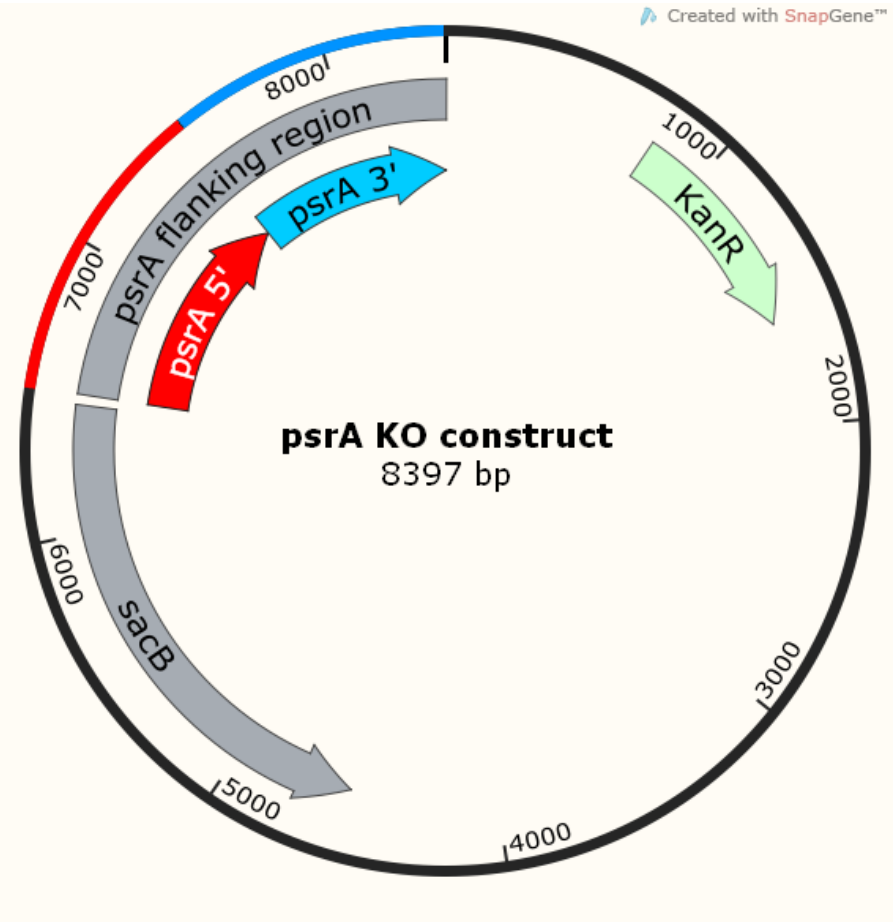

Figure 3.7: Genetic map of psrA knockout plasmid.

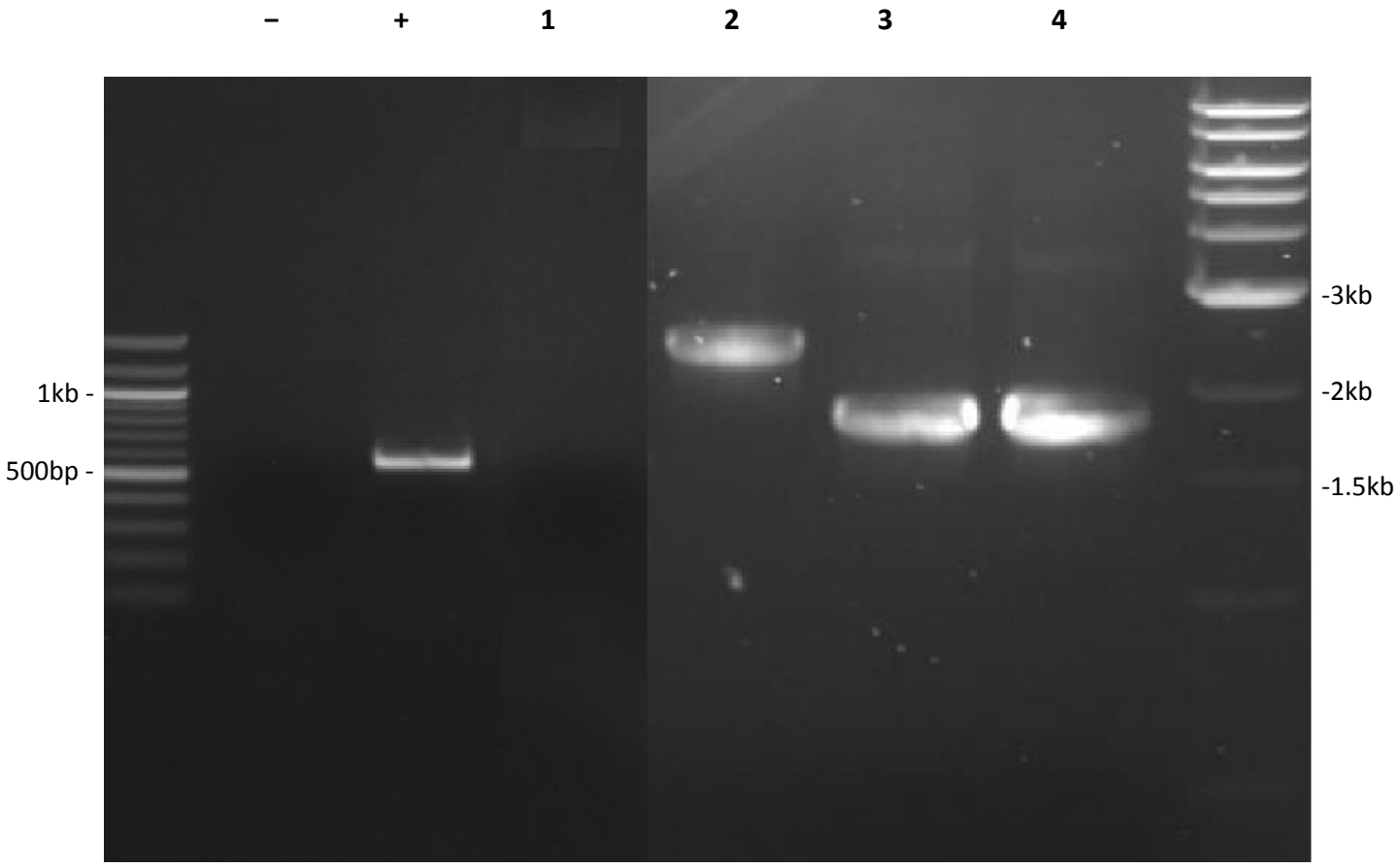

Figure 3.8: ***ΔpsrA* in-frame deletion verification by PCR.** PCR was performed on the *ΔpsrA* genome using psrA int and psrA flanking primer sets. Sign – and + represent negative control and positive control, respectively. Following samples represent different PCR conditions: 1- internal psrA primer set on *ΔpsrA* genome, 2- Flanking primers on Lp02 genome (positive control), 3&4- flanking primers with *ΔpsrA* genome. Samples were loaded on 1% agarose gel with 100bp DNA ladder and the gel electrophoresis was performed for 30 min at 100V.

3.2.3 Δ*psrA* complement plasmid construction

For the complement studies, pJB908 vector (Figure 3.9) was used to clone in *psrA* gene with its native promoter. The optimum annealing temperature of the psrA complement primer set (Table 2.3) was determined to be 53.9^0C through a gradient PCR. The *psrA* gene with its promoter region was amplified using Q5® high fidelity polymerase and cloned between SacI and KpnI restriction sites of the pJB908. The colonies carrying the pJB908::psrA plasmid were screened using the psrA complement primer set and the plasmid from selected colony was verified by sequencing.

3.2.4 Growth kinetic studies

To determine if the Δ*psrA* mutant had any growth defects *in vitro,* a growth kinetic assay was performed in a 96-well plate for 24hrs at 37^0C with Lp02, Δ*psrA* mutant and Δ*psrA* complement strains. The assay results showed that all three strains demonstrated comparable growth kinetics (Figure 3.10). Moreover, growth kinetics were also useful in identifying different growth phases with the post exponential phase starting at 14hr time point (Figure 3.10).

3.3 PsrA protein purification

To evaluate the protein-DNA interaction, PsrA was cloned into pET16b vector for recombinant protein expression. PsrA was tagged with 10 histidine residues at the N-terminus and was purified using the nickel-charged gravity column (see Methods and Materials). The eluted sample was run on 12% SDS-PAGE and stained with Coomassie blue after which no other non-specific bands or contaminations were observed suggesting a

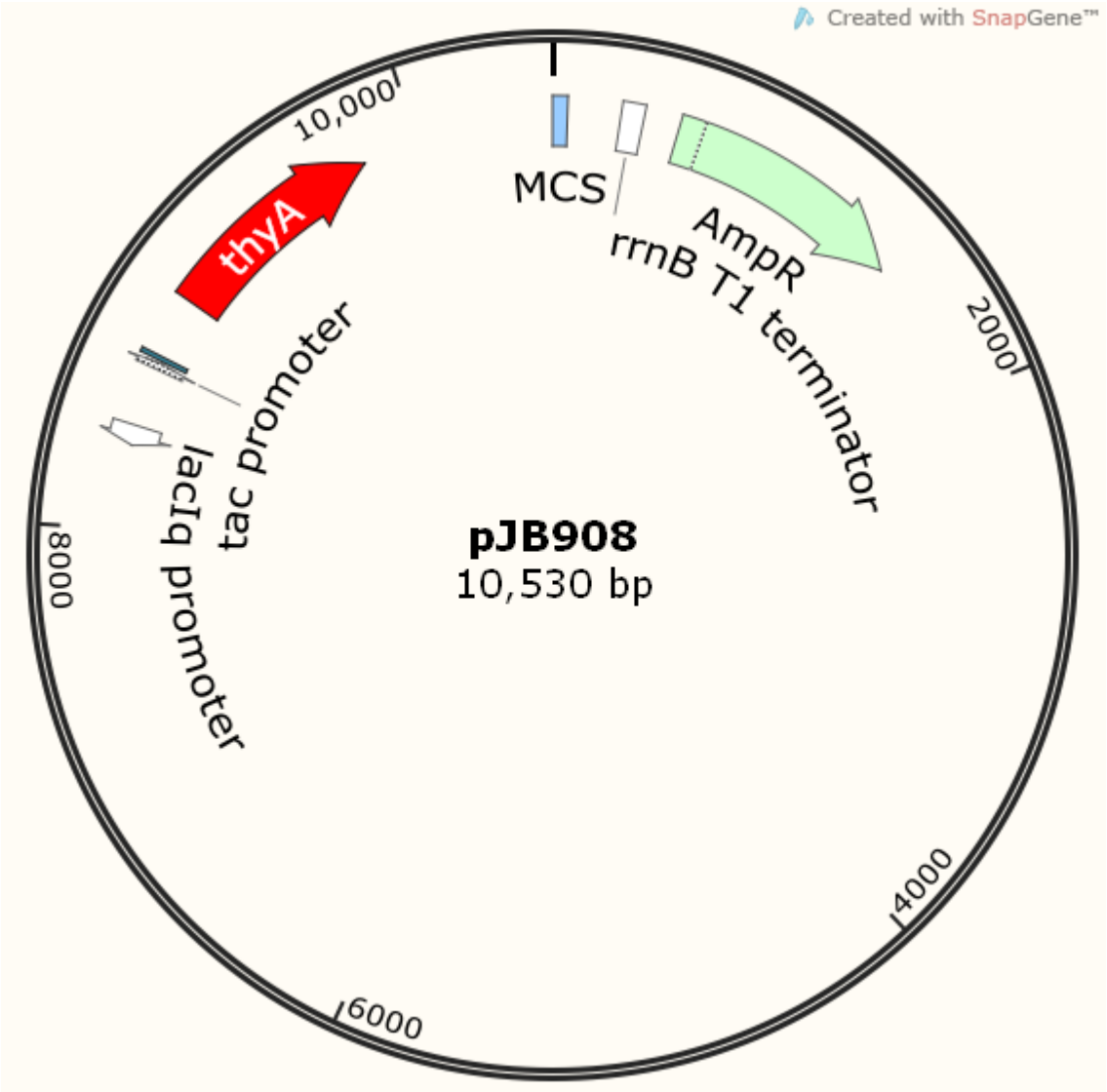

Figure 3.9: Plasmid map of pJB908 vector which was used to construct complement strains

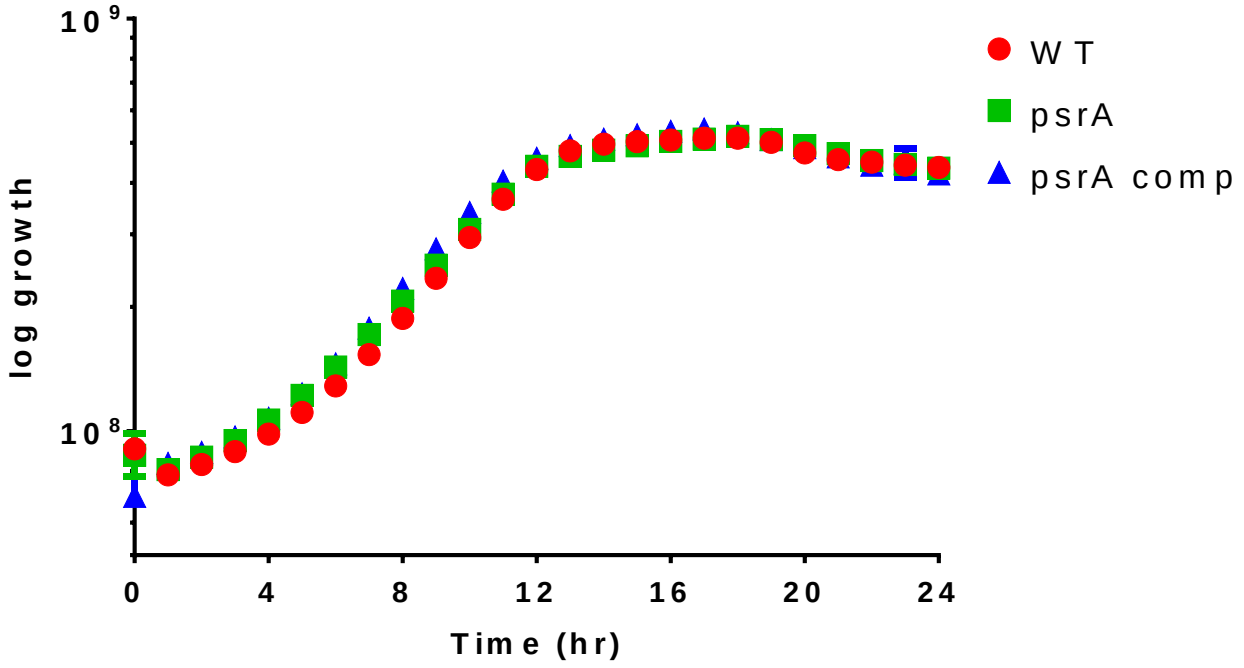

Figure 3.10: **Growth kinetics comparison of Lp02 (WT) and *ΔpsrA* mutant strains.** Growth kinetics was performed in 96-well plates for 24hrs. Data represents an average from three independent experiments and SEM are shown in error bars.

high purity level of the eluted PsrA (Figure 3.11). The use of protease inhibitor cocktail and HiTrap™ Heparin HP column was considered as an extra step to ensure the purity of the protein. Finally, the protein was concentrated and filtered using an Amicon® Ultra 10K Centrifugal filter units. During the purification process several samples were taken to evaluate potential contaminations (i.e. additional proteins that were inadvertently co-purified) and an SDS-PAGE was performed to visualize the protein bands after staining (Figure 3.12). As shown, no contaminants (non-specific bands) were found in the concentrated protein stock which was determined to be 10.59μg/μL (481μM).

3.4 PsrA involvement in non-coding RsmY & RsmZ and IHF regulation

3.4.1 PsrA and RsmY/Z interaction

3.4.1.1 GFP expression profiles of RsmZ in Lp02, and Δ*psrA*

Recently, it was reported that LetA and LpIHF are both required for the expression of the non-coding RNAs, RsmY and RsmZ (Pitre *et al.*, 2013). However, the promoter activity assessment via GFP reporter assays indicated the presence of an additional but unidentified regulator responsible for the basal expression of these non-coding RNAs. This unknown protein was hypothesised to be PsrA and several GFP reporter assays were performed in different strain backgrounds to evaluate this possibility.

For the GFP reporter assay, the pBH6119 promoterless vector (Figure 2.1) was used. Truncated promoter regions upstream of RsmZ and RsmY were cloned into pBH6119 (Table 2.2). A schematic of the truncated promoter GFP constructs is shown in Figure 3.13. The Z1 construct contains a 316bp region of the RsmZ promoter region which was

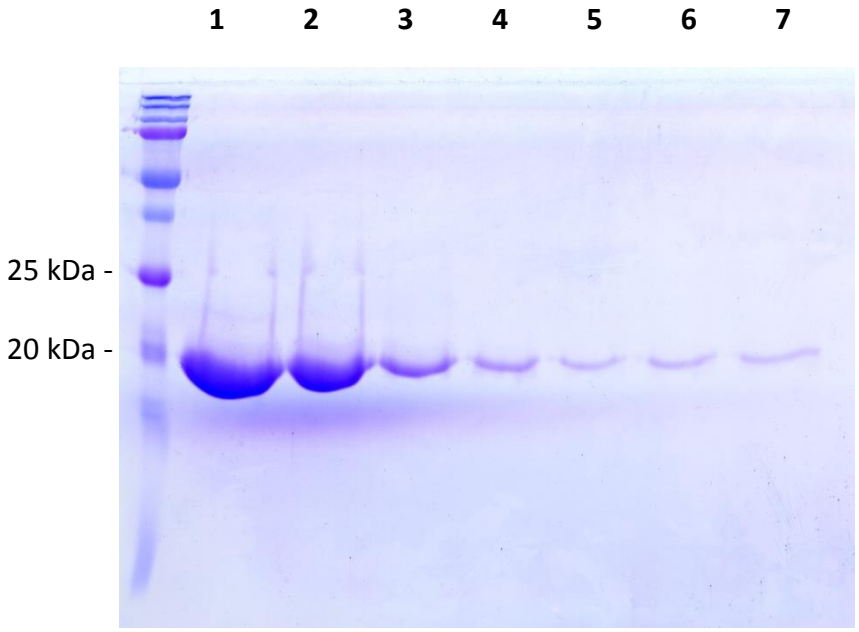

Figure 3.11: **Eluted fractions from nickel-charged gravity column.** Protein samples were eluted from the nickel-charged gravity column in the elution buffer. 5µL of samples was run on the 12% gel and was stained with Coomassie blue stain. Lanes 1-7 represent different protein fractions eluted from the column. Approximate size of PsrA is 20 kDa.

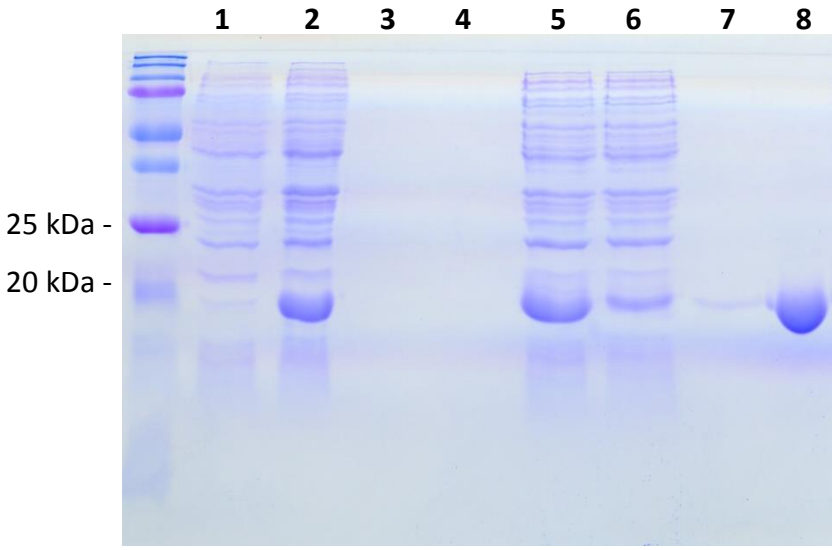

Figure 3.12: Assessment of the Protein purification procedure. Samples were taken during the protein purification to track down any potential artifact or contamination. 5µL of samples was run on the 12% gel and was stained with Coomassie blue stain. Samples were loaded in following order: 1:pre-induction, 2: post-induction, 3&4: supernatant resulting from pelleted induced cells, 5: soluble fraction of French pressed cells post centrifugation, 6: discarded flow through from the gravity column, 7: wash samples from the gravity column, 8: final purified and concentrated PsrA product.

considered to be the full length promoter region (Figure 3.13A). The Z2 and Z3 constructs were truncated from 5' end of the full length promoter and each contained 268 and 172bp in size, respectively (Figure 3.13A). As mentioned previously, the growth kinetics generated in 96-well plates were also useful in determining the different growth phases of the *L. pneumophila* growth cycle.

3.4.1.1.1 GFP expression profiles of RsmZ in Lp02

All three RsmZ GFP reporter plasmid constructs were electroporated in Lp02, Δ*ihf,* Δ*letA* and Δ*psrA* mutant strains. The activities of the truncated promoter regions were measured and represented as normalised fluorescent values (see Methods and Materials) over time. In Lp02 wildtype, exponential growth started at 8 hour time point, whereas the post-exponential growth phase was initiated at 18 hour time point. The GFP expression from the Z1 construct (carrying full length promoter) appeared at very high levels in first few hours (lag phase) with a steady decline in the RFU/OD_{600} units as the cells started to transition to the exponential growth phase (Figure 3.14A). During the post exponential phase, the GFP expression went back up and this trend was expected as it was documented in other research studies (Figure 3.14A) (Sahr *et al.*, 2009; Pitre *et al.*, 2013). Similar GFP expression patterns were also observed for the Z2 construct in the Lp02 background with RFU/OD_{600} values starting from 1000 during the first few hours. The Z2 graph greatly resembled the Z1 graph except the Z2 graph was shifted downwards by about 750 RFU/OD_{600} units (Figure 3.14A). The difference in the GFP expression between Z1 and Z2 constructs is believed to be a result of additional unknown regulatory controls. The fluorescent levels from the Z3 construct were very low as expected since most of the

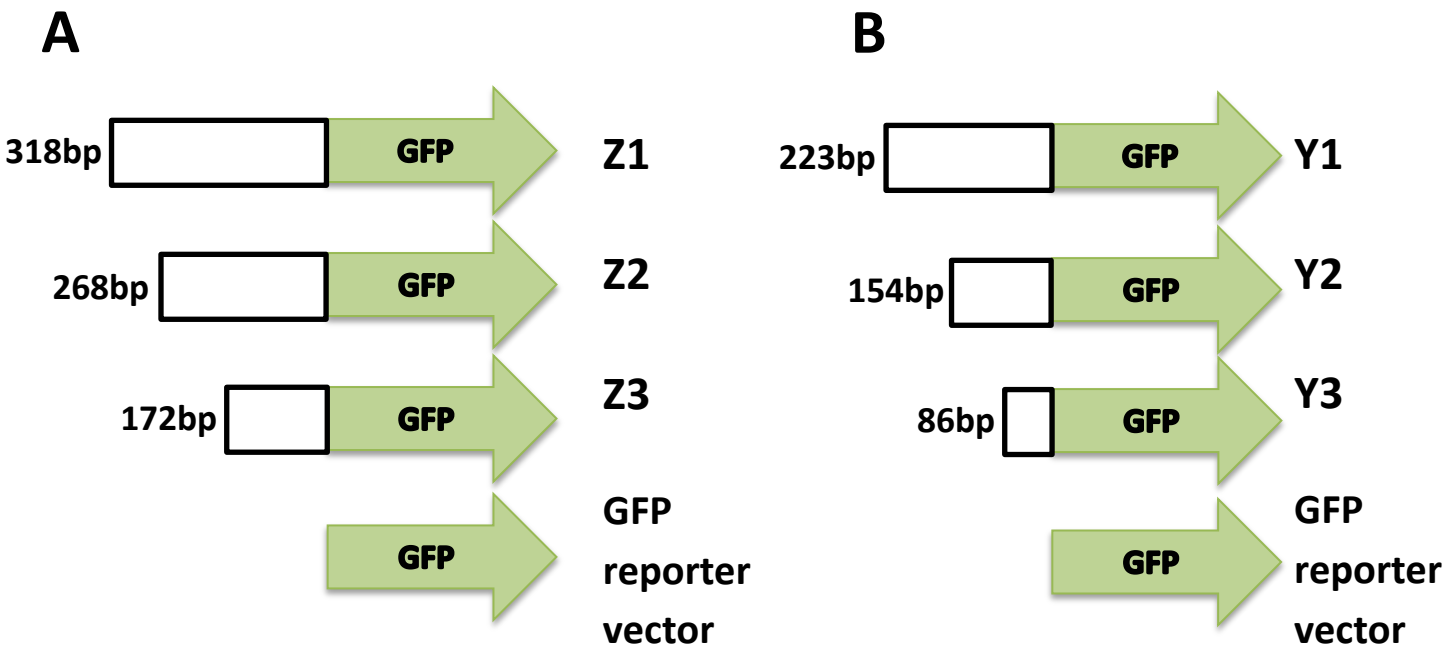

Figure 3.13: RsmZ (A) and RsmY (B) GFP constructs design. Truncated promoter regions of RsmZ and RsmY non coding RNAs were cloned into BamHI/XbaI sites of pBH6119. Figures adapted from Pitre, Tanner, Patel, & Brassinga, 2013.

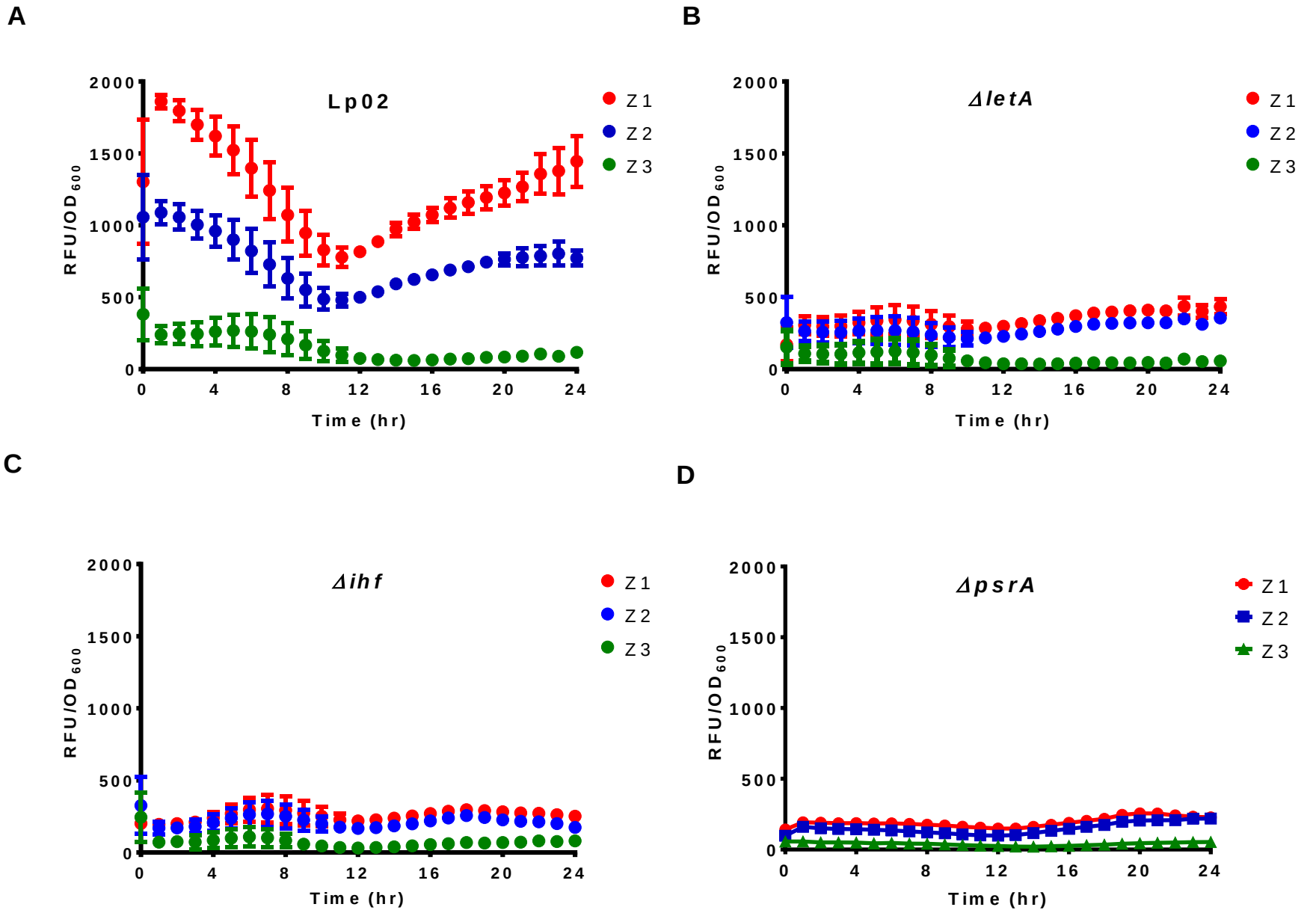

Figure 3.14: **Expression profiles of RsmZ promoter GFP reporter constructs**. Fluorescence was detected from the RsmZ GFP reporter constructs on an hourly basis for 24 hours in Lp02 (WT) (A), *ΔletA* (B), *Δihf* (C), and *ΔpsrA* (D) strain backgrounds. Normalised RFU/OD_{600} units were plotted and the error bars represents SEM. Data represents an average from three independent experiments. Panels A-C adapted from (Pitre *et al.*, 2013).

promoter region was truncated. It is noted that during the lag growth phase, a slight peak in expression was observed suggesting the presence of a few regulatory sites within the Z3 promoter region.

3.4.1.1.2 GFP expression profiles of RsmZ in Δ*letA*

Since LetA has been recently identified to regulate the RsmZ expression (Sahr *et al.*, 2009), the Δ*letA* mutant strain was used in the GFP reporter assay as a control. As expected, GFP expression from the Z1 construct was significantly lower in comparison to levels observed in the Lp02 strain background. Interestingly the Z2 construct had very similar fluorescent expression profile to that of Z1 (Figure 3.14B). Moreover, during the first 8 hours a minor peak in the GFP expression was observed and a slight elevation in the RFU/OD_{600} units was also detected at post-exponential growth phase (Figure 3.14B). The expression profile of the Z3 construct was unaltered from the expression profile for Z2; however, during the first 8 hours the values were lower but the overall pattern with a minor peak was distinct. The overall conclusion is that LetA is an essential positive regulator of RsmZ correlating with similar findings in other studies (Figure 3.14B) (Sahr *et al.*, 2009; Pitre *et al.*, 2013). Thus, deletion of LetA protein is enough to reduce the majority but not all of the RsmZ expression from all three constructs.

3.4.1.1.3 GFP expression profiles of RsmZ in Δ*ihf*

The GFP expression profiles of RsmZ truncated promoter constructs in the Δ*ihf* mutant strain background were obtained in a similar manner as above. All three RsmZ truncated promoter constructs had very similar expression profiles to the expression

profiles achieved in the Δ*letA* mutant strain background (Figure 3.14C)(Pitre *et al.*, 2013). Like in the mutant strain background, the fluorescent levels were at basal levels indicating that LpIHF may be another essential positive regulator of RsmZ (Figure 3.14C). Thus, deletion of LpIHF is sufficient to bring the RsmZ expression down to basal levels.

3.4.1.1.4 GFP expression profiles of RsmZ in Δ*psrA*

As mentioned earlier, PsrA directly regulates the expression of the RsmZ in *Pseudomonas* species and it was hypothesized that PsrA could be responsible for the basal level expression in *L. pneumophila*. To this end, the three RsmZ truncated promoter GFP reporter constructs were electroporated into the Δ*psrA* mutant strain to assess the GFP expression profile. Interestingly, the promoter activity for Z1 and Z2 promoter constructs was much more reduced in comparison to levels observed in the Δ*ihf* and Δ*letA* strain backgrounds. Notably, the slight elevation during the first 8 hours in the Δ*ihf* and Δ*letA* strain backgrounds was absent in the Δ*psrA* strain background (Figure 3.14D). The expression profile from the Z3 construct barely showed activity unlike in the Lp02, Δ*ihf* and Δ*letA* strain backgrounds suggesting that PsrA has some regulatory control in the Z3 promoter region (Figure 3.14D). Thus, it appears that PsrA is another positive regulator of RsmZ since its deletion abolishes the majority of RsmZ expression.

Thus, these GFP reporter assays showed that IHF, LetA and PsrA are all required for RsmZ expression and absence of any of these proteins results in a severe decrease in RsmZ expressions.

3.4.1.2 GFP expression profiles of RsmY in Lp02, and Δ*psrA*

As mentioned earlier, in *Pseudomonas* species, PsPsrA regulates the RsmZ expression but not RsmY. However, initial bioinformatics pattern search revealed 3 binding sites for PsPsrA in the RsmY promoter region (Table 3.2). So to determine if PsrA has a role in the regulation of RsmY, the Y1, Y2 and Y3 truncated promoter GFP reporter constructs (Table 2.2 and Figure 3.13B) (Pitre *et al.*, 2013) were electroporated into the Δ*psrA* mutant strain. These GFP constructs have been used in a previous study to examine the RsmY promoter activity and these same three constructs were used in this study.

As previously shown, in the Lp02 strain background, full length promoter Y1 construct showed high GFP expression during the lag growth phase (Figure 3.15A) (Pitre *et al.*, 2013). However, a steady decline in the levels was noticeable when bacterial cells transitioned into the exponential growth phase. The levels increased once more when the cells transitioned into the post-exponential growth phase (Figure 3.15A). The GFP expression profile of the Y1 promoter construct was very similar to the profile of the Z1 promoter construct but with lower fluorescence values. The GFP expression profile of the Y2 promoter construct, truncated by 69bp from the 5' end, was compared to that of the Y1 promoter construct in the Lp02 strain background (Figure 3.15A). Surprisingly, the fluorescence expression from the Y2 promoter construct was completely abolished suggesting that the regulatory controls lie within the -223 to -154 promoter region. The Y3 promoter construct also had the similar expression profile as that of the Y2 promoter construct (Figure 3.15A).

In the Δ*psrA* mutant strain, the loss of GFP expression was observed from the Y1 promoter construct indicating that PsrA is essential for the RsmY expression. Similar

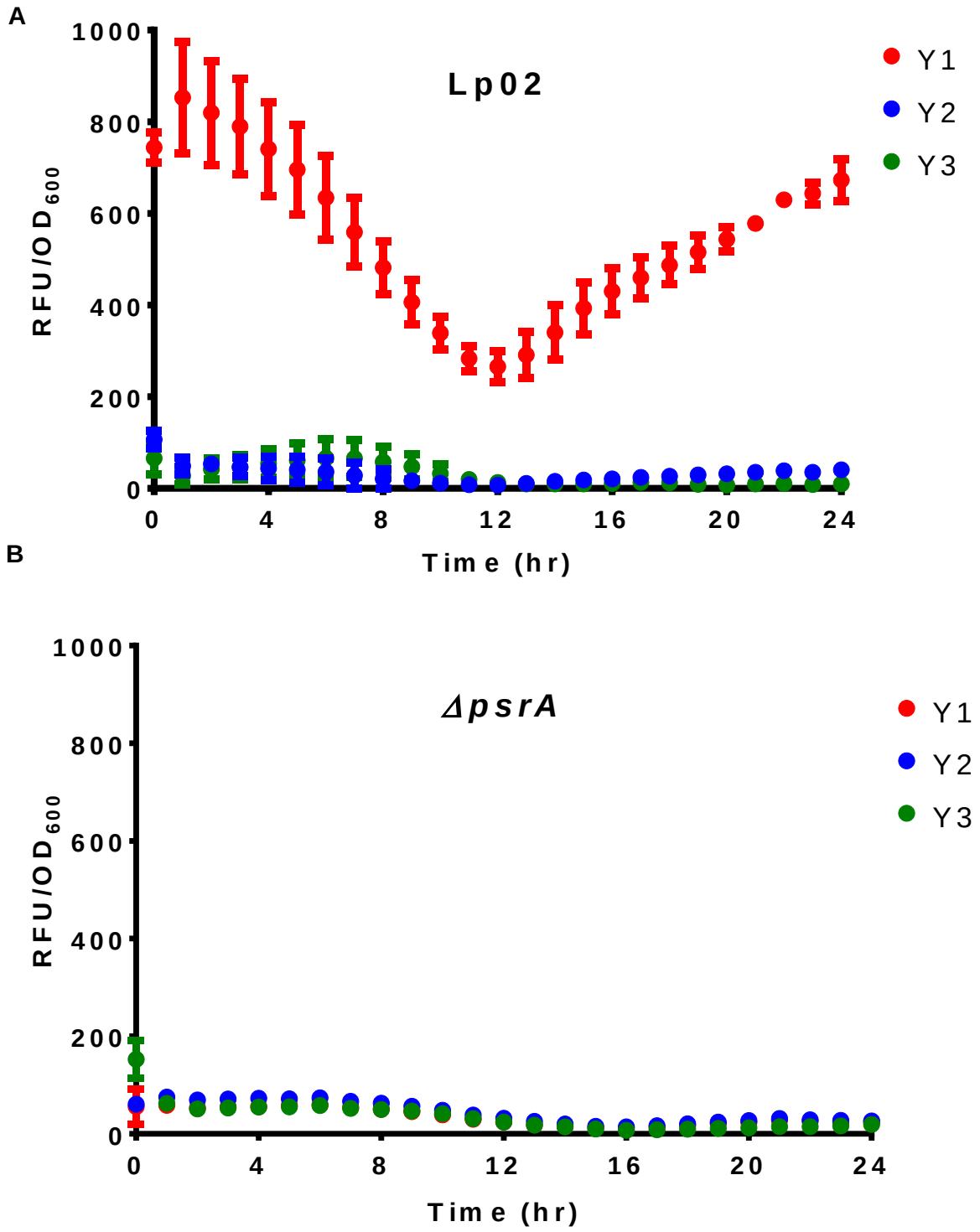

Figure 3.15: **Expression profiles of RsmY promoter GFP reporter constructs**. Fluorescence was detected from the RsmY GFP reporter constructs on an hourly basis for 24 hours in Lp02 (WT) (A), and *ΔpsrA* (B) strain backgrounds. Normalised RFU/OD_{600} units were plotted and the error bars represents SEM. Data is representative of one experiment. Data represents an average from three independent experiments. Figure A made by Chantelle A. Pitre. Figures adapted from (Pitre *et al.*, 2013).

profiles were seen from the Y2 and Y3 promoter constructs with no significant differences in the expression values like in the Lp02 strain background (Figure 3.15B). These results suggest that the binding site of PsrA resides in first 69bp at the 5' end of the Z1 promoter region and loss of this protein results in drastically reduced expression of this non-coding RNA.

3.4.1.3 EMSAs

Electrophoretic mobility shift assays (EMSAs) were performed to determine whether the regulation of RsmZ and RsmY by PsrA was direct or indirect (see Methods and Materials). EMSAs were done using the radiolabelled full-length promoter regions (probes) of RsmZ and RsmY. If PsrA binds to the promoter region, then it will form a DNA/protein complex which will migrate slower than free DNA on a non-denaturing gel, producing a shift in band sizes. The purified recombinant PsrA protein was used in a gradient of concentrations to evaluate its affinity for the RsmZ and RsmY probes. Different sizes of the band shifts resulted indicating that PsrA binds directly to both RsmZ and RsmY promoter regions (Figure 3.16). Moreover, it was found that 11.4μM PsrA is sufficient to fully shift the radiolabelled RsmZ and RsmY probes. However, at higher protein concentrations (>20 μM), larger shifts were produced indicating the possibility of PsrA binding to more than one site in the RsmY and RsmZ promoter regions as evidenced by the formation of larger DNA/protein complexes (Figure 3.16).

Thus, PsrA protein appears binds to the promoter regions of RsmY and RsmZ directly and therefore, positively regulates the expression of RsmY and RsmZ (Figures 3.14, 3.15 and 3.16). To further validate these interactions, co-competing DNA was used in EMSA

A) RsmZ

PsrA (µM)	0	9.1	11.4	15.9	34	45	15
Specific Comp.	-	-	-	-	-	-	+

B) RsmY

0	9.1	11.4	15.9	34	45	15
-	-	-	-	-	-	+

Figure 3.16: **Radiolabelled Electromobility shift assay was performed with RsmZ (A) and RsmY (B) full length promoter region**. Gradient of PsrA concentration was used as indicated above with approximately 1000 cpm of RsmZ probe and the samples were ran on a 6% TBE acrylamide gel in 0.5x TBE buffer. The bands were visualised using the Molecular Imager PharosFX™ Plus system.

studies where non-labelled RsmZ and RsmY promoter regions were included in the same reaction with radiolabelled RsmZ and RsmY probes. If the interaction is specific, the non-labelled promoter regions will out-compete the radiolabelled probes for PsrA binding. As shown in Figure 3.16, the shift was not present when non-labelled RsmZ and RsmY promoter regions were used to compete with the respective radiolabelled probes.

3.4.1.4 DNaseI footprint studies

To precisely determine the PsrA binding site within the RsmZ promoter region, the antisense strand was radiolabelled with ^{32}P. Approximately 60,000 cpm of this labelled probe was used per reaction (see Methods and Materials). Approximately 10 µg of PsrA protein was added to the binding reaction and the PsrA-bound probe was digested with DNaseI for 90 sec. The digested DNA sample was then extracted and loaded on an 8% polyacrylamide sequencing gel along with a sequencing ladder generated with the PR RsmZ primer via Sequenase™ Quick Denature Plasmid DNA Sequencing Kit. After drying, the gel was then exposed to Carestream® Kodak® BioMax® MS film overnight (see Methods and Materials). After the film development, two separate protected regions were visible indicating possible binding sites of PsrA. The protected region from DNaseI digestion (i.e. footprint) was then aligned with the sequencing ladder and the sequence was read in 5' to 3' direction (Figure 3.17). The sequence was reverse complemented and aligned against the RsmZ promoter sequence available on the Legiolist *L. pneumophila* Philadelphia 1 type strain genome database. The binding region of PsrA after the alignment is shown in Figure 3.18A. The binding site appears to cover the -35 promoter element and the upstream region; thus, it seems that PsrA could facilitate the assembly of other regulatory factors to

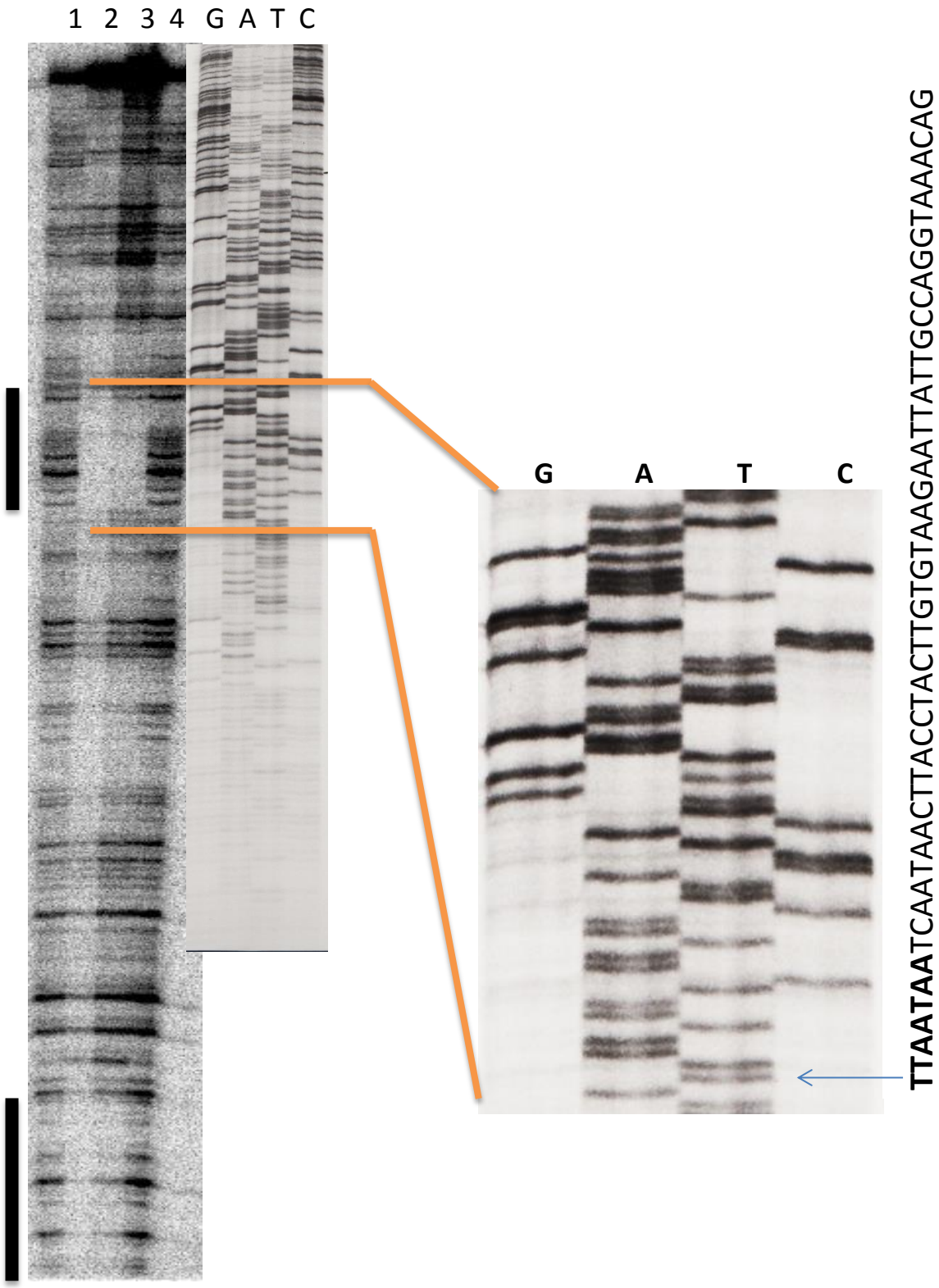

Figure 3.17: **DNaseI footprint analysis of RsmZ promoter region**. Samples resulting from DNaseI digestion of ^{32}P-labelled antisense RsmZ promoter (~60,000 cpm per lane) with no protein (lanes 1&4), 10µg of PsrA (lanes 2&3) are shown with the accompanying sequencing ladder. The samples were run on an 8% TBE acrylamide gel and the protected region from DNaseI digestion is shown in the inset picture with the DNA sequence in the order of G, A, T, C. The bands were visualised using the Molecular Imager PharosFX™ Plus system. Shaded bars indicate PsrA DNA footprints.

A

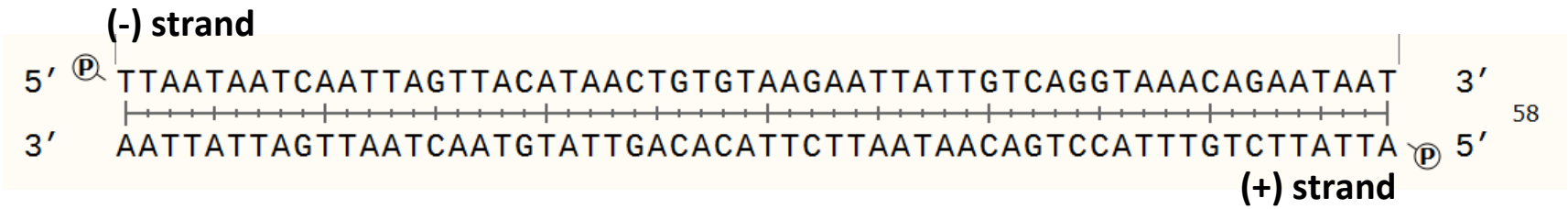

B

ATAAAATGACGTTATTTAAGCTGTAATTGATGTAAGAAATTTCTCAATTCCATAGAAGAAATTATTCTGTT

TACCTGACAATAATTCTTACACAGTT**ATGTAA**CTAATTGATTATTAATAAAATAAA**TATATA**AGGCTATTT

-35 box -10 box

CTGAGTTGAAAATAGTATTGAGTGAAAATGTGATTTAGCACCTTGCGCTTCCCCCATTCAATTGCTAAATT

TTAATCAAGACTTATATGGATA

Figure 3.18: **RsmZ promoter analysis.** A) PsrA binding site on RsmZ promoter after comparative analysis of binding site from Figure 3.17 to the Legiolist genome sequence database. B) The -10 and -35 promoter elements are underlined. The grey region represents the PsrA-bound region from Figure 3.17 and the *rsmZ* coding sequence is shown in red.

initiate the transcription of *rsmZ* (Figure 3.18B). The -10 and -35 promoter elements for the RsmZ promoter region were predicted using the BPROM program (Solovyev V, 2011). As mentioned above, a second protection site was found from the DNaseI footprint experiments; however, the sequencing ladder did not extend enough to align and read the sequence. Interestingly, the PsPsrA consensus binding site (C/GAAACN$_{2-4}$ GTTTG/C) was not present in the promoter region shown in Figure 3.18A suggesting that PsrA could potentially have a very different binding site from PsPsrA.

3.4.2 PsrA and IHF interaction

Recently, LetA and RpoS were characterised as regulators of *ihfA* and *ihfB* genes in *L. pneumophila* (Pitre *et al.*, 2013). According to the GFP expression profiles that detail the promoter activities of *ihfA* and *ihfB* in various strain backgrounds, LetA seemed to be repressing the transcription of the *ihfA and ihfB* genes during the lag and post exponential growth phases (Figure 5.2 and 5.3)(Pitre *et al.*, 2013). In addition, RpoS was found to be essential for *ihfA* and *ihfB* gene expression (Pitre *et al.*, 2013).

3.4.2.1 GFP expression profiles of *ihfA* and *ihfB* in Lp02 and Δ*psrA* strain backgrounds

Bioinformatic analyses showed multiple sites that match the consensus PsPsrA binding site sequence within the promoter regions of *ihfA* and *ihfB* genes. To investigate whether these sites are also recognised by PsrA, the full-length *ihfA* (α1) and *ihfB* (β1) promoter GFP reporter constructs (Table 3.2) (Pitre *et al.*, 2013) were electroporated into Lp02 and *ΔpsrA* mutant strains. These constructs have been described in previous study

(Pitre *et al.*, 2013). The promoter activities via GFP expression profiles were assessed in 96-well plates over a period of 24 hours as described earlier.

3.4.2.1.1 GFP expression profiles of *ihfA* in Lp02 and *ΔpsrA* strain backgrounds

In the Lp02 strain background, the fluorescent levels were initially high for the α1 promoter construct during the lag growth phase which gradually declined during the transition to the exponential growth phase and increased once during the transition to post-exponential growth phase (Figure 3.19A). In the Δ*psrA* mutant strain background, the fluorescent levels dropped three-fold in comparison to those in the Lp02 strain background during the lag growth phase (Figure 3.19A). However, after the transition into the exponential growth phase, the GFP expression profile in the Δ*psrA* strain was very similar to that observed in the Lp02 strain background. During the exponential and post-exponential growth phases, there was an average difference of approximately 200 RFU/OD_{600} units in fluorescent expression in the *ΔpsrA* strain background in comparison to levels observed in the wildtype Lp02 strain background (Figure 3.19A). Thus, these results suggest that PsrA is acting as an activator of *ihfA* and is required for its full expression.

3.4.2.1.2 GFP expression profiles of *ihfB* in Lp02 and Δ*psrA* strain backgrounds

The expression profiles of the β1 promoter construct in Lp02 and Δ*psrA* strain backgrounds were generated in similar manner as for the α1 promoter construct. In the Lp02 strain background; there was no GFP expression present during the first 8 hours representing the lag growth phase. However, the fluorescent levels increased at a steady rate throughout the exponential growth phase with leveling off the values during post-

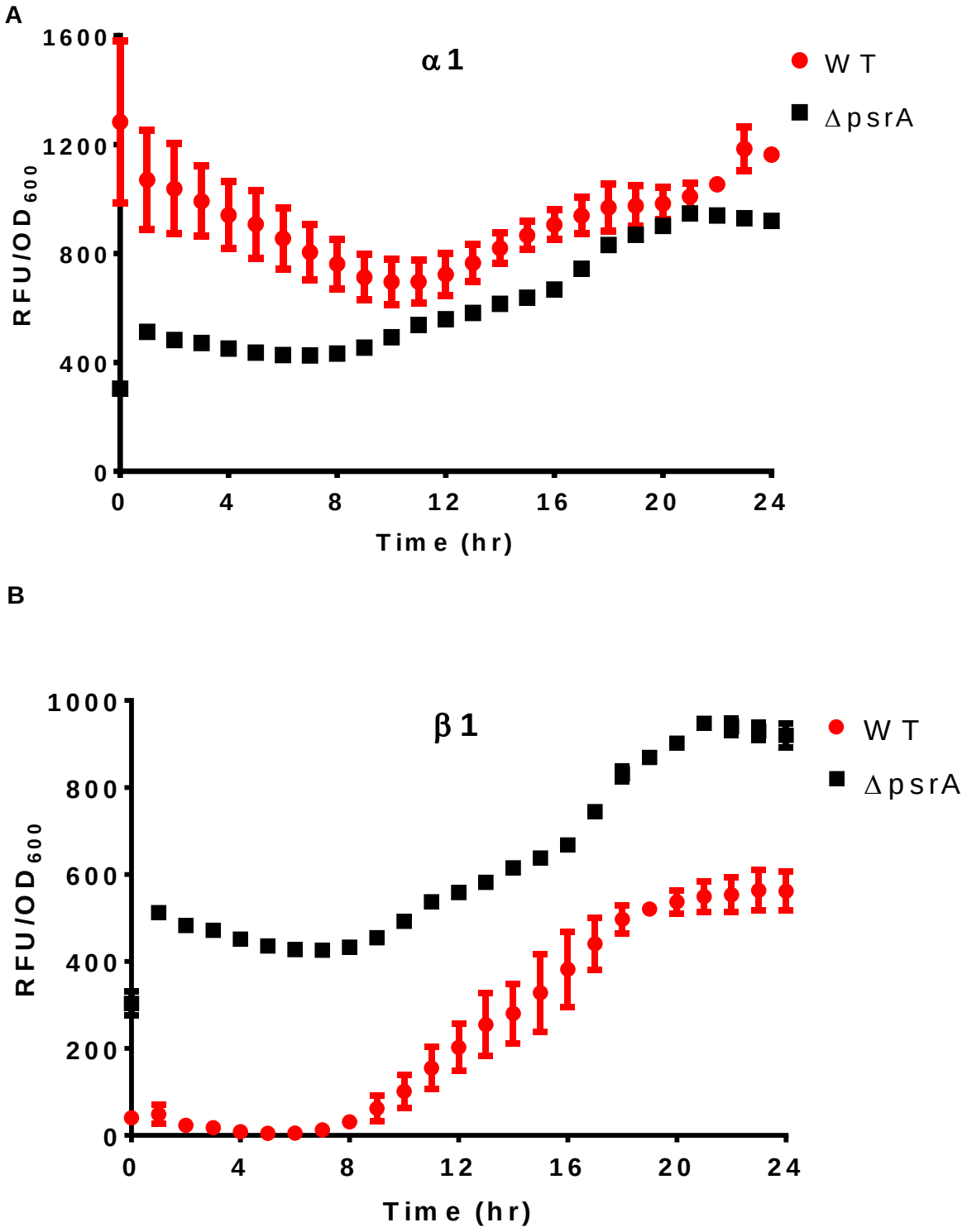

Figure 3.19: **Expression profiles of *ihfA* (α1) and *ihfB* (β1) GFP reporter constructs**. The activity of α1 and β1 GFP promoter constructs carrying full length promoter regions of *ihfA* and *ihfB* genes, respectively, were assessed. Florescence was detected from the α1 (A) and β1 (B) GFP reporter constructs on an hourly basis for 24 hours in Lp02 (WT), and *ΔpsrA* background. Normalised RFU/OD_{600} units were plotted and the error bars represents SEM. Data represents an average from three independent experiments.

exponential growth phase (Figure 3.19B). Thus, it would appear that the *ihfB* promoter is primarily active during exponential and post-exponential growth phases.

In the Δ*psrA* strain background, in contrast to that observed with the α1 promoter construct, the β1 construct demonstrated a similar GFP expression profile but with higher fluorescent levels. The fluorescent levels during the first 8 hours stayed relatively constant at approximately 500 RFU/OD_{600} units in the Δ*psrA* strain background whereas in the Lp02 strain background, there were minimal to no fluorescent levels (Figure 3.19B). In the Δ*psrA* strain background, the fluorescent levels of the β1 construct gradually increased during the exponential growth phase with higher levels detected during the transition to post-exponential growth phase. Overall the GFP expression profile from the Lp02 strain background was elevated by approximately 500 RFU/OD_{600} units in the Δ*psrA* mutant strain background (Figure 3.19B). These results indicate that PsrA is acting as a negative regulator of *ihfB* since the absence of PsrA results in increased expression.

3.4.2.2 EMSAs

To further determine the mode of action regarding the regulation of *ihfA* and *ihfB* by PsrA, EMSA studies were performed. Gradient of PsrA protein concentrations were used in EMSA reactions with several different controls since this is the first evidence of these genes being regulated by PsrA. As shown in Figure 3.20, both radiolabelled (*ihfA* and *ihfB* probes) bound to PsrA and shifted at the concentration of 14 μM. At higher concentrations, higher band shifts were achieved suggesting the presence of multiple PsrA binding sites within *ihfA* and *ihfB* promoter regions. This result correlates with the bioinformatics pattern search results (Table 3.2 and Figure 3.20). Bovine serum albumin (BSA) was also included

A) *ihfA*

PsrA (µM)	0	4.6	9	14	23	32	30	30	30
Specific Comp.	-	-	-	-	-	-	-	-	+
BSA	-	-	-	-	-	-	+	-	-
magA	-	-	-	-	-	-	-	+	-

B) *ihfB*

0	4.6	9	14	23	32	30	30	30
-	-	-	-	-	-	-	-	+
-	-	-	-	-	-	+	-	-
-	-	-	-	-	-	-	+	-

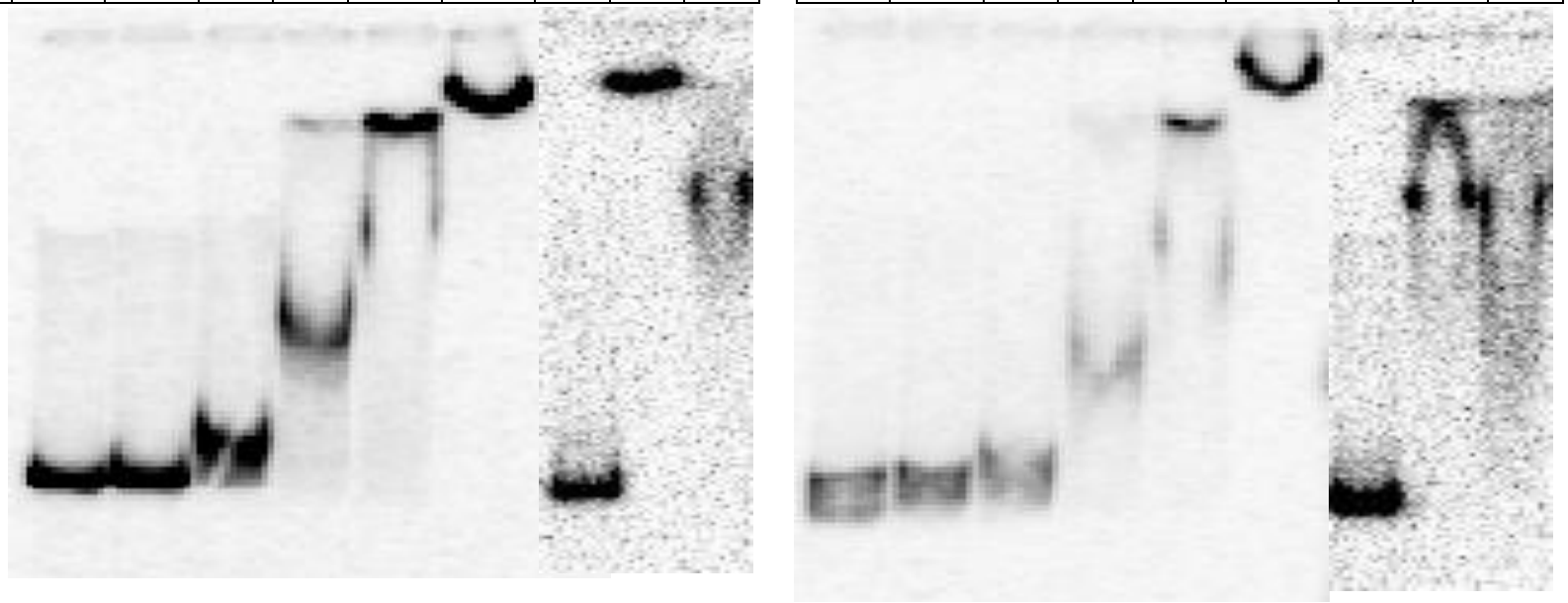

Figure 3.20: Radiolabelled Electromobility shift assay was performed with *ihfA* (A) and *ihfB* (B) full length promoter region. Gradient of PsrA concentration was used as indicated above with approximately 1000 cpm of each probe. The samples were run on a 6% TBE acrylamide gel in 0.5x TBE buffer. The bands were visualised using the Molecular Imager PharosFX™ Plus system.

in one of the reactions in place of PsrA to rule out any artifacts or contaminations. No shifts were visible when BSA was used instead of PsrA which confirmed the stable DNA/protein interactions (Figure 3.20). As an additional control, the internal coding region of *magA* gene was used. The rationale for this is that as PsrA is a transcriptional regulator, it should not bind to the internal coding region of *magA*. As expected, the eight times the DNA concentration of *magA* did not cause the shift to disappear further confirming the specificity of the PsrA in binding sites in the *ihfA* and *ihfB* promoter regions (Figure 3.20). Lastly, non-labelled competing DNA of *ihfA* and *ihfB* was used as another control which dissipated the band shift confirming the specificity of PsrA for sites within *ihfA* and *ihfB* promoter regions (Figure 3.20). Thus, PsrA directly binds to sites within *ihfA* and *ihfB* promoter regions with apparent equal affinity to regulate their gene expressions.

3.4.2.3 DNaseI footprint studies

To identify the precise location of the sites bound by PsrA within the *ihfA* and *ihfB* promoter regions, DNaseI footprinting studies were done in a similar manner as described for the upstream region of *rsmZ*. Approximately 10 µg of PsrA protein was used in the binding reactions with ^{32}P-labelled antisense *ihfA* and *ihfB* promoter fragments. The accompanying sequencing ladders were prepared with the PR ihfα P1 and PR ihfβ P2 primers (Table 2.3).

As shown in Figure 3.21, a clear footprint was observed within the *ihfA* promoter region. Two regions were protected from bound PsrA; however only one of the protected regions was used for further analysis since the sequencing ladder did not extend far enough to detail the DNA sequence of the second protected region. The first protected site

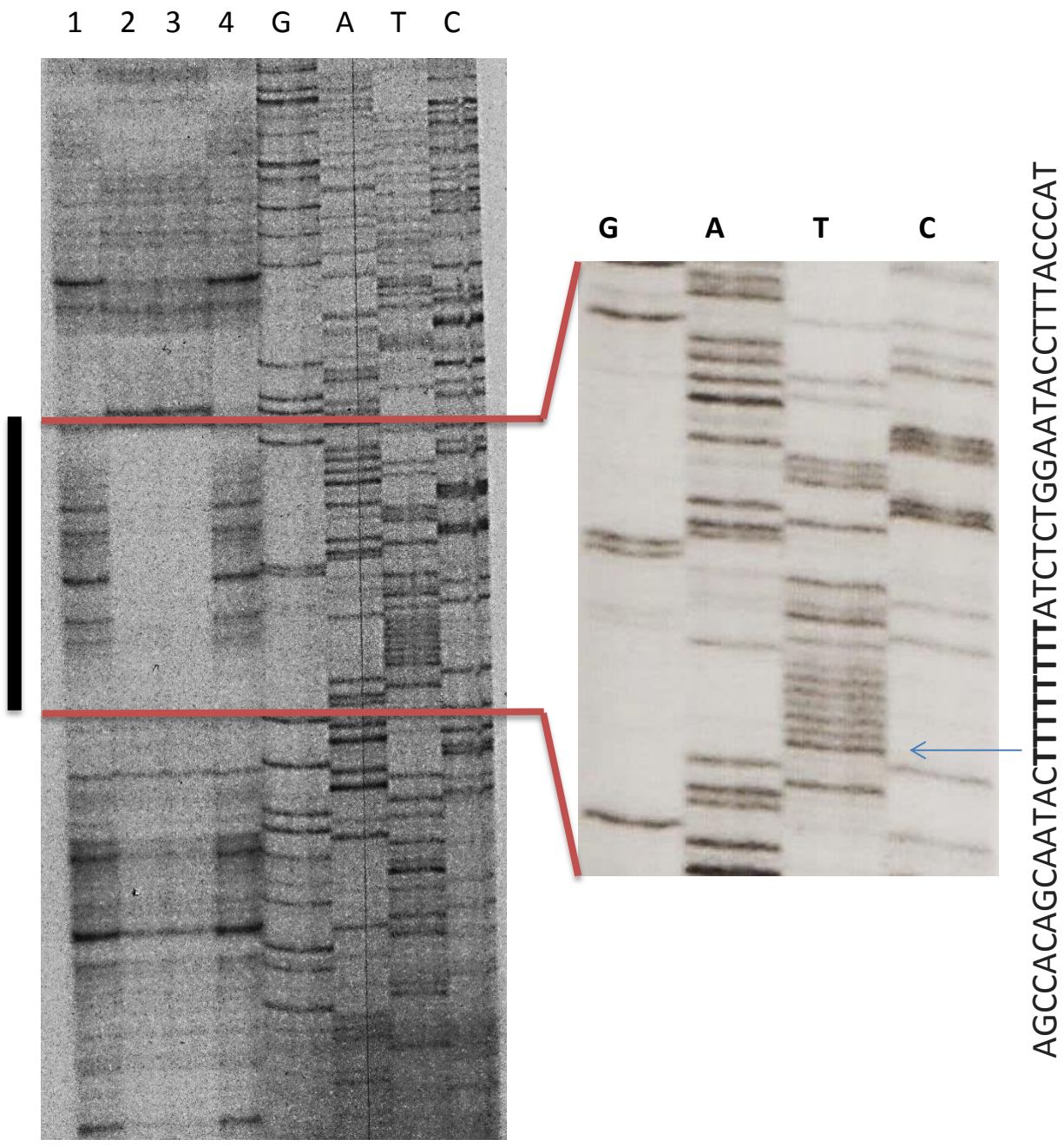

Figure 3.21: **DNaseI footprint analysis of *ihfA* promoter region**. Samples resulting from DNaseI digestion of ^{32}P-labelled antisense *ihfA* promoter (~60,000 cpm per lane) with no protein (lanes 1&4), 10µg of PsrA (lanes 2&3) are shown with the accompanying sequencing ladder. The samples were run on a 8% TBE acrylamide gel and the protected region from DNaseI digestion is shown in the inset picture with DNA sequence in the order of G, A, T, C. Shaded bars indicate PsrA DNA footprint.

A

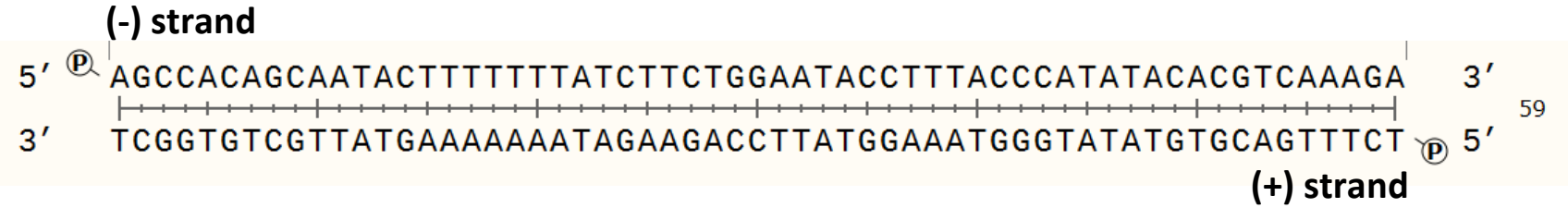

B

TTCCTGGTTGATAGGCAGATAAGTGCCATGCAGATTGAGCGAGTAATCAGAAATACAGTTAAAGAGG

ATTGGTTAAAATCGTTTGACGTCTTTGACGTGTATATGGGTAAAGGTATTCCAGAAGATAAAAAAAG

TATTGCTGTGGCTATGACACTACAAGACGATACTCGAACTTTAG**TTGATG**CCGAGATCAATTTAACA

-35 box

ATTAGTG**CTATAAT**CAAGAAACTGGAAAATGAATTTTCAATCCTTTTGAGGGAATGATCGTGAACGC

-10 box

ACTAAGCAAAGCAATAATGGCAGAAA

Figure 3.22: *ihfA* promoter analysis. A) PsrA binding site on *ihfA* promoter after comparative analysis of the binding site from Figure 3.21 to the Legiolist genome sequence database. B) The -10 and -35 promoter elements are shown in green and blue, respectively. The grey region represents the PsrA-bound region from Figure 3.21 and the *ihfA* coding sequence is shown in red.

was aligned with the *ihfA* sequencing ladder and the binding site sequence was read in the 5' to 3' direction. The sequence was reverse complemented for further comparison with the Legiolist *L. pneumophila* genome database. In Figure 3.22A, the deduced PsrA binding site sequence is shown which is located about 100bp upstream from the ATG start codon of *ihfA* gene (Figure 3.22B). It appears that the region bound by PsrA does not affect any regulatory elements thus supporting its role as a positive regulator of *ihfA* gene.

The *ihfB* promoter region was also analyzed to characterise PsrA binding site(s). DNaseI footprinting reactions were done as described in Methods and Materials. The PR ihfβ P1 primer (Table 2.3) was used to generate the sequencing ladder to be run alongside footprinting samples on a sequencing gel. One protected region was observed in the resultant footprint (Figure 3.23). Because of the fuzzy and crowded banding pattern on the sequencing ladder, few mismatches were observed which were corrected by alignment of the sequence with the Legiolist genome sequence database. The corrected PsrA binding site sequence is shown in Figure 3.24A. It appears that PsrA covers a large region within the *ihfB* promoter that excludes the -10 and -35 promoter elements (Figure 3.24B). Thus, the placement of the binding site does not explain how PsrA is able to prevent the transcription of *ihfB*.

3.5 PsrA involvement in RpoS and PsrA (auto-regulation) regulation

Studies with *P. putida* showed that PsPsrA is involved in the regulation of *rpoS* and *psrA* genes. Evidence to support this finding comes from radiolabelled EMSAs and DNaseI footprint studies that showed a direct interaction of PsPsrA and the upstream promoter

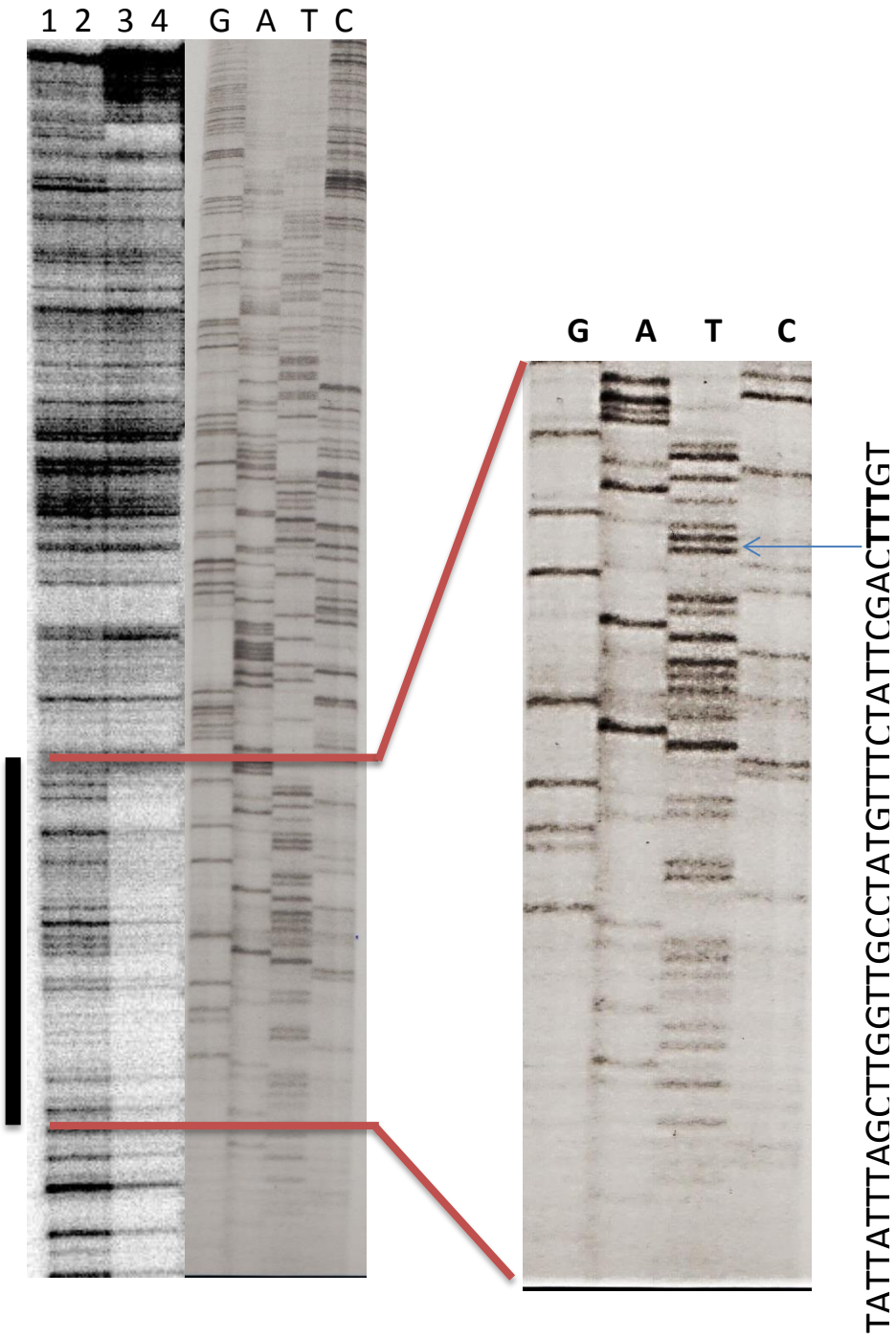

Figure 3.23: DNaseI footprint analysis of *ihfB* promoter region. Samples resulting from DNaseI digestion of ^{32}P-labelled antisense *ihfB* promoter (~60,000cpm per lane) with no protein (lanes 1&2), 10µg of PsrA (lanes 3&4) are shown with the accompanying sequencing ladder. The samples were run on a 8% TBE acrylamide gel and the protected region from DNaseI digestion is shown in inset picture with the DNA sequence in the order of G, A, T, C. Shaded bars indicate PsrA DNA footprints.

A

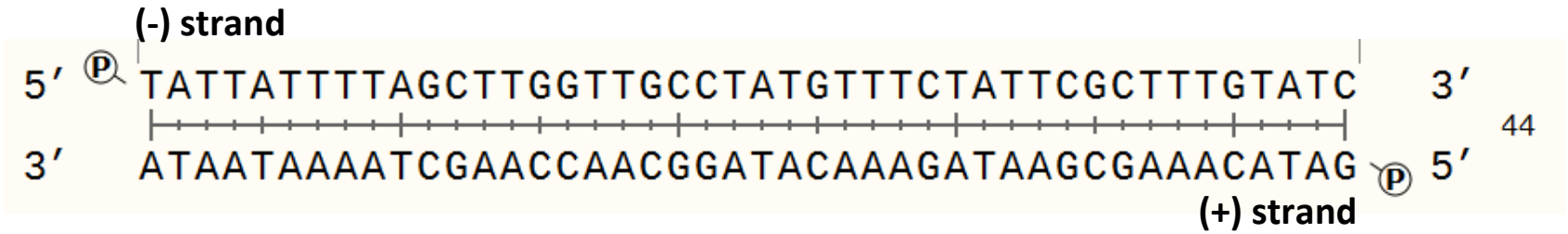

B

CTAACCAGC**TTGAAA**ACATTGAATAATTTTTTACCCGAA**CTATACT**TATAAAATCAAATGGGAAATT

-35 box -10 box

GTCAGCGCCTGATGTGTCTTGGTAGCAGACATTAGGCCAGTTGCTCAGCTCGTGGAGTTTATTTTAG

TATCGGCCACCCGTGTTTCAAGATACAAAGCGAATAGAAACATAGGCAACCAAGCTAAAATAATAGA

GGATGCAATCGGTCTATTAAATACGCGACAAAACGAGGTGAGTATATGATTAAATCCGAACTCATTG

AACACATCGCTGCTCGA

Figure 3.24: *ihfB* promoter analysis. A) PsrA binding site within the *ihfB* promoter region after comparative analysis of the binding site from Figure 3.23 to the Legiolist genome database. B) The -10 and -35 promoter elements are underlined. The grey region represents the region bound by PsrA from Figure 3.23 and the *ihfB* coding sequence is shown in red.

regions of these genes. PsPsrA was determined to bind the -59 to -35 bp region upstream of the +1 transcription start site inferring its role as a positive regulator of *rpoS* expression. Conversely, PsPsrA bound a -18 to +20 bp region overlapping the promoter and coding sequence of *psrA* inferring its role as a repressor of the *psrA* expression. Thus, *P. putida* PsPsrA was found to be an activator of *rpoS* but repressor of *psrA* (negative auto-regulation).

So to address this possibility in *L. pneumophila*, *rpoS* and *psrA* promoter regions were cloned in pBH6119 promoterless GFP reporter vector (Figure 2.1). These GFP reporter constructs (Table 2.3) were electroporated into wild-type Lp02 and Δ*psrA* mutant strains for implementation in GFP reporter assays to develop the expression profiles. Further analyses were done using EMSAs and DNaseI footprinting.

3.5.1 PsrA and RpoS interaction

3.5.1.1 GFP expression profiles of RpoS in Lp02 and *ΔpsrA*

As mentioned above, to determine if PsrA is involved in the regulatory control of *rpoS* gene expression, the full-length *rpoS* promoter-GFP construct (Table 2.2) was used in GFP reporter assays. In the Lp02 wild-type strain background, the expression profile initiated around 200 RFU/OD_{600} units (Figure 3.25A). For the first 8 hours, there was a gradual minor decline in the fluorescent values; however, during the exponential growth phase the fluorescent values started to increase at a slow and steady rate to a maximum of around 400 RFU/OD_{600} units during the transition to post-exponential growth phase

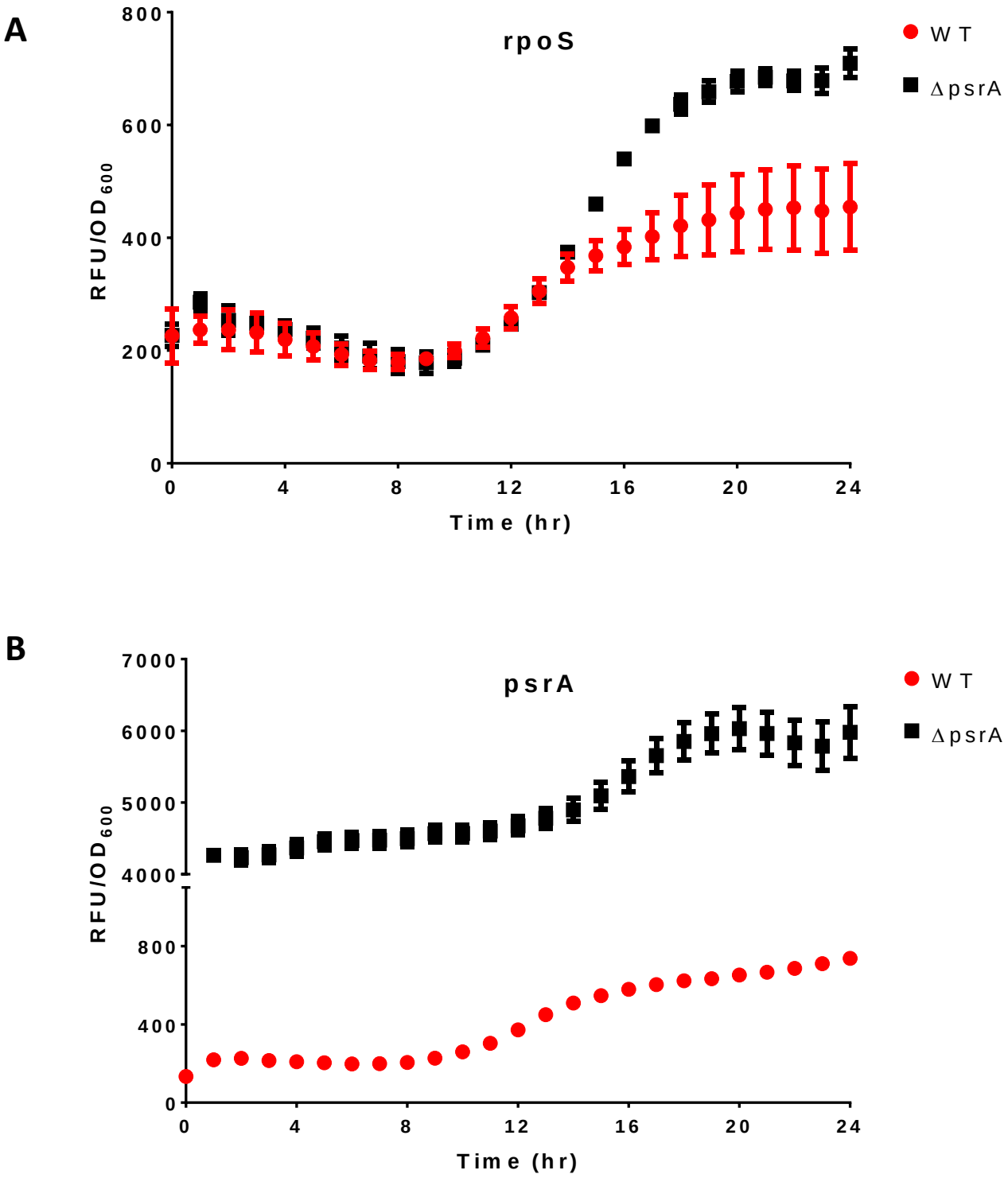

Figure 3.25: Expression profiles of *rpoS* and *psrA* promoter GFP reporter constructs. Florescence was detected from the *rpoS* (A) and *psrA* (B) promoter GFP reporter constructs on an hourly basis for 24 hours in the Lp02 (WT), and *ΔpsrA* strain backgrounds. Normalised RFU/OD_{600} units were plotted and the error bars represents SEM. Data represents an average from three independent experiments.

(Figure 3.25A). This expression profile correlated with the documented *rpoS* expression profile reported elsewhere (Hales and Shuman, 1999).

In the Δ*psrA* mutant strain background, the fluorescent values were slightly elevated during the first 8 hours comparison to levels observed in the wild-type Lp02 strain background (Figure 3.25A). There was no difference in fluorescent values during log growth phase; however, the fluorescent levels were about 300 units higher in the post-exponential growth phase (Figure 3.25A). Overall, PsrA seems to be acting as a weak repressor of *rpoS* gene expression since the change in fluorescent values is not significant for most of the time points.

3.5.1.2 EMSAs

Bioinformatic analyses using the reported PsPsrA consensus binding site sequence predicted multiple binding sites within the *rpoS* promoter region (Table 3.2). To evaluate the possible PsrA/*rpoS* promoter region interactions, EMSAs were performed as described earlier. As shown in Figure 3.26A, only 9μM PsrA concentration was sufficient to fully shift the radiolabelled *rpoS* promoter region probe. Higher band shifts were achieved with increased protein concentrations. The radiolabelled *rpoS* promoter region probe did not shift when BSA was used in place of PsrA further confirming the specificity of the PsrA/*rpoS* promoter region interaction (Figure 3.26A). In addition, non-labelled *magA* DNA and non-labelled *rpoS* DNA were also used in a similar manner as described in previous experiments to verify the specificity of the band shifts (Figure 3.26A). Thus, it was determined that PsrA directly binds sites within the *rpoS* promoter region to regulate its expression.

A) RpoS

PsrA (µM)	0	5	9	18	27	36	45	30	30	30
Specific Comp.	-	-	-	-	-	-	-	-	-	+
BSA	-	-	-	-	-	-	-	+	-	-
magA	-	-	-	-	-	-	-	-	+	-

B) PsrA

0	5	9	18	27	36	45	30	30	30
-	-	-	-	-	-	-	-	-	+
-	-	-	-	-	-	-	+	-	-
-	-	-	-	-	-	-	-	+	-

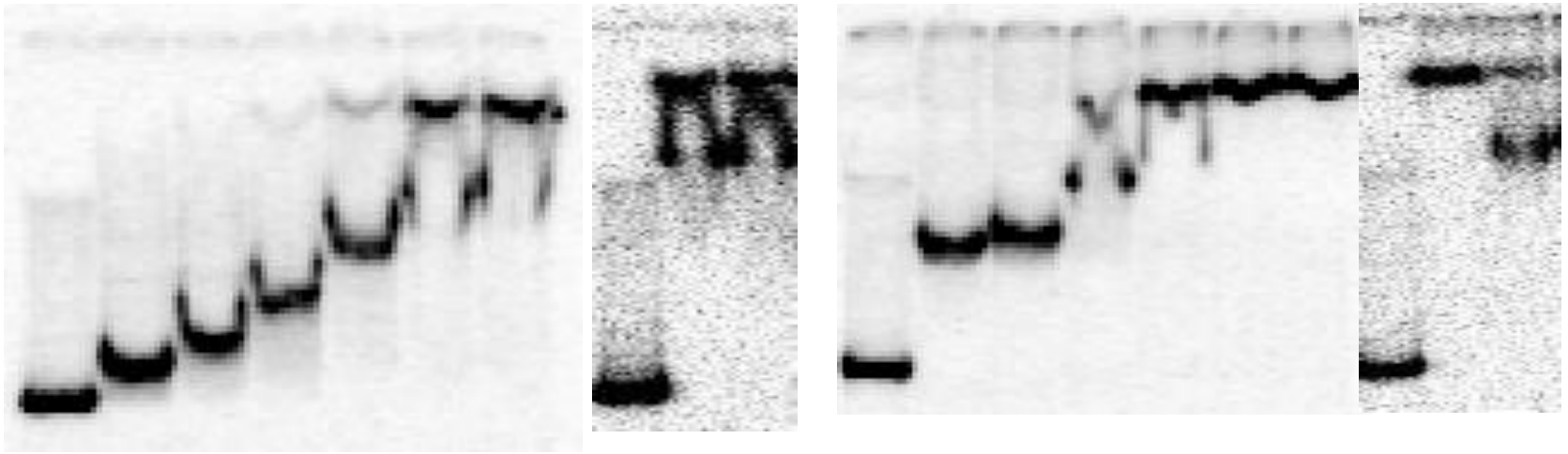

Figure 3.26: Radiolabelled Electromobility shift assay was performed on *rpoS* (A) and *psrA* (B) full length promoter region. Gradient of PsrA concentration was used as indicated above with ~1000cpm of each probe. The bands were visualised using the Molecular Imager PharosFX™ Plus system.

3.5.1.3 DNaseI footprint studies

To precisely identify the PsrA binding site(s) within the *rpoS* promoter region, DNaseI footprinting studies were performed by labelling the antisense strand of *rpoS* promoter with ^{32}P (see Methods and Materials). In Figure 3.27, three protected regions are observed in the resultant DNaseI footprint. It is difficult to deduce the DNA sequence corresponding with the first protected region due to the compression of the DNA sequence ladder. However, the DNA sequence can be read for the second and third protected regions (Figure 3.27). This second protected region is unusually large suggesting that more than one PsrA homodimer could be binding within this region of the promoter. The binding site sequence was determined by alignment with the sequencing ladder, reverse complemented and cross-referenced with the Legiolist genome database. The binding site sequence is shown in Figure 3.28A. Further analyses showed that binding by PsrA overlaps the -10 and -35 promoter elements along with first 40bp of the *rpoS* coding sequence suggesting that PsrA is a repressor of *rpoS* gene correlating with the result of the GFP reporter assay (Figure 3.28B). This finding is very different from the reported finding that PsPsrA is an activator of *rpoS* expression in *P. putida* (Kojic *et al.*, 2002).

3.5.2 PsrA auto-regulation

In *P. putida*, PsPsrA was found to be negatively autoregulated. To determine if PsrA is also autoregulated in *L. pneumophila,* GFP reporter assays, EMSAS and DNaseI footprint studies were undertaken.

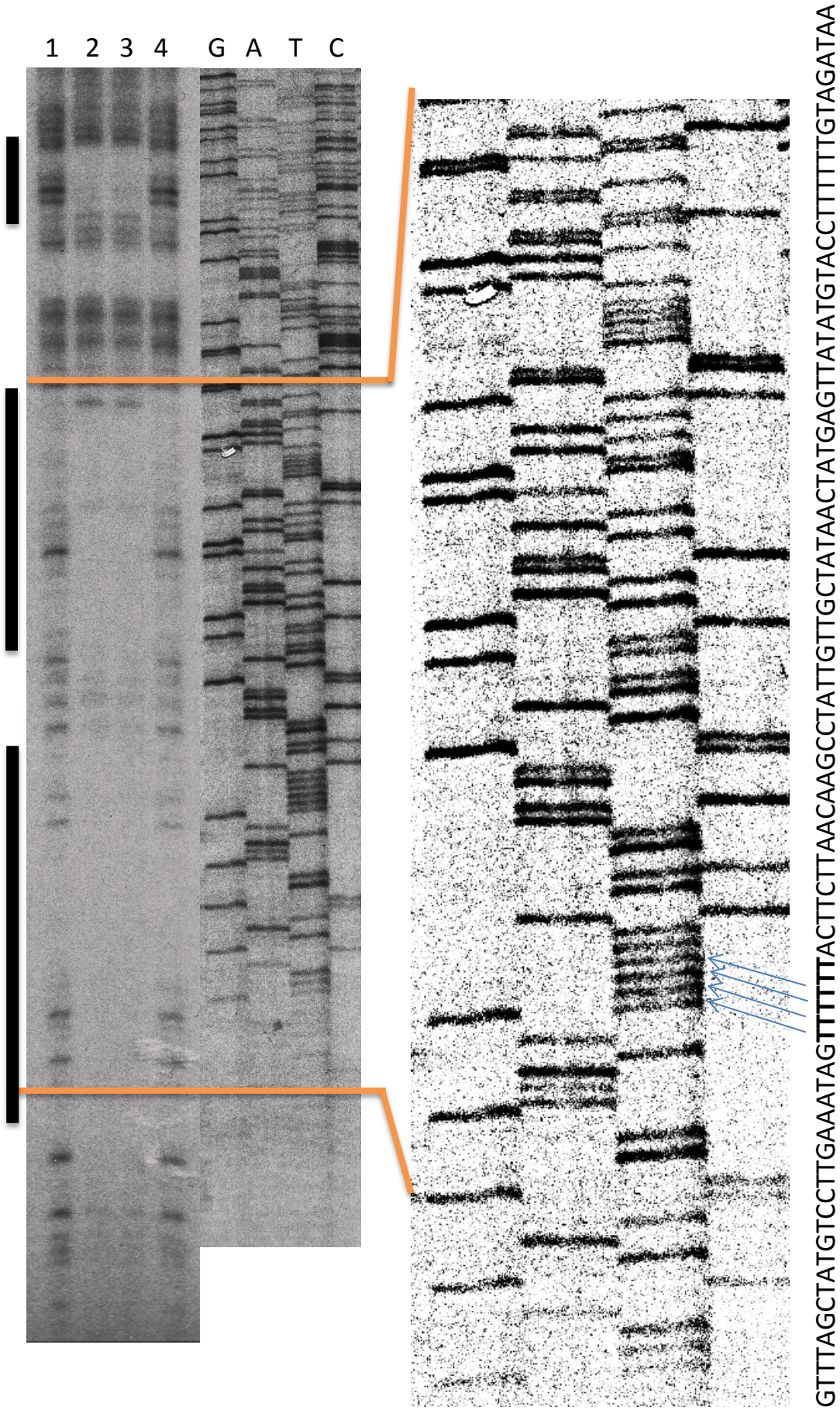

Figure 3.27: **DNaseI footprint analysis of *rpoS* promoter region**. Samples resulting from DNaseI digestion of ^{32}P-labelled antisense *rpoS* promoter (60,000cpm per lane) with no protein (lanes 1&4), 10µg of PsrA (lanes 2&3) are shown with the accompanying sequencing ladder. The samples were run on 8% TBE acrylamide gel and the protected region from DNaseI digestion is shown in the inset picture with the DNA sequence in the order of G, A, T, C. Shaded bars indicate PsrA DNA footprints.

A

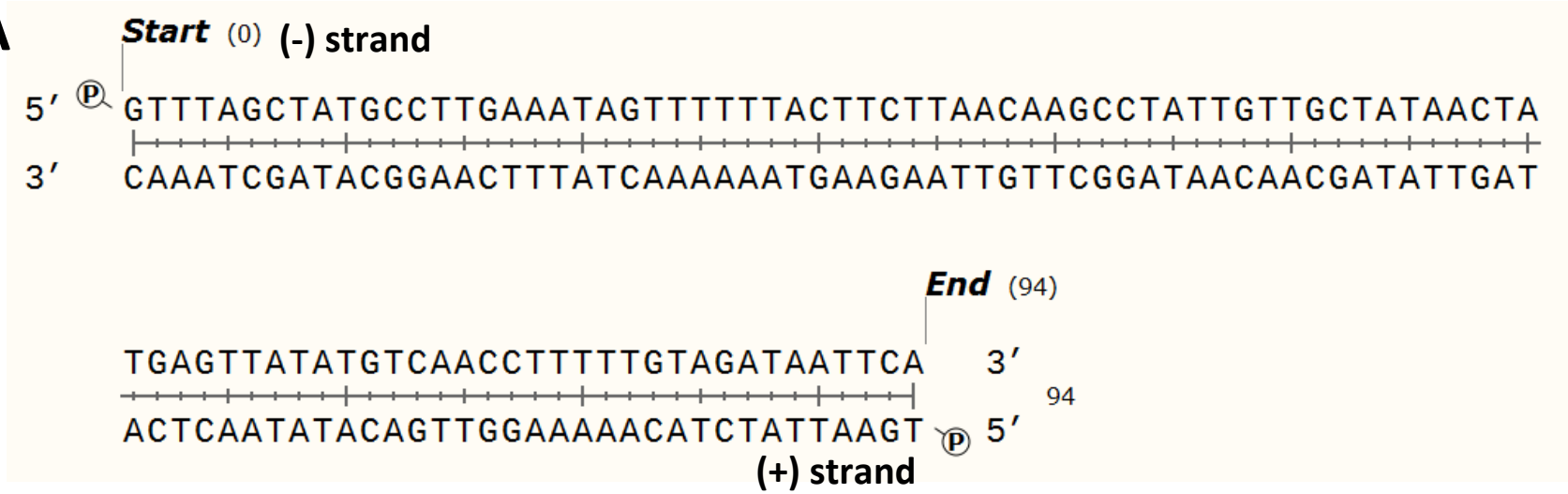

B

AACACAGTAATGAATATTTAACTGCATACGGCAACAATGCCAGAAACCTGGTGACAGAAGGACAGCG

CGTTAATGCAGGGCAGGTAATAGCAGAAGCTGGGTTAATAGATAGATCATACTGGGGTGTGCATTTT

GAAATTAGAAGAGCAGGGGTGCCAGTTAATCCA**TTGAAT**TATCTACAAAAAGGTTGACA**TATAAC**TC

-35 box -10 box

ATAGTTATAGCAACAATAGGCTTGTTAAGAAGTAAAAAACTATTTCAAGGCATAGCTAAACATATAG

GTGATACAATGCAAGATGATGAAGAGCCAATT

Figure 3.28: *rpoS* promoter analysis. A) PsrA binding site within *rpoS* promoter region after comparative analysis of binding site from Figure 3.27 to the Legiolist genome sequence database. B) The -10 and -35 promoter elements are underlined. The grey region represents the PsrA- protected region from DNaseI digestion from Figure 3.27 and the *rpoS* coding sequence is shown in red.

3.5.2.1 GFP expression profiles of PsrA in Lp02 and Δ*psrA*

The full-length promoter region upstream of *psrA* was cloned in pBH6119 promoterless GFP reporter vector and electroporated into wildtype Lp02 and Δ*psrA* mutant strains. In the Lp02 strain background, fluorescent levels were found to be constant for approximately 16 hours and increased to higher levels in late-log and post-exponential growth phases to a maximum of about 800 RFU/OD_{600} units (Figure 3.25B). Thus it seems that PsrA is expressed mainly during post-exponential and stationary phase.

Interestingly, in the Δ*psrA* mutant strain background, the fluorescent values were significantly elevated. Like the profile observed in the Lp02 strain background, the fluorescent values stayed constant but at a higher level of about 4000 RFU/OD_{600} units (Figure 3.25B). During the late-log growth phase, the fluorescent levels started to increase rapidly reaching the maximum level of 6000 RFU/OD_{600} units at post-exponential growth phase (Figure 3.25B). Clearly, PsrA expression was significantly elevated in the absence of PsrA strongly suggesting its role as a negative auto-regulator.

3.5.2.2 EMSAs

To determine if PsrA can functionally recognise binding sites in the upstream promoter region of *psrA*, an EMSA was performed with purified recombinant PsrA and radiolabelled *psrA* promoter region in a similar manner as for EMSAs with PsrA and the *rpoS* promoter region. As shown in Figure 3.26B, the radiolabelled *psrA* promoter region probe was fully shifted at the concentration of only 5μM PsrA. Higher protein concentrations produced higher band shifts suggesting the presence of more than one

binding site (Figure 3.26B). This observation correlated with the bioinformatics analyses that revealed multiple PsPsrA binding sites within the *psrA* promoter region (Table 3.2). The BSA control did not shift the probe and *magA* DNA did not affect the shift; both confirming the stability and specificity of the PsrA/*psrA* promoter region interaction (Figure 3.26B). In addition, co-competing non-labelled *psrA* promoter region DNA weakened the band shift. Thus, PsrA is a strong negative autoregulator with high affinity for binding sites in the *psrA* upstream promoter region.

3.5.2.3 DNaseI footprint studies

To precisely identify the psrA binding sites within the *psrA* promoter region, DNaseI footprint studies were done as described in Methods and Materials. Briefly, the antisense strand of the *psrA* promoter region was labelled with ^{32}P, incubated with PsrA and run on a sequencing gel along with a sequencing ladder generated using PR psrA primer (Table 2.3). Four protected sites were observed within the *psrA* promoter indicating the presence of multiple binding sites (Figure 3.29). This result is supported by the results obtained with EMSAs, GFP reporter assays, and bioinformatics analyses. The sequence aligned with the protect regions was read in the 5' to 3' direction, reverse complemented and cross referenced with Legiolist genome sequence database. The final analysed sequences are shown in Figure 3.30A. Even though there were 4 protected regions present, the sequencing read was long enough to deduce the binding site sequence for the second, third and fourth footprint regions and these regions were selected for further promoter analysis (Figure 3.30A). The first binding site covers a fairly large region that is located just upstream of the -10 box overlapping the -35 box. The second binding site covers the -27 to

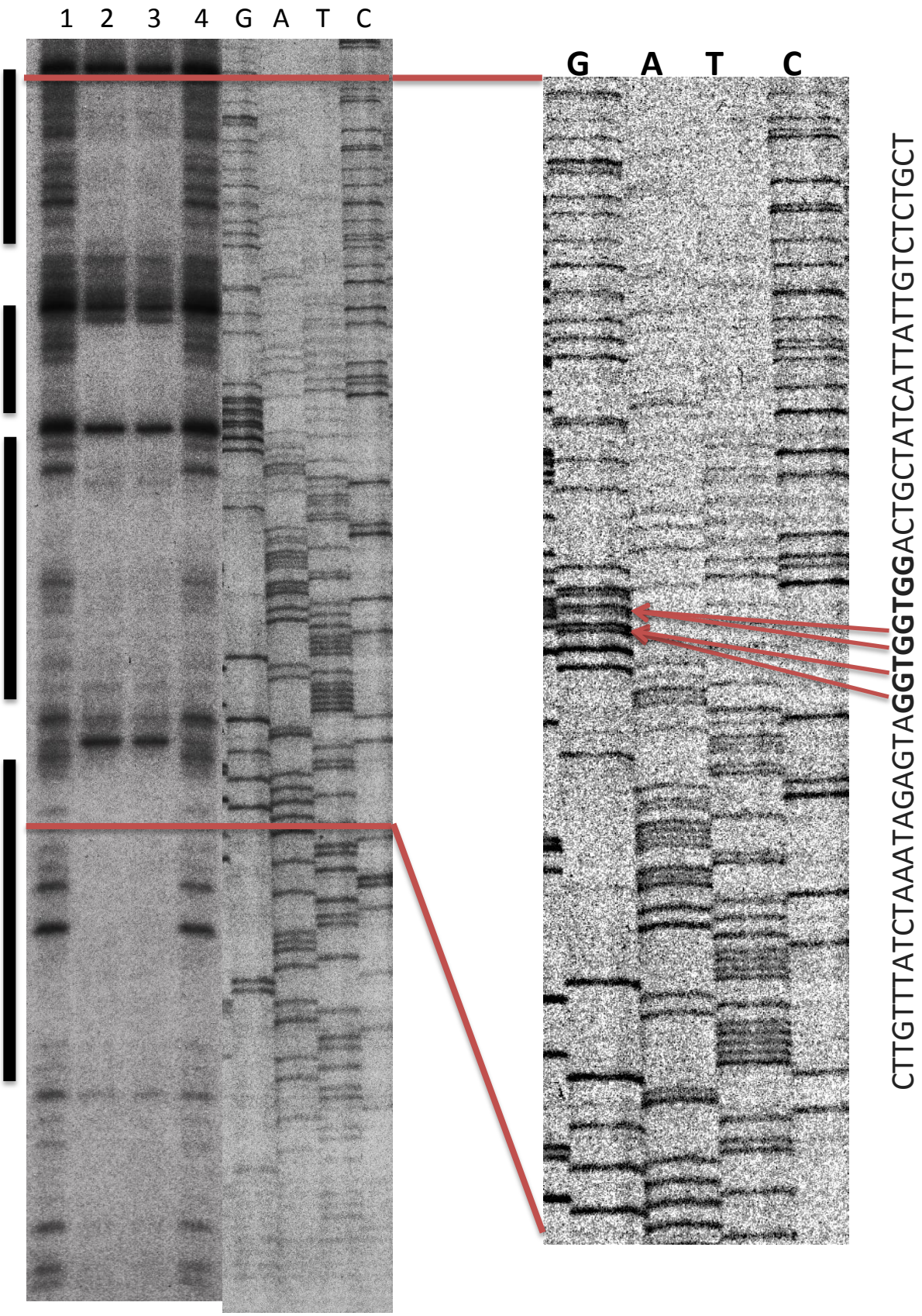

Figure 3.29: **DNaseI footprint analysis of *psrA* promoter region**. Samples resulting from DNaseI digestion of ^{32}P-labelled antisense *psrA* promoter (~60,000cpm per lane) with no protein (lanes 1&4), 10µg of LpPsrA (lanes 2&3) are shown with the accompanying sequencing ladder. The samples were run on a 8% TBE acrylamide gel and the protected region from DNaseI digestion is shown in the inset picture with the DNA sequence in the order of G, A, T, C. Shaded bars indicate PsrA DNA footprints.

A

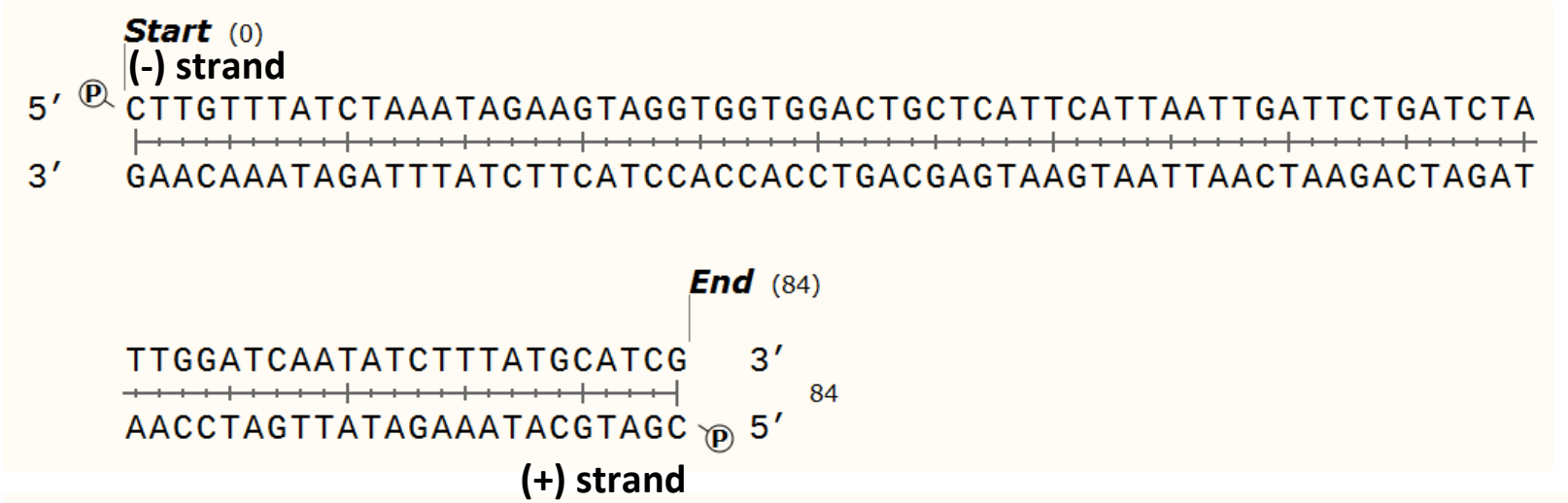

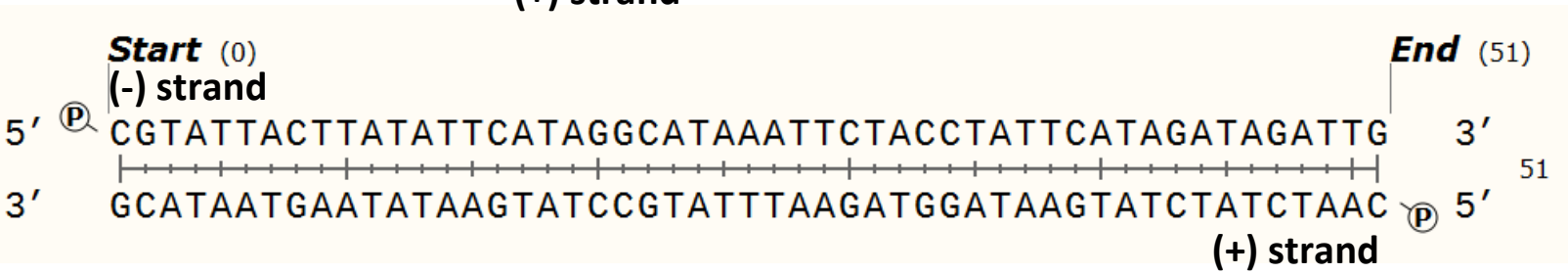

B

GACATAAAGTCTTTAAGGCCAATTGACATAGCGATGCATAAAGATATTGATCCAATAGATCAGAATC

AATTAATGAATGAGCAGTCCACCACCTAC**TTCTAT**TTAGATAAACAAGTGTTATTTTAATTTGA**TAT**

-35 box -10

AGAAAACTATAAAAAGCTTGACAATCTATCTATGAATAGGTAGAATTT**ATG**CCTATGAATATAAGTA

box

ATACGAAAGAACGGATATTAGCAGTTGCGGAAGCATTGATCCAAAAAGACGGATATAACGCCTTTAG

Figure 3.30: ***psrA* promoter analysis**. A) PsrA binding sites within the *psrA* promoter region after comparative analysis of binding site from Figure 3.29 to the Legiolist genome sequence database. B) The -10 and -35 promoter elements are underlined. The grey region represents the protected region bound by PsrA from Figure 3.29 and the *psrA* coding sequence is shown in red.

+24 bp region on the *psrA* promoter (Figure 3.30B). Thus, the second binding site also includes several base pairs of the coding sequence which further supports the results of the EMSAs and GFP reporter assays as well as the bioinformatic analyses that PsrA is a negative autoregulator.

3.6 PsrA involvement in regulation of the Dot/Icm secretion system components

In *P. aeruginosa,* PsPsrA was found to directly regulate the type III secretion system as well as several effector proteins. Components of the type III secretion system is expressed and assembled when *Pseudomonas* species encounter an eukaryotic cell (Shen *et al.*, 2006). Upon the activation of this system, several effector proteins are translocated to the host cytoplasm where they modulate the host cell processes to circumvent the host immune response (Newton *et al*., 2010; Shen *et al*., 2006). Similarly, *L. pneumophila* employs the Dot/Icm secretion system to alter and evade the host cellular responses (Newton *et al.*, 2010). There are several transcriptional factors identified in *L. pneumophila* that regulate the expression of the Dot/Icm secretion system as well as some of the effector proteins. To determine if PsrA is involved in the regulation of the Dot/Icm secretion system, bioinformatic analyses were performed and several genes of Dot/Icm secretion system were found to have multiple sites that match the consensus PsPsrA binding site sequence (Table 3.2).

Due to time constraints, *icmR, icmT, icmV* and *dotD* were selected to study the PsrA involvement; since the GFP reporter constructs carrying the full-length promoter region of these genes were previously constructed (Table 2.3). Pattern search on the Legiolist database showed multiple potential binding sites on the prompter regions of these genes.

To validate these findings, GFP reporter assays, EMSAs and DNaseI footprinting studies were carried out.

3.6.1 Expression profiles of *icmR, icmT,* and *icmV* in Lp02 and *ΔpsrA*

IcmR has been previously identified as an essential protein for intracellular survival of *L. pneumophila* in U937 macrophage cell line; however it is not required for LCV formation (Coers *et al.*, 2000). Moreover, it was hypothesized that IcmR interacts with IcmQ and forms a translocation complex which is used to deliver effector proteins to the host cell (Coers *et al.*, 2000). Thus, IcmR is one of the key components of this Dot/Icm secretion system. In the wildtype Lp02 strain background, the fluorescent values are stable at ~600 RFU/OD_{600} units during the first 12 hours and then increases reaching the maximum level of about 1600 RFU/OD_{600} units post-exponential growth phase (Figure 3.31A). Thus, IcmR is expressed mainly in the late log and post-exponential growth phase. In the Δ*psrA* mutant strain background, the fluorescent values were significantly reduced for all growth phases in comparison to values in the wild-type strain background although slightly elevated values were observed in late log and post-exponential growth phase. The fluorescent values are constant at about 200 RFU/OD_{600} for first 8 hours which starts to climb up very slowly during late log phase to a maximum level of 400 units (Figure 3.31A). Thus, it seems that PsrA is acting as a positive regulator and is required for full expression of *icmR*.

IcmT is another component of the *dot*/*icm* secretion system which is required for pore formation mediated cytolysis after the intracellular replication stage (Molmeret, 2002). Thus, IcmT is required to egress *L. pneumophila* from macrophages and protozoa.

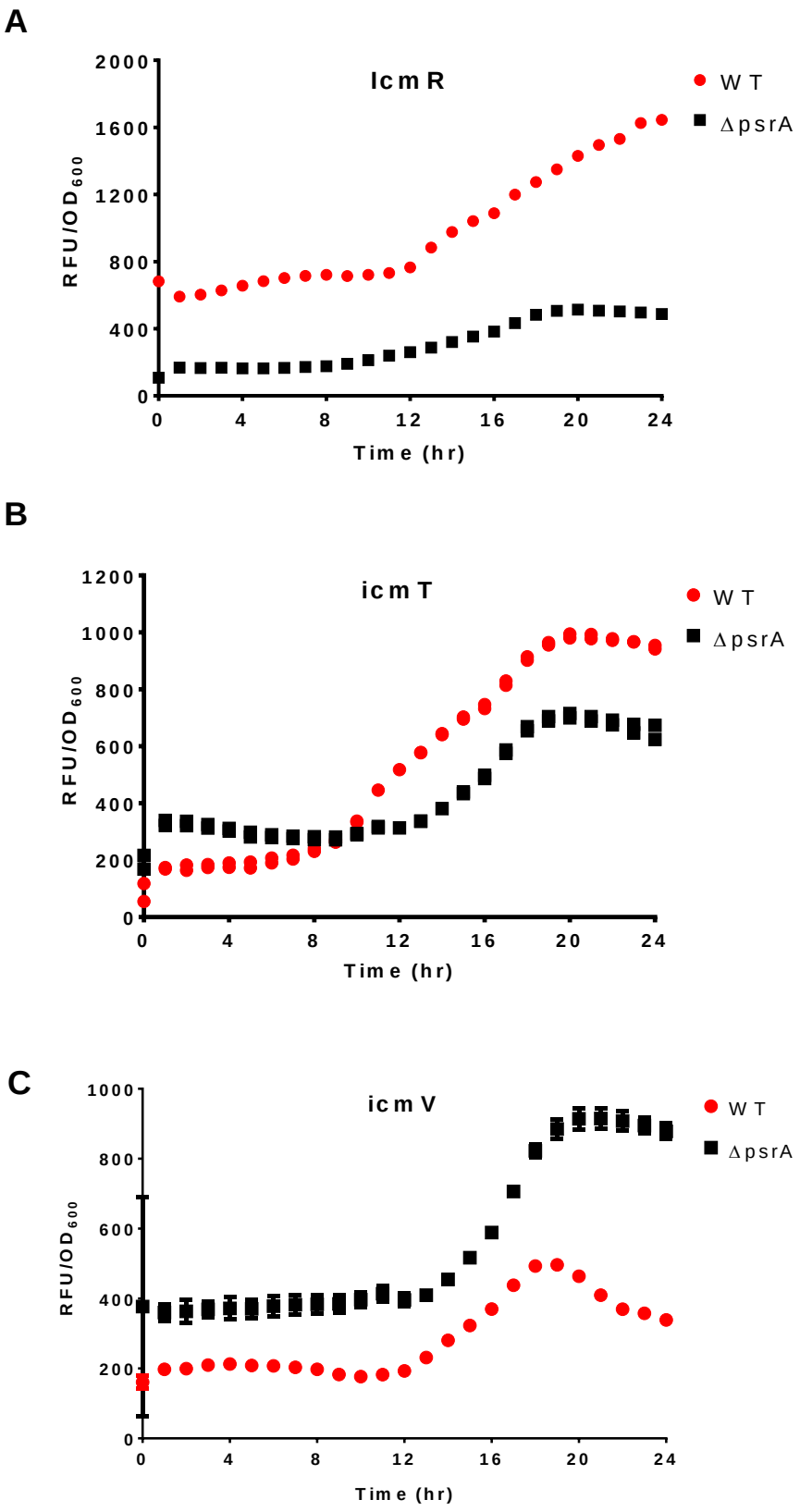

Figure 3.31: Expression profiles of *icmR*, *icmT* and *icmV* GFP constructs. Fluorescence was detected from the icmR (A), icmT (B) and icmV (C) GFP promoter reporter constructs on an hourly basis for 24 hours in Lp02 (WT), and *ΔpsrA* strain backgrounds. Normalised RFU/OD_{600} units were plotted and the error bars represents SEM. Data represents an average from three independent experiments.

Moreover, PsPsrA binding sites were found within the promoter region of *icmT* and thus GFP reporter assays were carried out for further investigate this possibility in *L. pneumophila*. In Lp02 strain background, the fluorescent values remained unchanged at ~ 200 RFU/OD_{600} units during lag growth phase; however, the fluorescent values increased rapidly during the exponential growth phase reaching the maximum levels of 1000 RFU/OD_{600} during post-exponential growth phase (Figure 3.31B). In the *ΔpsrA* strain background, no significant differences were found when comparing the fluorescent values to those observed in the Lp02 strain background for the first 8 h period. However, during the exponential and post-exponential growth phases, the fluorescent values are on average ~200 RFU/OD_{600} units lower in the *ΔpsrA* mutant strain background in comparison to the values observed in the Lp02 strain background (Figure 3.31B). Thus, PsrA is acting as an activator of *icmT* and is required for its full expression.

IcmV has been described as an inter-membrane protein but not much is known about its function (Bandyopadhyay *et al*., 2004). However, *dotA* and *icmW*, the components of *dot*/*icm* system, are important for the formation of the LCV and intracellular growth in macrophage (Roy *et al.*, 1998; Coers *et al.*, 2000). Interestingly, *dotA* and *icmW* genes are transcribed from the same *icmV* promoter region. Unlike the previous GFP reporter assays, a translational fusion of IcmV-GFP construct was used and the expression of this protein was evaluated in different strain backgrounds. In Lp02 strain background, the fluorescent values stayed constant at 200 RFU/OD_{600} units throughout the lag and early log growth phases. The fluorescent levels increased during the late-log growth phase reaching the maximum level of 1000 RFU/OD_{600} units in the post-exponential growth phase (Figure 3.31C). In the Δ*psrA* mutant strain background, the fluorescent values were constant at 400

RFU/OD_{600} units for the first 12 hours with an increase in levels to ~900 RFU/OD_{600} units in late log growth and post-exponential growth phases (Figure 3.31C). Taken together, these results strongly indicate that PsrA is a negative regulator of the *icmV* gene expression. Thus, it appears that PsrA tightly regulates the expression of several key components of type IV secretion system in *L. pneumophila.*

3.6.1.1 Radiolabelled EMSA and DNaseI footprinting studies on *icmR* promoter

To further study the mode of action of PsrA on *icmR* promoter, EMSAs were performed using similar controls and reaction conditions as described earlier (see Methods and Materials). It was found that PsrA directly binds to the *icmR* promoter. Only 18μM of PsrA is required to fully shift the *icmR* promoter region probe (Figure 3.32). Higher protein concentration resulted in higher band shifts supporting the multiple site prediction from bioinformatics results. BSA and non-labelled competing DNA produced no shift and *magA* DNA had no effect on the shift (Figure 3.32). Thus, PsrA appears to be a direct regulator of *icmR*.

To further define the binding sites in the *icmR* promoter region, DNaseI footprinting was performed as described above. Unlike the other gene targets, the sense strand of the *icmR* promoter region was labelled with ^{32}P and DNaseI digestion was performed after the protein binding reaction. As shown in Figure 3.33, only one protected region was seen on the footprint gel. To deduce the binding site sequence, the PF icmR primer (Table 2.3) was used to generate a sequencing ladder and run with the footprinting samples (Figure 3.33). The sequence corresponding to the protected region was read from the sequencing ladder in the 5' to 3' direction. The sequence was then further verified by comparing it with the

PsrA (µM)	0	9	18	36	54	72	90	15	15	15
Specific Comp.	-	-	-	-	-	-	-	-	+	-
BSA	-	-	-	-	-	-	-	+	-	-
magA	-	-	-	-	-	-	-	-	-	+

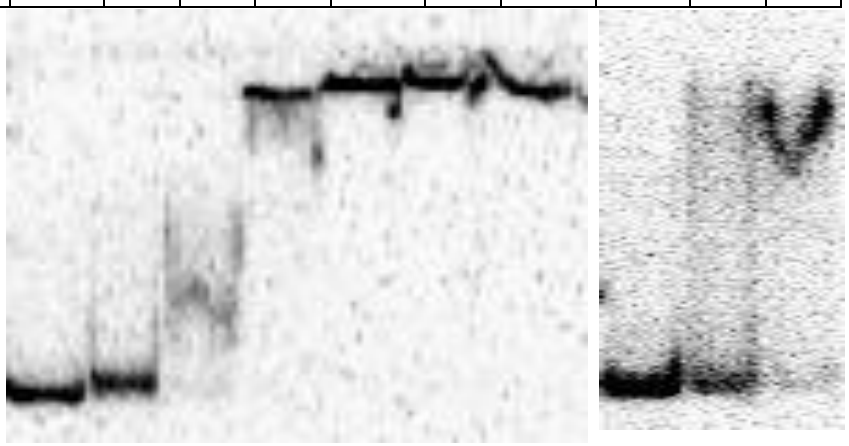

Figure 3.32: Radiolabelled Electromobility shift assay was performed on IcmR full length promoter region. Gradient of PsrA concentration was used as indicated above with 1000cpm of each probe. The bands were visualised using the Molecular Imager PharosFX™ Plus system.

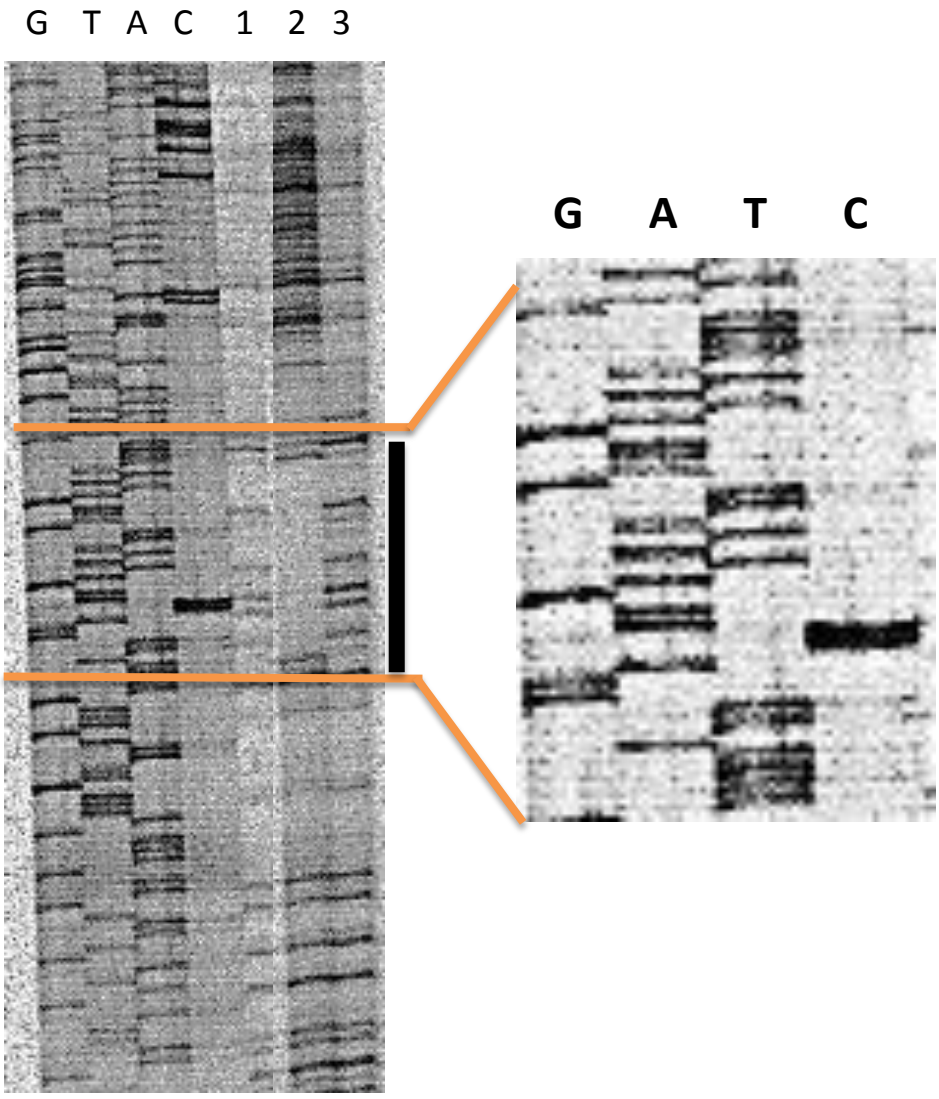

Figure 3.33: **DNaseI footprint analysis of *icmR* promoter region**. Samples resulting from DNaseI digestion of ^{32}P-labelled sense *psrA* promoter region (~60,000cpm per lane) with no protein (lanes 1&3), 10µg of LpPsrA (lane 2) are shown alongside with the sequencing ladder. The samples were run on an 8% TBE acrylamide gel and the protected region is shown in the inset picture with the sequence. Shaded bars indicate PsrA DNA footprints.

Legiolist genome sequence database and the final confirmed sequence is shown in Figure 3.34A. PsrA covers a 30bp area that includes the -35 promoter element and the upstream region (Figure 3.34B). This kind of regulatory arrangement supports the role of PsrA as an enhancer or positive regulator of *icmR*.

3.6.2 PsrA and Dot components interaction

In *L. pneumophila,* DotD has been characterised as lipoprotein which is shown to be required for intracellular growth in HL-60 derived macrophages and protozoa (Yerushalmi *et al.*, 2005). This gene was selected for further analyses since the full-length *dotD* promoter region was already cloned into the GFP promoterless pBH6119 plasmid (Table 2.2). This dotD GFP reporter plasmid was then electroporated into wild-type Lp02 and Δ*psrA* mutant strains to assess the expression profiles.

3.6.2.1 Expression profiles of *dotD* in Lp02 and *ΔpsrA*

Interestingly, a complete different expression profile was observed for the dotD promoter GFP construct in comparison to profiles for the *icm* gene promoters in the Lp02 strain background. A slow and steady increase in fluorescent values was seen in the first 8 hours. The values increased at a faster rate during log and post-exponential growth phases up to the maximum level of 3500 RFU/OD_{600} units (Figure 3.35). The overall expression profile in the Δ*psrA* mutant strain background was strikingly similar to the one seen in the Lp02 strain background with minor differences noted during lag, log and post-exponential growth phases (Figure 3.35). Thus, it seems that PsrA is a positive regulator with a minor role in the regulation of *dotD* expression.

A

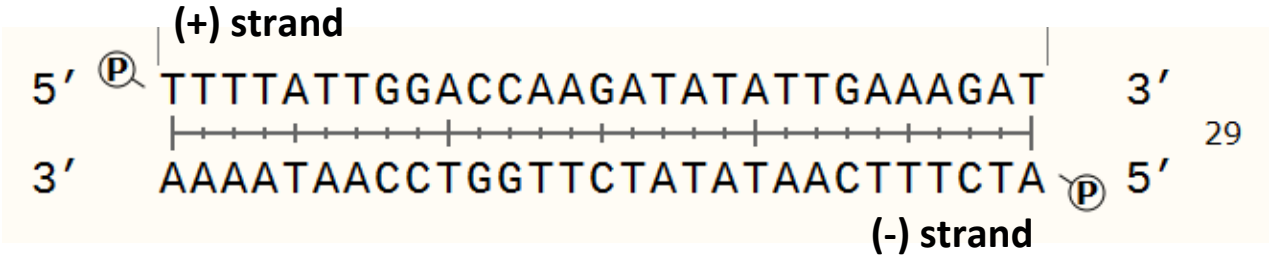

B

TGATTATACTCCCCTGGATGAGTTAATGTATGATTAGTTGTTTGTAAAGAATTAGAAAGTTTTATTG

GACCAAGATATA**TTGAAA**GATATATTTTGATATATG**TAAAGT**AAGAGATTTAGCTCAGGAGTGGTAA

-35 box -10 box

TAATGGGTAATAATACTGATGACAGTGCACGAAATCCATTTGGTTTTTATACGCCACCTCGTGTTAA

AGAGATAGGTGAACCTGATGTAACTGATGCTACTCTAGGCAGTGTCTATAGTGAAATTATTTCACCG

GTAA

Figure 3.34: ***icmR* promoter analysis**. A) PsrA binding site within the *icmR* promoter region after comparative analysis of the binding site from Figure 3.33 to the Legiolist genome sequence database. B) The -10 and -35 promoter elements are underlined. The grey region represents the protected region from Figure 3.33 and the *icmR* coding sequence is show in red.

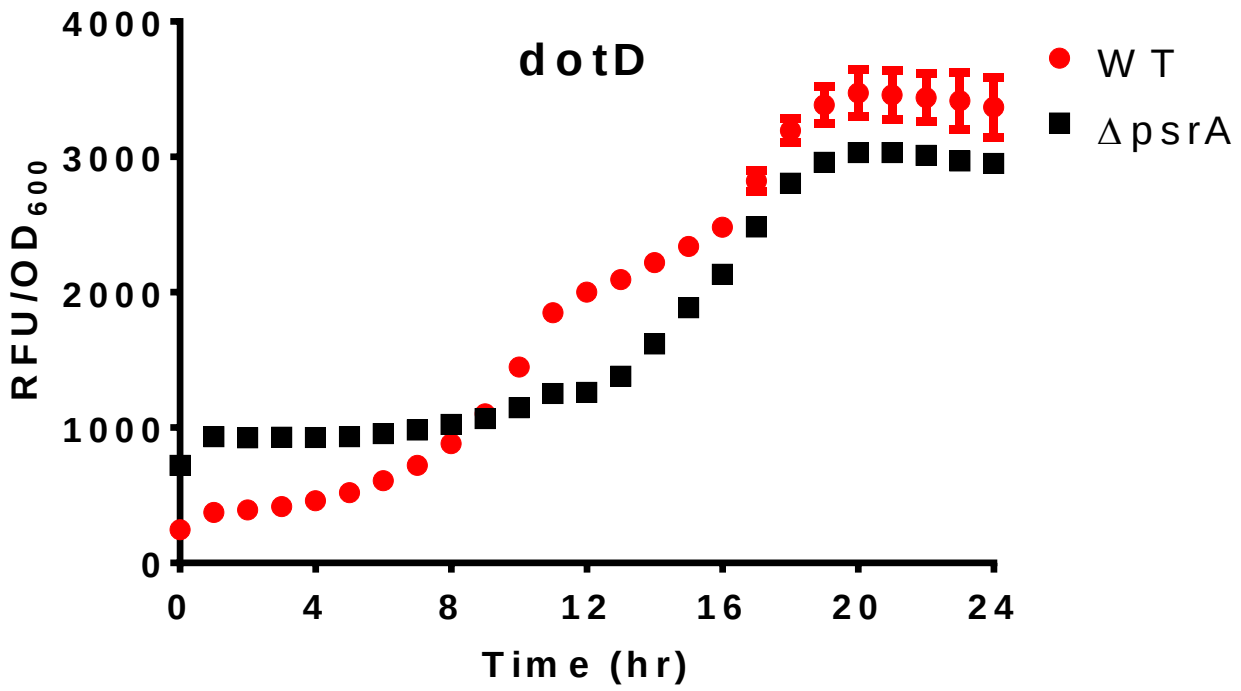

Figure 3.35: Expression profiles of *dotD* promoter GFP reporter constructs. Fluorescence was detected from the *dotD* promoter GFP reporter construct on an hourly basis for 24 hours in Lp02 (WT), and *ΔpsrA* strain backgrounds. Normalised RFU/OD_{600} units were plotted and the error bars represents SEM. Data represents an average from three independent experiments.

3.7 PsrA involvement in regulation of flagella and oxidative stress response

Motility is one of the features which are expressed during post-exponential growth phase or in response to stress. Flagellin is a major component of the flagellum complex and is encoded by *flaA* gene in *L. pneumophila* (Heuner *et al.*, 1995; Hammer and Swanson, 1999). The flagellum is a complex made of several subunits and is responsible for providing the motility to CLFs (Heuner *et al.*, 1995). Moreover, bacteria use several regulators like OxyR during the post-exponential growth phase to cope with the oxidative stress. In *L. pneumophila* OxyR has been identified to regulate several hydroperoxide reductase systems (LeBlanc *et al.*, 2008). Thus, *flaA* and *oxyR* are two genes that are expressed during stress conditions and thus they could be good indicators of post-exponential growth phase of *L. pneumophila.* So to determine the potential role of PsrA in the regulation of *flaA* and *oxyR* genes, GFP reporter assays, and EMSA studies were performed.

3.7.1 Expression profile of *flaA* in Lp02 and *ΔpsrA*

The *flaA* promoter GFP reporter construct from Hammer & Swanson, 1999 was used to determine the expression profile in wild-type Lp02 and Δ*psrA* strain backgrounds. In Lp02 strain background, fluorescent levels are initially at high levels with a steady decline in levels for the first 15 hours that includes lag and log growth phases (Figure 3.36A). During the post-exponential growth phase, the fluorescent values increased at a rapid rate reaching the maximum of 3000 RFU/OD_{600} units in post-exponential growth phase (Figure 3.36A). In the Δ*psrA* strain background, the fluorescent values initially started at 800 RFU/OD_{600} units with a steady decline during the lag and log growth phases with

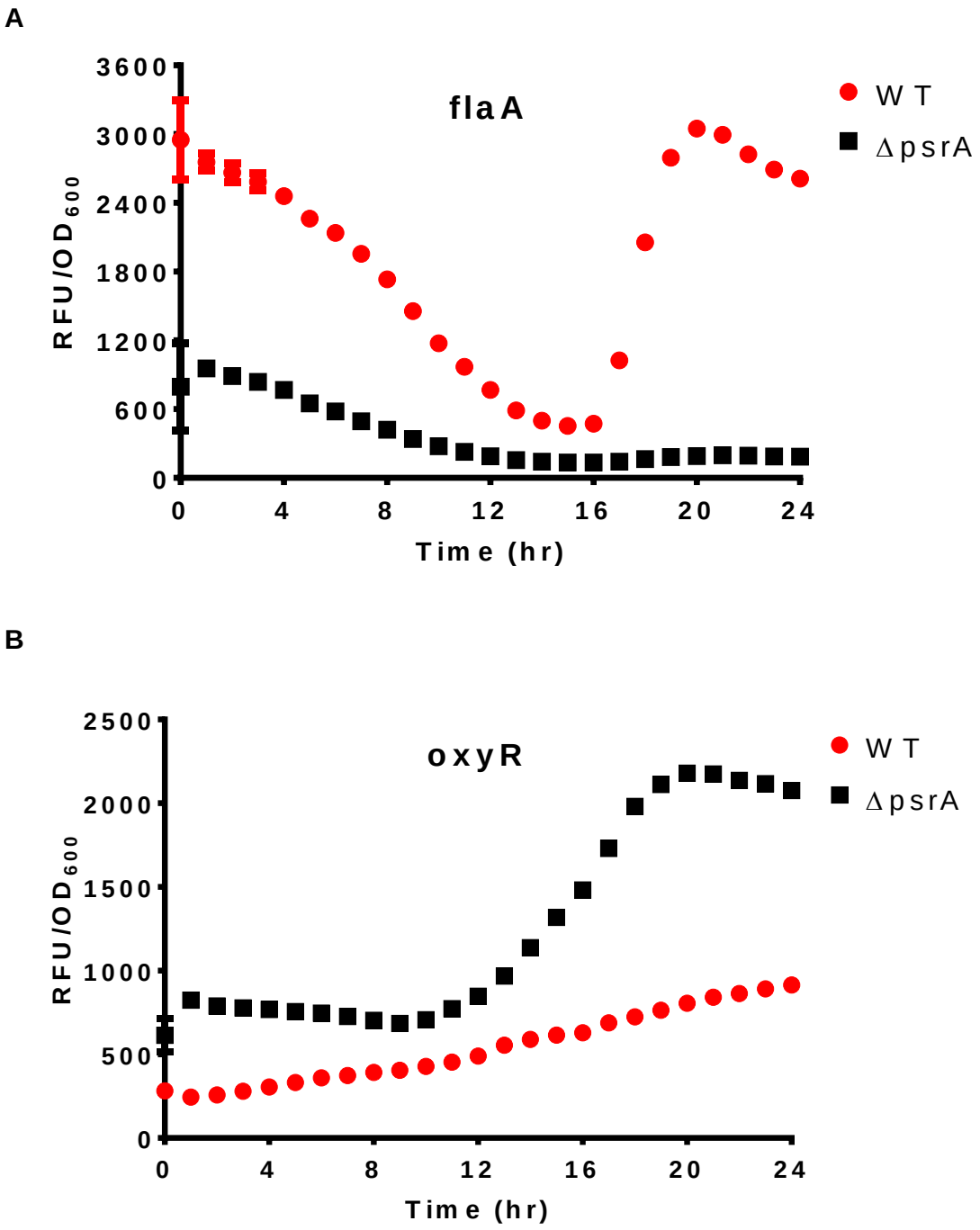

Figure 3.36: Expression profiles of *flaA* and *oxyR* promoter GFP reporter constructs. Fluorescence was detected from the *flaA* (A), and *oxyR* (B) promoter GFP reporter constructs on an hourly basis for 24 hours in Lp02 (WT), and *ΔpsrA* strain backgrounds. Normalised RFU/OD_{600} units were plotted and the error bars represents SEM. Data represents an average from three independent experiments.

expression decreased to basal levels in post-exponential growth phase (Figure 3.36A). Thus, it seems that PsrA is required for full expression of *flaA.*

3.7.2 Expression profile of *oxyR* in Lp02 and *ΔpsrA*

Similarly, GFP reporter assays were employed to determine the potential role of PsrA in the regulation of *oxyR.* The full-length *oxyR* promoter region was cloned into pBH6119 and electroporated into wild-type Lp02 and Δ*psrA* strains. In the Lp02 strain background, the expression profile showed fluorescent values increasing a steady rate from ~200 RFU/OD_{600} units in lag growth phase to ~700 RFU/OD_{600} units in the post-exponential growth phase (Figure 3.36B). Whereas in the Δ*psrA* mutant strain background, the fluorescent values were relatively constant at 700 RFU/OD_{600} units for the first 12 hours with a rapidly increased rate during log phase to a maximum level of 2000 RFU/OD_{600} units in the post-exponential growth phase (Figure 3.36B). Thus, PsrA appears to be a strong repressor of *oxyR* since absence of PsrA results in increased *oxyR* expression.

3.7.3 EMSAs

To further investigate the regulation of *oxyR* gene by PsrA, EMSAs were performed as described previously. The results are represented in Figure 3.37. Similar to other EMSA studies, 18μM PsrA was sufficient to bind and fully shift radiolabelled *oxyR* promoter region probe DNA. Higher protein concentrations caused higher band shifts indicating the possibility of more than one binding site (Figure 3.37). The BSA, non-labelled *magA* DNA and non-labelled competing DNA controls verified the specificity of the DNA/protein

PsrA (µM)	0	9	18	36	54	72	90	15	15	15
Specific Comp.	-	-	-	-	-	-	-	-	+	-
BSA	-	-	-	-	-	-	-	+	-	-
magA	-	-	-	-	-	-	-	-	-	+

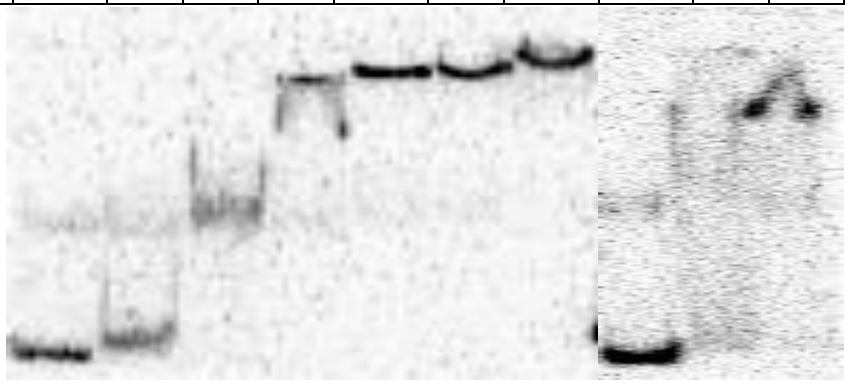

Figure 3.37: Radiolabelled Electromobility shift assay was performed on *oxyR* full length promoter region. Gradient of PsrA concentration was used as indicated above with ~1000cpm of probe in each lane. The bands were visualised using the Molecular Imager PharosFX™ Plus system.

interactions (Figure 3.37). Thus, PsrA appears to bind the *oxyR* promoter region directly, regulating the activity of this promoter region.

3.8 Consensus sequence analysis for PsrA binding site

To further characterise the binding site sequence of PsrA, the binding site sequences identified in all promoter regions tested were compiled to generate a consensus binding site sequence (Figure 3.38). It seems that PsrA prefers the thymine (T) rich region as its binding site and two sequence motifs were found in the consensus binding site sequence (Figure 3.38). However, this predicted consensus sequence had too much variation with inconsistency in the gap regions. So T-rich short regions were then hypothesised to be a part of the binding site of PsrA and they were included in the alignment instead of the whole DNaseI protected regions. The alignment showed the following well conserved regions with scores >~60: TWYTTAM (Figure 3.39). This consensus sequence was found multiple times in the promoter regions of the genes investigated in this study. Because of the low variability and adequate spacing between two binding sites, this consensus sequence was accepted as the binding site for the homodimer regulatory protein PsrA.

3.9 Intracellular growth kinetics using U937 macrophage cell line

According to the molecular assays done in this study, PsrA appears to play a central role in the regulation of various post-exponential traits that includes virulence factors. However, to examine the physiological effects of the Δ*psrA* mutant strain, infection studies were performed using the U937 human monocytic cell line. Differentiated U937 cells were infected with wildtype Lp02, *ΔdotA, ΔpsrA* and *ΔpsrA* comp (harboring wildtype *psrA* gene

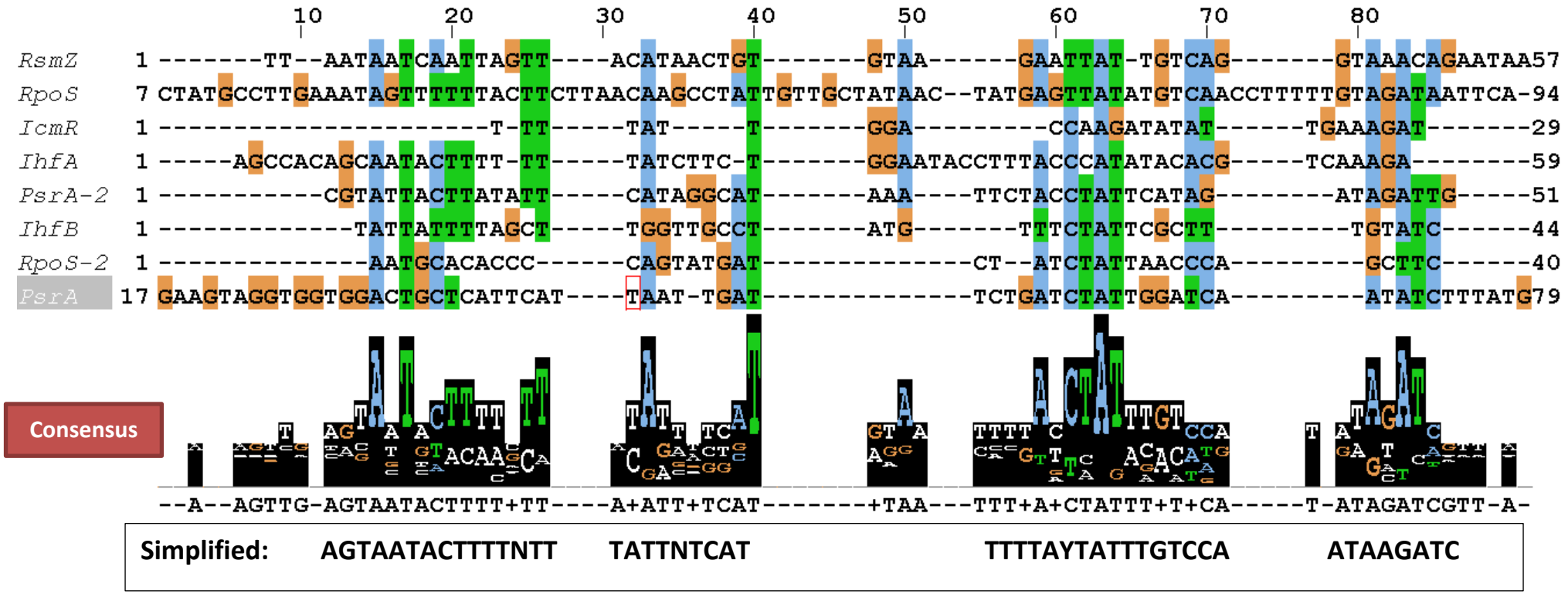

Figure 3.38: PsrA protected region alignment. All the data from promoter analysis were compiled together and sequence alignment was performed to identify the potential consensus sequence in the regions protected from the DNaseI digestion.

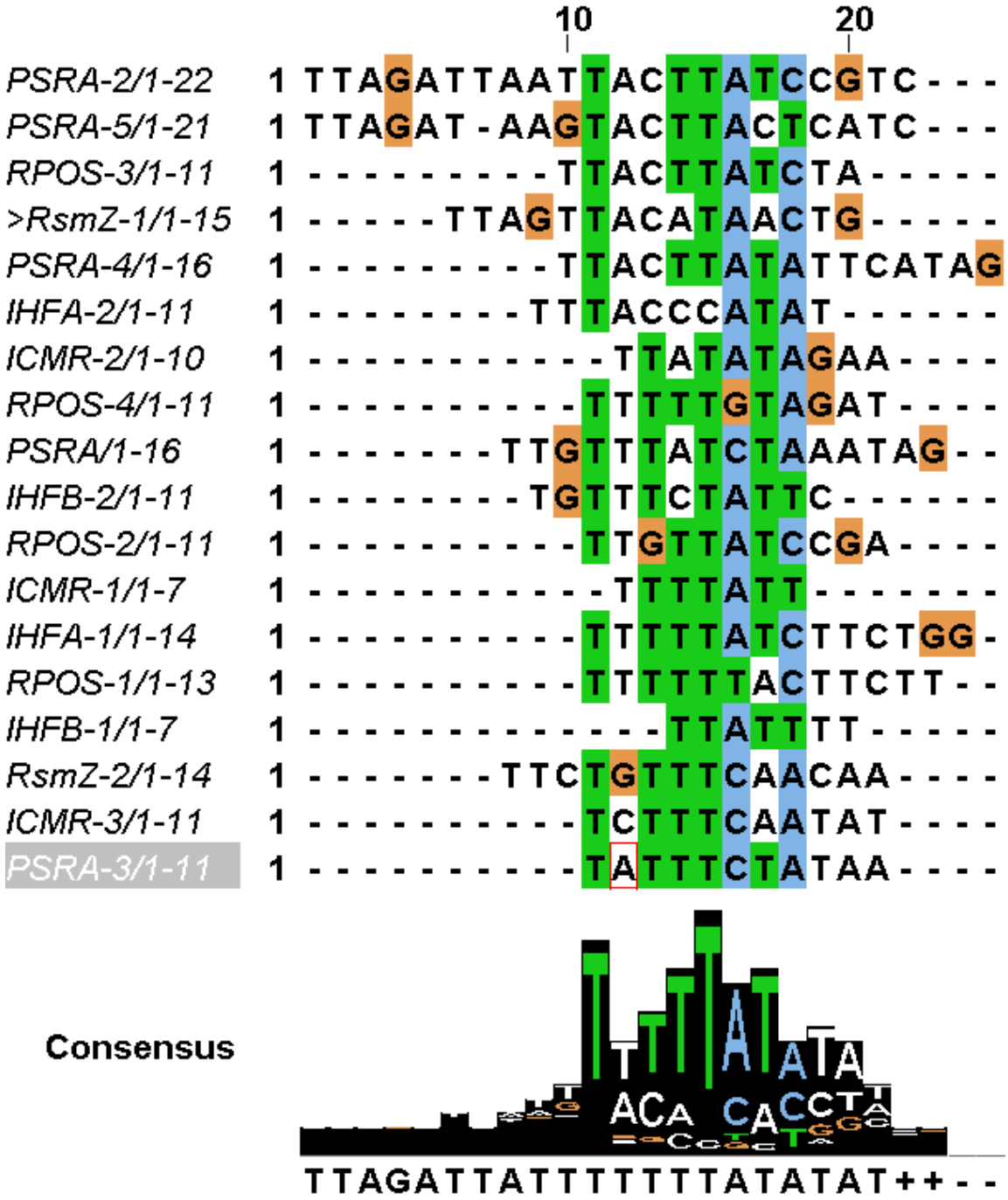

Figure 3.39: Consensus sequence analysis. The thymidine rich regions from the regions protected after the DNaseI digestion were included in one alignment. The alignment was performed on ClustalW2.1 server.

on pJB908) strains to assess the bacterial intracellular growth kinetics. The cells were infected at the MOI of 2, and at selected time points the CFUs were determined by serial dilution plating method for each strain. Interestingly, the *ΔpsrA* mutant strain showed a severe intracellular growth defect in comparison to Lp02. Moreover, bacteria extracted from the lysed macrophage cells formed very small colonies in comparison to the colony size from by the Lp02 strain. While a complemented strain was included in this infection assay, the plasmid-borne PsrA was unable to rescue the wildtype phenotype (Figure 3.40). To validate the experiment, the *ΔdotA* mutant strain was included in the infection studies as a negative control and as expected this mutant was unable to replicate within the macrophage and thus has demonstrated a severe growth defect (Figure 3.40). Thus, it appears that the *ΔpsrA* mutant is defective for intracellular replication in U937 differentiated human macrophages.

3.10 Immunofluorescence studies

To further examine the infection process of the Δ*psrA* mutant strain in U937 macrophage cells, immunofluorescence studies were performed using the Lp02, *ΔdotA, ΔpsrA* and *ΔpsrA* compl strains. Infections were performed in a similar manner as in the intracellular growth kinetics studies; however, this time the macrophage cells were adhered to the coverslips for microscopic examination. After 24 hours of incubation, the cells were then treated with anti-DAPI, anti-Calnexin and anti-Lp1 antibodies to stain the cell nucleus, endoplasmic reticulum (ER) and LPS of *L. pneumophila*, respectively. As shown in Figure 3.41, the wildtype Lp02 strain successfully infected most of the cells as LCVs were clearly visible and lots of rod forms of *L. pneumophila* were present within LCVs or

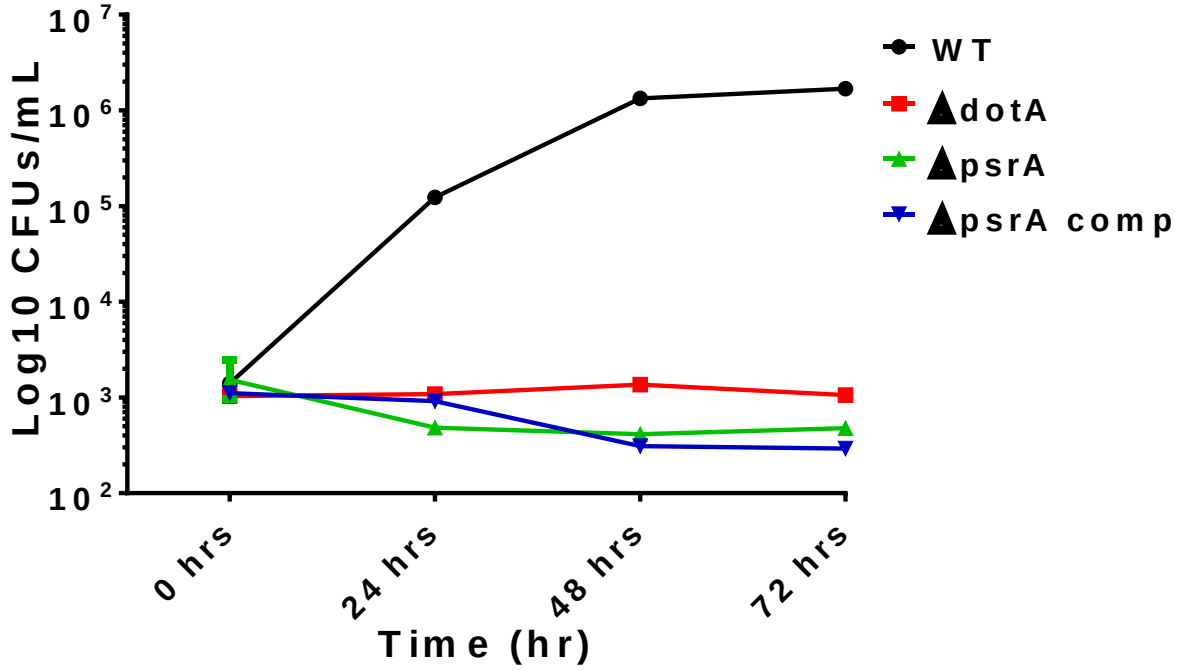

Figure 3.40: Intracellular growth kinetics in U937 cells. Lp02 WT, *ΔdotA, ΔpsrA* and *ΔpsrA* complement strains were used to infect U937 human macrophage cells at a MOI of 2. Macrophage cells were lysed at selected time points and CFU counts were determined via serial dilution plating method. The error bars represents SEM. Data represents an average from three independent experiments.

associated with the ER membrane (Figure 3.41). Thus Lp02 was able to evade the lysosomal degradation and replicate within LCVs. The Δ*dotA* mutant strain was used as a negative control and as expected no LCV formation was observed with very few rod forms present in the cytoplasm (Figure 3.42). Judging from the low bacterial cell count, it was believed that the Δ*dotA* mutant strain was unable to replicate within the macrophages as expected because of the lack of LCV formation. In the case of Δ*psrA* infections, the macrophage cells were healthy and no rod-forms were visible. This clearly shows that all the bacterial cells were degraded. Moreover, no LCVs were found with this strain further supporting the molecular studies (Figure 3.42). However, the Δ*psrA* complement strain was unable to rescue the wildtype phenotype and similar phenotype as in *psrA* mutant was observed (Figure 3.43). Thus, Δ*psrA* mutant is unable to survive within macrophage and gets degraded by the lysosomal pathway within first 24 hours.

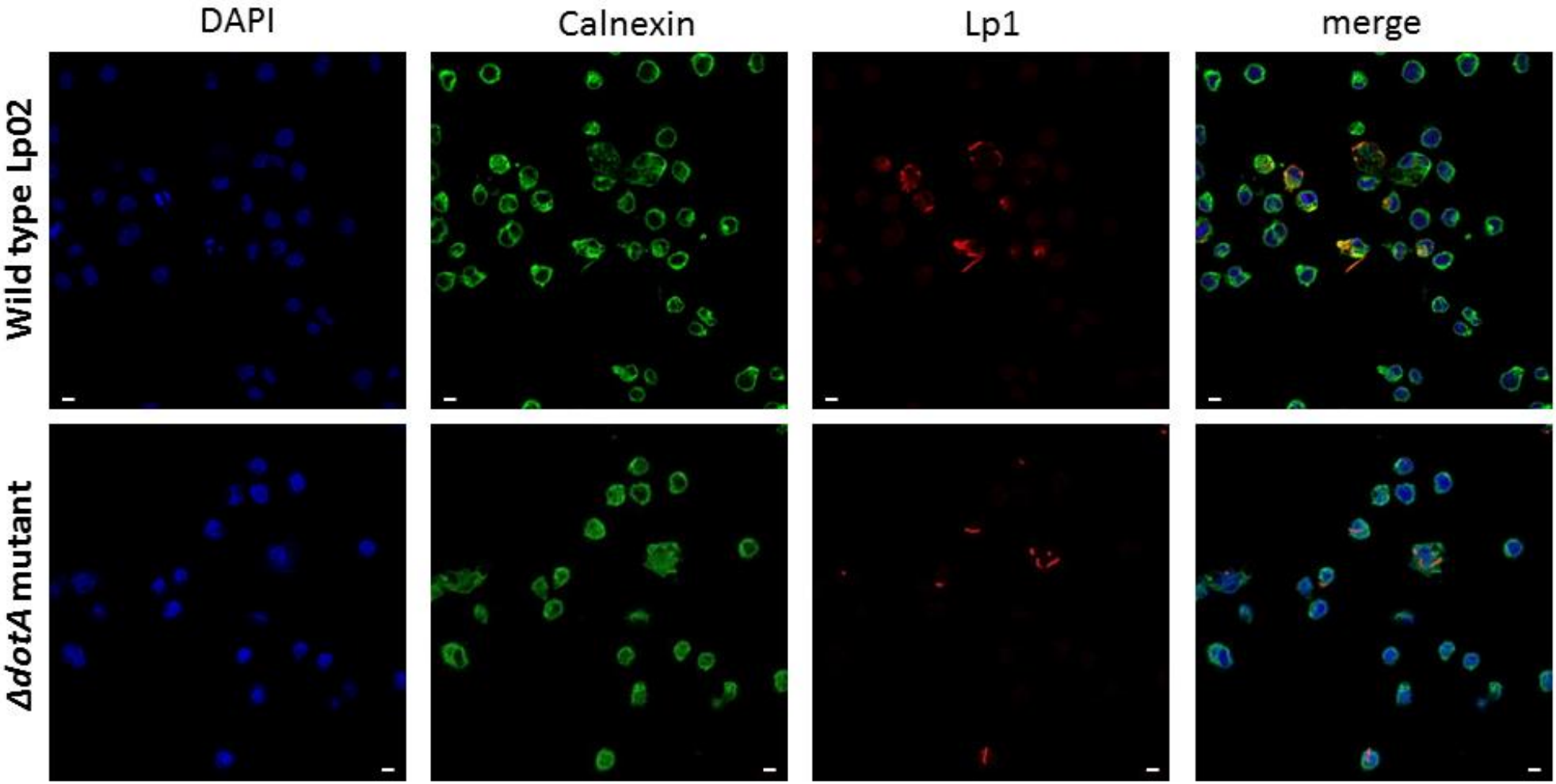

Figure 3.41: Immunofluorescence studies with wildtype Lp02 and *ΔdotA* mutant strains. Lp02 and *ΔdotA* stains were used to infect U937 cell line for 1hr with MOI of 2. After 24 hours of incubation, the cells were stained with anti-DAPI, anti-Calnexin and Lp1 which stain nucleus, ER and *L. pneumophila*, respectively. The cells were imaged under LSM 700 confocal microscope. Scale bars: 5µm

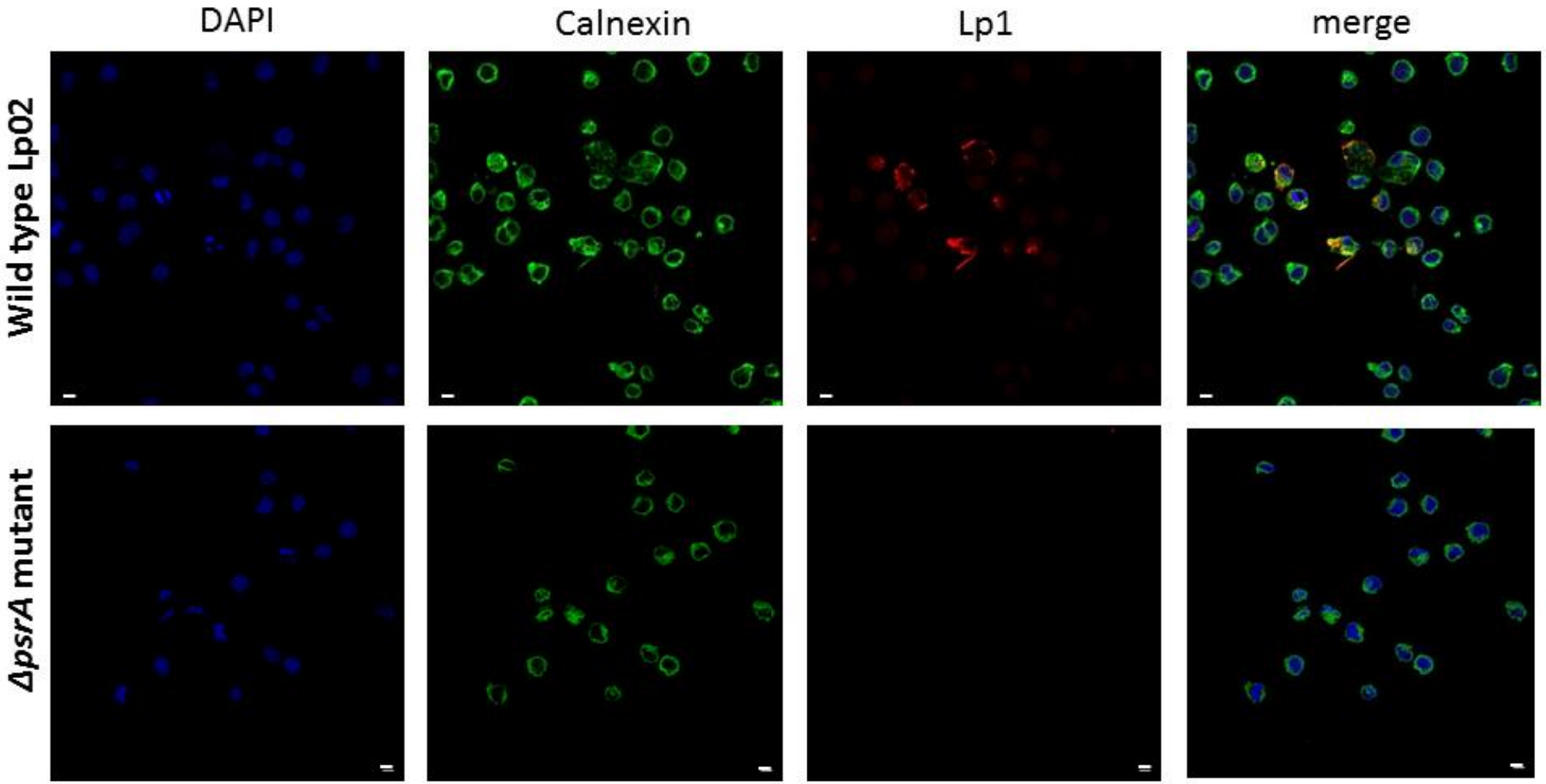

Figure 3.42: Immunofluorescence studies with wildtype Lp02 and *ΔpsrA* mutant strains. Lp02 and *ΔpsrA* stains were used to infect U937 cell line for 1hr with MOI of 2. After 24 hours of incubation, the cells were stained with anti-DAPI, anti-Calnexin and Lp1 which stain nucleus, ER and *L. pneumophila*, respectively. The cells were imaged under LSM 700 confocal microscope. Scale bars: 5µm

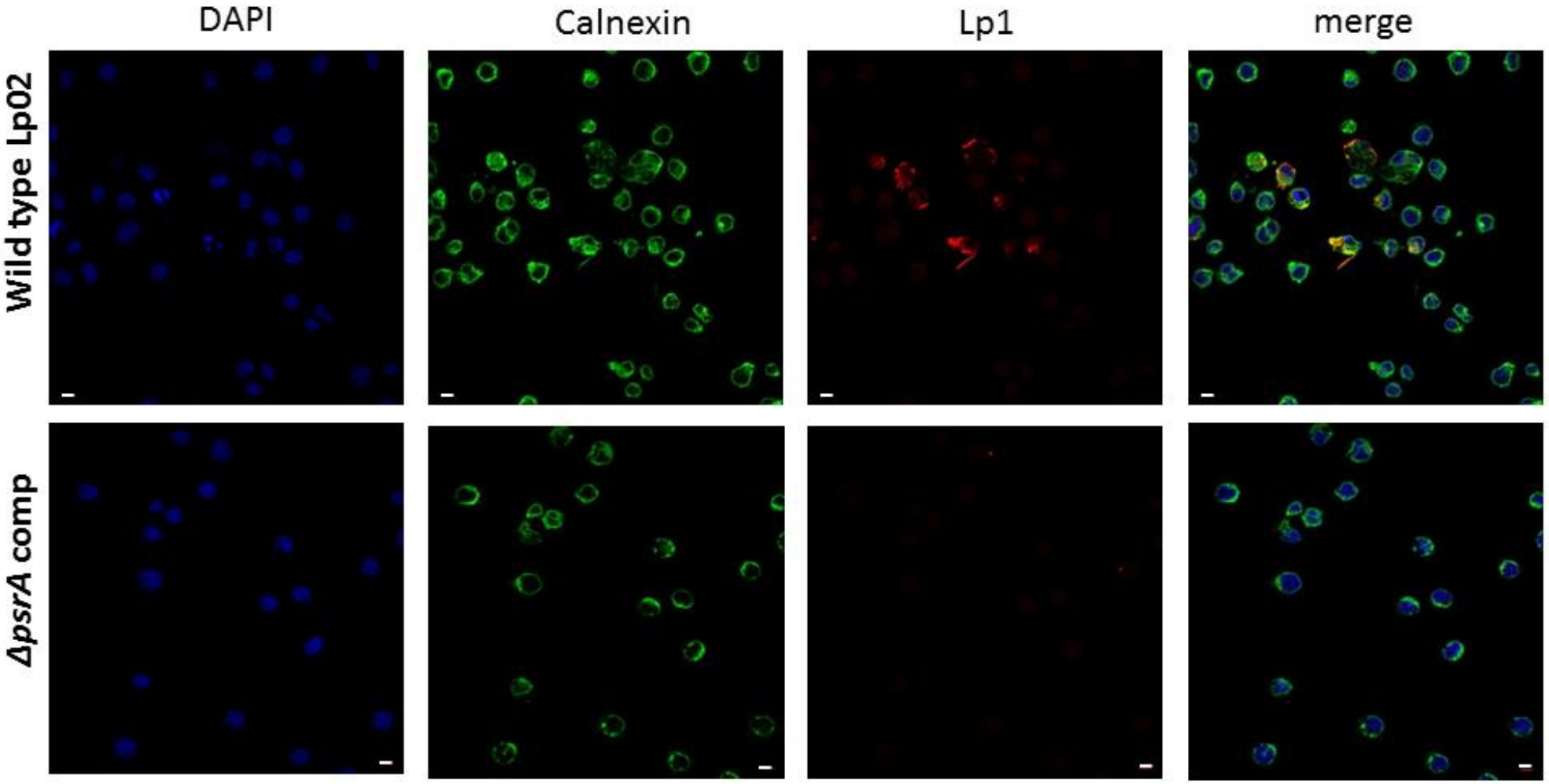

Figure 3.43: Immunofluorescence studies with wildtype Lp02 and *ΔpsrA* complement mutant strains. Lp02 and *ΔpsrA* compl stains were used to infect U937 cell line for 1hr with MOI of 2. After 24 hours of incubation, the cells were stained with anti-DAPI, anti-Calnexin and Lp1 which stain nucleus, ER and *L. pneumophila*, respectively. The cells were imaged under LSM 700 confocal microscope. Scale bars: 5µm

Chapter 4: Discussion

Legionella pneumophila, an intracellular pathogen of protozoa, is well known for its dimorphic life cycle that alternates between the vegetative replicative form (RF) and cyst-like form (CLF) (Garduño, Margot, & Hoffman, 2002). CLFs has been shown to be hyper infectious and it is believed that upon inhalation of aerosols containing CLFs by humans, *L. pneumophila* opportunistically infect alveolar macrophages, eventually causing a typical pneumonia known as the Legionnaires' disease or legionellosis in immunocompromised or elderly individuals (Garduño, 2007). The LetA-RsmYZ-CsrA regulatory cascade and the Dot/Icm secretion system along with the effector proteins have been shown to be vital for infection and intracellular survival of *L. pneumophila* within macrophages (Hammer, Tateda, & Swanson, 2002; Lynch *et al*., 2003; Rasis & Segal, 2009; Segal, Feldman, & Zusman, 2005). Regulatory proteins such as IHF have been shown to be involved in the regulation of cyst-biogenesis (Morash *et al*., 2009). In addition, the CpxR/CpxA and PmrB/PmrA are two-component systems associated with the regulation of the Dot/Icm secretion system and the effector proteins (Gal-Mor and Segal, 2003; Zusman *et al.*, 2007). Thus, virulence traits in *L. pneumophila* are regulated by a variety of regulatory proteins; however, not much is known about the triggers which initiate the transformation from RF to CLFs. As previously stated, inhibition of fatty acid biosynthesis, excess amount of short chain fatty acids and accumulation of guanosine tetraphosphate (ppGpp) can initiate the stringent response ultimately leading to cyst-biogenesis (Edwards, Dalebroux, & Swanson, 2009; Hammer & Swanson, 1999). In *Pseudomonas* species, a TetR-family regulator, PsPsrA was found to regulate several virulence traits by responding to the changes in fatty acid levels in the surroundings (Kang *et al.*, 2009; Kang *et al.*, 2008). In this study, we show that

a novel TetR family regulator, PsrA (Lpg1967), orthologous to PsPsrA controls the expression of several proteins known to be associated with virulence in *L. pneumophila.*

4.1 PsrA, a TetR family transitional regulator

In *Pseudomonas* species, PsPsrA has been characterised as a TetR-family regulator and is found to be involved in various processes ranging from energy metabolism to the regulation of type III secretion system (Kojic *et al*., 2005; Shen *et al.*, 2006). Moreover, PsPsrA was found to regulate the genes associated with motility and quorum sensing and it seems that PsPsrA is playing a prominent role in virulence in *Pseudomonas* species by responding to the chances in fatty acid levels in surroundings (Kang *et al.*, 2008). Interestingly, PsrA has only been studied in *Pseudomonas* species and *A. vinelandii,* so not much is known about the regulatory functions of its orthologues in other bacteria.

The purpose of this study was to identify and characterise the PsPsrA orthologue in *L. pneumophila.* The TetR family regulator PsrA (Lpg1967) has a predicted helix-turn-helix (HTH) DNA binding domain located within first 60 amino acid region (Table 3.1). Moreover, this gene was predicted with extremely low coverage and low score suggesting a poor homology between PsrA and PsPsrA (Table 3.1). Thus, to further verify the homology, secondary structures of both proteins were compared using PRALINE and InterProScan 5, and PsrA was confirmed to be a TetR family regulator with DNA binding domain at the N-terminus. Further analysis of their crystal structures showed that both proteins are homodimers and structurally similar over all 10 α-helices (Figure 3.1). With the poor homology and sequence differences in mind, it was believed that PsrA might not respond similarly to the fatty acid changes in the surroundings and could very well have completely different consensus binding site sequence than PsPsrA.

The footprint assays performed in this study showed that PsrA recognised the following consensus sequence which is rich in thymidine (T) and adenine (A): TWYTTAM (W: A or T; Y: C or T; M: A or C). This sequence is completely different from PsPsrA consensus sequence (C/GAAACN$_{2\text{-}4}$GTTTG/C) as expected from the bioinformatic analyses. More variation in the PsrA consensus binding site sequence was seen in comparison to that of PsPsrA suggesting the extensive and diverse regulatory role of PsrA in *L. pneumophila.* To further examine the role of PsrA, in-frame deletion of *psrA* gene was performed in *L. pneumophila* and the loss of *psrA* was confirmed by PCR and sequencing.

4.2 The regulation of *ihfA* and *ihfB* by PsrA

In *E. coli,* integration host factor (EcIHF) is a heterodimeric protein encoded by *himA* and *himD* genes and it is believed that EcIHF controls the expression of genes by inhibiting or promoting the interaction of other regulators or proteins with DNA (Aviv and Giladi, 1994). IHF is highly conserved in many bacteria, and in *E. coli* it is known to be involved in cell differentiation and virulence by acting as a transcription regulator (Aviv and Giladi, 1994). In *Vibrio cholera*, VcIHF is known to regulate pilus and cholera toxin, and similar results have also been found in other bacteria (Stonehouse *et al.*, 2008).

In *L. pneumophila,* IHF is encoded by *ihfA* and *ihfB* genes and studies involving gene deletion strains showed that IHF is required for cyst-biogenesis (Morash *et al.*, 2009). These genes are positively regulated by RpoS and negatively regulated by LetA (Figure 5.2, 5.3) (Pitre *et al*., 2013). Thus, RpoS, LetA and IHF are required for full expression of *ihfA* and *ihfB*; however, here we show the first evidence of *ihfA* and *ihfB* being regulated by PsrA. Even though the TetR family regulators have been classified to be repressors in most cases (Ramos *et al.*, 2005), in *L. pneumophila* PsrA positively regulates *ihfA* expression and

is required for its full expression. Footprint studies on *ihfA* promoter showed that PsrA was binding upstream of the -35 promoter element suggesting a possible regulation by Class I activation where PsrA could be recruiting the polymerase to the promoter (Figure 3.22B)(Browning and Busby, 2004). Furthermore, PsrA negatively regulates the expression of *ihfB* since the expression was doubled in the absence of PsrA. Promoter analysis on *ihfB* gene showed that PsrA does not cover the -35 and -10 promoter elements like in the other cases to prevent the recognition of the promoter by RNA polymerase holoenzyme (Figure 3.24B). Moreover, it seems that *ihfB* is the limiting factor for the heterodimeric IHF protein levels since it is expressed at very low levels compare to *ihfA*. Footprint analysis showed more than one protected regions and due to the short sequencing ladders, it was not possible to get the sequence for the other footprints. However, this result does support the bioinformatic analyses and EMSA studies showing more than binding sites for PsrA within these promoter regions. Thus, it seems that by regulating *ihfB,* PsrA can tightly control the expression of the functional IHF protein. Since IHF has been shown to be involved in cyst-biogenesis and RsmYZ regulation, it can be argued that PsrA could exert similar effect as IHF in *L. pneumophila*.

Further comparison of the GFP expression profiles of *ihfA* and *ihfB* in Δ*rpoS*, *ΔletA* and Δ*ihf* background indicated that IHF could be negatively auto regulated; however, the results were inconclusive (Pitre *et al.*, 2013b). To address this issue, Δ*rpoS*Δ*letA* double mutant was created with an assumption that RpoS and LetA are the only regulators of *ihfA* and *ihfB* genes. It was found that IHF positively regulates *ihfA* and *ihfB* genes (Figure 5.4, 5.5). Oddly, the *ihfA* gene expression profile in Δ*rpoS*Δ*letA* strain was very similar to the one seen in the *ΔpsrA* mutant strain background. Thus, it is not clear about *ihfA* being

autoregulated by IHF since PsrA is also acting as activator; however, the data presented in this study is sufficient to determine that *ihfB* is positively regulated by IHF.

4.3 The regulation of *rpoS* and *psrA* genes

Research studies in *Pseudomonas* species have shown that PsPsrA controls the expression of *rpoS* gene and is negatively autoregulated as its expression in *ΔpsrA* mutant strain background was significantly elevated (Kojic *et al.*, 2002). Thus, PsPsrA was identified to be a strong regulator of these genes and this orthologous function was further investigated in *L. pneumophila.* Compared to the Lp02 strain, *rpoS* expression was barely affected in the Δ*psrA* mutant strain background with somewhat significant elevation in the expression values in the post-exponential growth phase (Figure 3.25A). Unlike in *Pseudomonas* species, PsrA acts as a repressor of *rpoS* gene and was found to have multiple binding sites within the *rpoS* promoter region as evidenced from the EMSA and DNaseI footprint studies. Promoter analysis showed that one of the protected regions covered the -35 and -10 promoter element along with the first 40 bp of the coding sequence of *rpoS* (Figure 3.28B). Thus, it seems that PsrA is preventing the transcription of the *rpoS* gene by the resulting steric hindrance from covering the promoter regulatory elements. It was believed that the binding of more than one PsrA protein within the *rpoS* promoter region was the reason behind this massive protected region. Judging by the promoter analyses, the repression of *rpoS* seems to be strongly regulated; however, the GFP reporter assays showed a minor effect on the regulation of *rpoS* gene. These results were contradicting and could indicate a possible competition between PsrA and other regulators for the binding site within the promoter region of *rpoS* gene.

Furthermore, there was a 20-fold increase in the *psrA* expression in the *ΔpsrA* mutant strain background indicating a strong negative auto-regulation by PsrA (Figure 3.25B). These results were confirmed by EMSAs and DNaseI footprint studies in which two protected promoter regions were identified within the *psrA* promoter region. The promoter analyses showed that PsrA covered the -35 promoter element and the ribosomal binding site along with first 50bp of the *psrA* coding sequence preventing the binding of RNA polymerase holoenzyme (Figure 3.30B). Similar results were shown with respect to the PsrA auto regulation in *Pseudomonas* species. Thus, PsrA seems to have a major effect on its own regulation and is expressed mainly during the post-exponential growth phase, whereas the RpoS expression is not significantly affected. Not much is known about regulation of RpoS during the post exponential growth phase in *L. pneumophila* and most of the studies have shown ppGpp being the key trigger responsible for the expression this gene (Molofsky and Swanson, 2004). In this study, we show PsrA as another regulator of *rpoS;* however, its effect on the *rpoS* expression is significant only in stationary growth phase. PsrA also had significant effect on the *oxyR* regulation as the GFP reporter assays showed a drastic hike in the expression of *oxyR* during the transition to post exponential growth phase in the *ΔpsrA* mutant strain background. Later it was found that this interaction is direct and thus it seems that PsrA might be repressing the expressions of *rpoS* and *oxyR* to efficiently utilize the nutrients and energy sources in the activation of virulence traits.

4.4 PsrA and the LetA-RsmYZ-CsrA regulatory cascade

LetA is a response regulator of LetA/LetS two component system and is known to control the expression of non-coding RNAs RsmY and RsmZ. Upon activation, the response

regulator LetA recognizes the TNAGAAATTTCTNA palindromic sequence located upstream of the RsmY and RsmZ non-coding RNAs and mediates the expression of these non-coding RNAs (Sahr *et al*., 2009). RsmY and RsmZ bind to CsrA which further promotes or represses the expression of specific mRNAs by binding near the ribosome binding site. In the presence of RsmY and RsmZ, CsrA is sequestered and the mRNAs for the virulence traits are available for translation (Sahr *et al*., 2009). Recently it was found that RsmY expression was completely abolished in *Δihf* and *ΔletA* mutant strains whereas RsmZ expression was reduced by 60% in these mutant strains (Pitre *et al*., 2013). These data indicated that RsmZ could be under control of other unknown regulator(s). Recently, PsPsrA was found to control the expression of RsmZ but not RsmY, in *Pseudomonas* species (Humair *et al.*, 2010).

Unlike in *Pseudomonas* species, both RsmY and RsmZ expressions were significantly reduced in the Δ*psrA* mutant strain background signifying the role of PsrA in their regulation in *L. pneumophila* (Figure 3.14D). The EMSAs and DNaseI footprint studies showed that PsrA had multiple binding sites within the promoter regions of both non-coding RNAs. RsmZ promoter analysis showed that PsrA covered the -35 promoter element showing a possible Class I activation regulation (Figure 3.18B). Moreover, it seems that three regulatory proteins (LetA, IHF and PsrA), are required for full expression of these noncoding RNAs. Noncoding RNAs RsmY and RsmZ are required for successful infection and intracellular growth within macrophages and protozoa (Sahr *et al*., 2009). These data explains why the Δ*psrA* mutant strain was defective in infecting and replicating within the U937 derived macrophages. Thus, the Δ*psrA* mutation effects a drastic reduction in the

expression of RsmY and RsmZ ultimately leading to impaired intracellular replication and defective infection cycle.

4.5 PsrA role in general virulence

As mentioned earlier, several regulatory systems have been identified to control the expression of the *dot/*icm genes. The CpxR/CpxA component system has been shown to regulate several dot/icm genes however; PmrB/PmrA is also believed to be more involved in the regulation of these genes (Gal-Mor and Segal, 2003; Zusman *et al.*, 2007).

In this study we report that PsrA is required for the full expression of *icmR, icmT, icmV* and *dotD* genes. However, the precise mode of action behind this regulation is not known except for *icmR* where EMSA and footprint studies have shown a direct regulation of by PsrA. The *icmR* promoter analyses showed that PsrA bound to a region that covered the -35 promoter element indicating the role of PsrA as an enhancer (Figure 3.34B). Moreover, *icmT* and *icmS* expression is driven by the same *icmT* promoter and since the GFP reporter assays showed positive regulation of *icmT* by PsrA (Figure 3.31B), it is assumed that PsrA exerts similar effect on the *icmS* expression. Similarly through the GFP reporter assays, PsrA was found to be an activator of *dotD* and repressor of *icmV* (Figure 3.31C, 3.35). Moreover, both *dotC* and *dotA* were thought to be regulated by PsrA since they are in operons and share promoter regions with *dotD* and *icmV*, respectively. Interestingly, *icmW* and *icmX* genes are divergently expressed from the *icmV* promoter, so it is very likely that these genes are also under PsrA regulatory control.

Thus, these data show that PsrA is required for full expression of several of the *dot*/*icm* genes and as mentioned earlier, the Dot/Icm secretion system is required for successful infection and intracellular replication within macrophages (Newton *et al*., 2010).

As shown in the immunofluorescence studies, no LCVs were found in U937 macrophages infected with Δ*dotA* or Δ*psrA* mutant strains indicating defective intracellular growth (Figure 3.41, 3.42). Likewise, the same defective intracellular growth phenotype was observed in macrophages infected with the Δ*psrA* complement strain (Figure 3.43). It is not clear the reason why the wild-type phenotype was not rescued. Once possibility could be the toxic effect from over-expression of PsrA as seen elsewhere (Papavinasasundaram *et al.*, 1998). Overall, PsrA seems to be deeply involved with the regulation of the whole type IV secretion system in *L. pneumophila.*

In *P. aeruginosa*, swarming motility was greatly impaired in the Δ*psrA* mutant strain (Overhage *et al.*, 2007). Swarming motility involves the use of flagella, type IV pili and genes from type II secretion system (Overhage *et al.*, 2007). In *L. pneumophila*, flagella are a key feature of CLFs with expression initiating in post-exponential growth phase. The GFP reporter assays determined that PsrA strongly regulates the expression of *flaA* and thus, PsrA was found to be a positive regulator of this gene (Figure 3.36). Thus, PsrA appears to be a global regulator that plays an integral role in expressing virulent traits during exponential and post-exponential growth phases in *L. pneumophila.*

4.6 Summary

In this study, a TetR-family regulator PsrA (Lpg1967), was identified as an orthologue of PsPsrA and was characterised to be a vital virulence factor in *L. pneumophila*. PsrA positively regulates the expression of RsmY and RsmZ non-coding RNAs directly. Moreover, *ihfA* and *ihfB* genes were also regulated by PsrA and thus, it is also associated with cyst-biogenesis. Interestingly, PsrA is negatively autoregulated as demonstrated with EMSAs and DNaseI footprint studies. In addition, weak negative regulation of *rpoS* gene by

PsrA was also observed. Moreover, the Dot/Icm secretion system components and flagellin were also regulated by PsrA showing an integral role of PsrA as a transcription regulator in governing the virulence cascade in *L. pneumophila*. Interestingly, PsrA recognises the following consensus sequence as the binding site: TWYTTAM, which is completely different from the PsPsrA palindromic binding sequence. In addition, the Δ*psrA* mutant was unable to grow within U937 macrophage cell line with defect in LCV formation. Thus, the proposed regulatory model of PsrA in *L. pneumophila* is shown in Figure 4.1.

4.7 Future directions

Now that we have identified PsrA as a critical virulence factor, the next thing will be to investigate if the PsrA activity can be affected by the fatty acid chain levels in the environment. DNaseI footprint studies on *rsmY* and *oxyR* promoter regions will be performed and these results will be used to further analyse the consensus binding site sequence. Since the Δ*psrA* complement stain failed to rescue the wildtype Lp02 phenotype, chemo luminescent immunoblots will be performed to confirm the PsrA protein production from the complement vector. In addition, q-PCR will be performed to further support the GFP reporter assay results. The regulatory role of PsrA will further be investigated with the following gene targets: *letA* and *dotA*. As mentioned in the discussion section, the autoregulatory role of IHF is still not clear and GFP expression from the α1 & β1 GFP promoter constructs will be measured in *ΔihfAΔihfBΔletAΔrpoSΔpsrA* mutant strain background since all three proteins are known to control their expression. Lastly, EMSAs studies will be performed with PsrA, LetA, RpoS and IHF to further determine the affinity of these proteins for promoter regions of target genes. These future experimental approaches

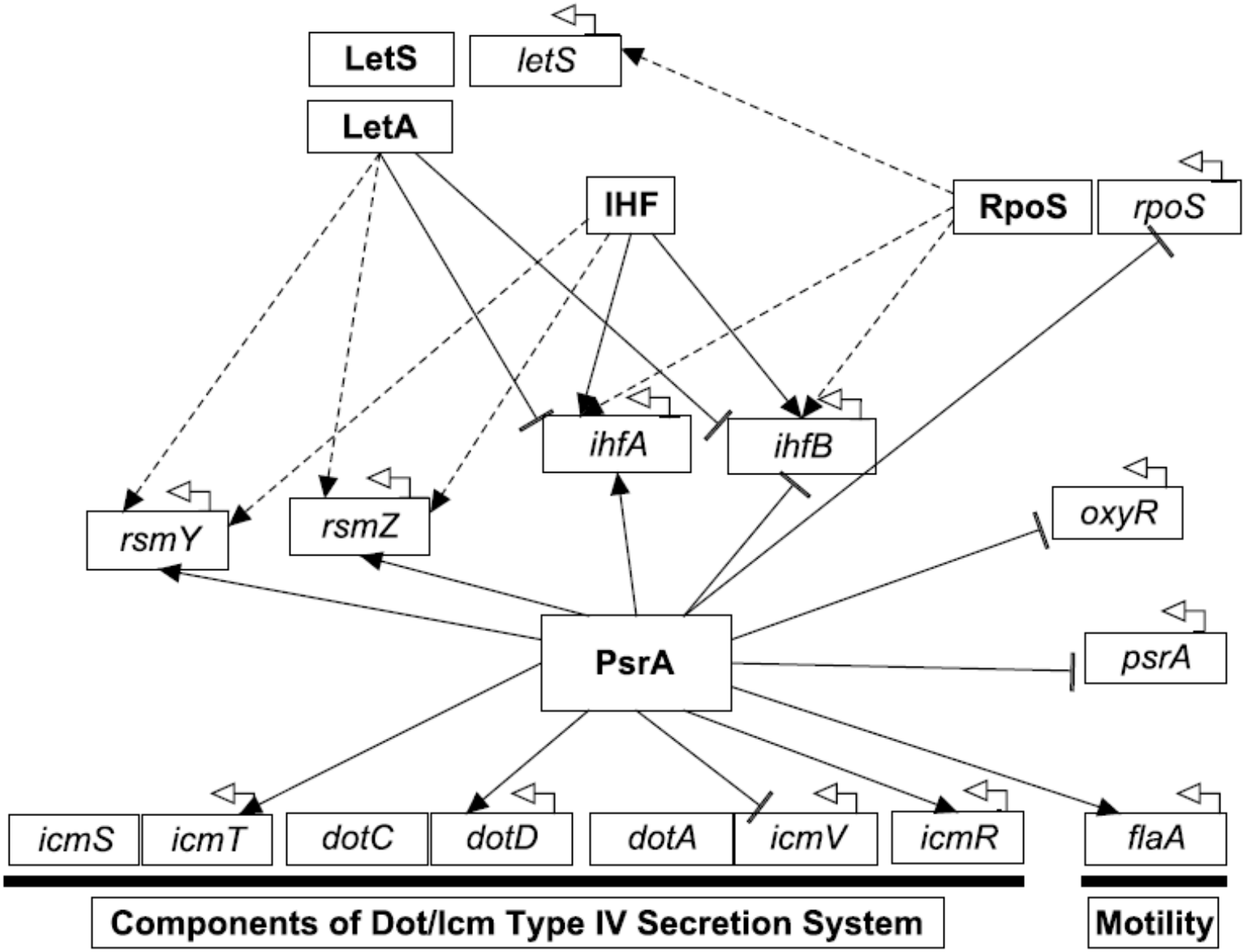

Figure 4.1: Proposed regulatory model involving PsrA. The results from the molecular studies were used to create the regulatory pathway for PsrA in *L. pneumophila* virulence as indicated by the solid lines. Interactions are represented by: arrows for positive regulation, T bar for negative regulation and dashed lines for previously known interactions. See text for details.

will be supported by infection studies in protozoa and macrophage cell-lines to differences, if any, in virulence.

Chapter 5: Appendix

5.1 LetA regulation in *ihfA* and *ihfB* genes

To evaluate the functional role LetA in the regulation of *ihfA* and *ihfB* genes, the truncated promoter GFP constructs of *ihfA* and *ihfB* were used (Figure 5.1) (Pitre *et al*., 2013). These reporter constructs have been previously described and were electroporated in Lp02 and Δ*letA* mutant strains to further evaluate the promoter activity of these genes via GFP reporter assays. In Lp02, the α1-7 GFP reporter constructs had very similar GFP expression levels which a steady after the lag phase. However, the α8 construct had the basal level of expression as expected since most of the *ihfA* promoter region is truncated from the 5'end (Figure 5.2A). During the lag growth phase the GFP expression from α1-8 constructs stayed constant in the Lp02 strain background (Figure 5.2A).

Interestingly, there was an increase of about 600 RFU/OD_{600} units in the GFP expression levels in the Δ*letA* mutant strain background (Figure 5.2B). During the lag growth phase there was a constant decline in fluorescent expression from the α1-7 constructs which started to increase at a steady rate during the exponential growth phase (Figure 5.2B). The α8 strain had very similar expression levels as in the Lp02 strain background; however, the expression was elevated by 500 units during the log growth phase in the Δ*letA* mutant strain background (Figure 5.2B). Thus, LetA seems to be acting as a repressor of *ihfB* gene.

Similarly, expression profiles for the β1-7 constructs were developed in the Lp02 and Δ*letA* mutant strain backgrounds. In Lp02, the expression was detected only from the β1-3 construct during the log and post-exponential growth phases (Figure 5.3A). The β4-7 constructs were defective in GFP expression suggesting that the regulatory controls lie

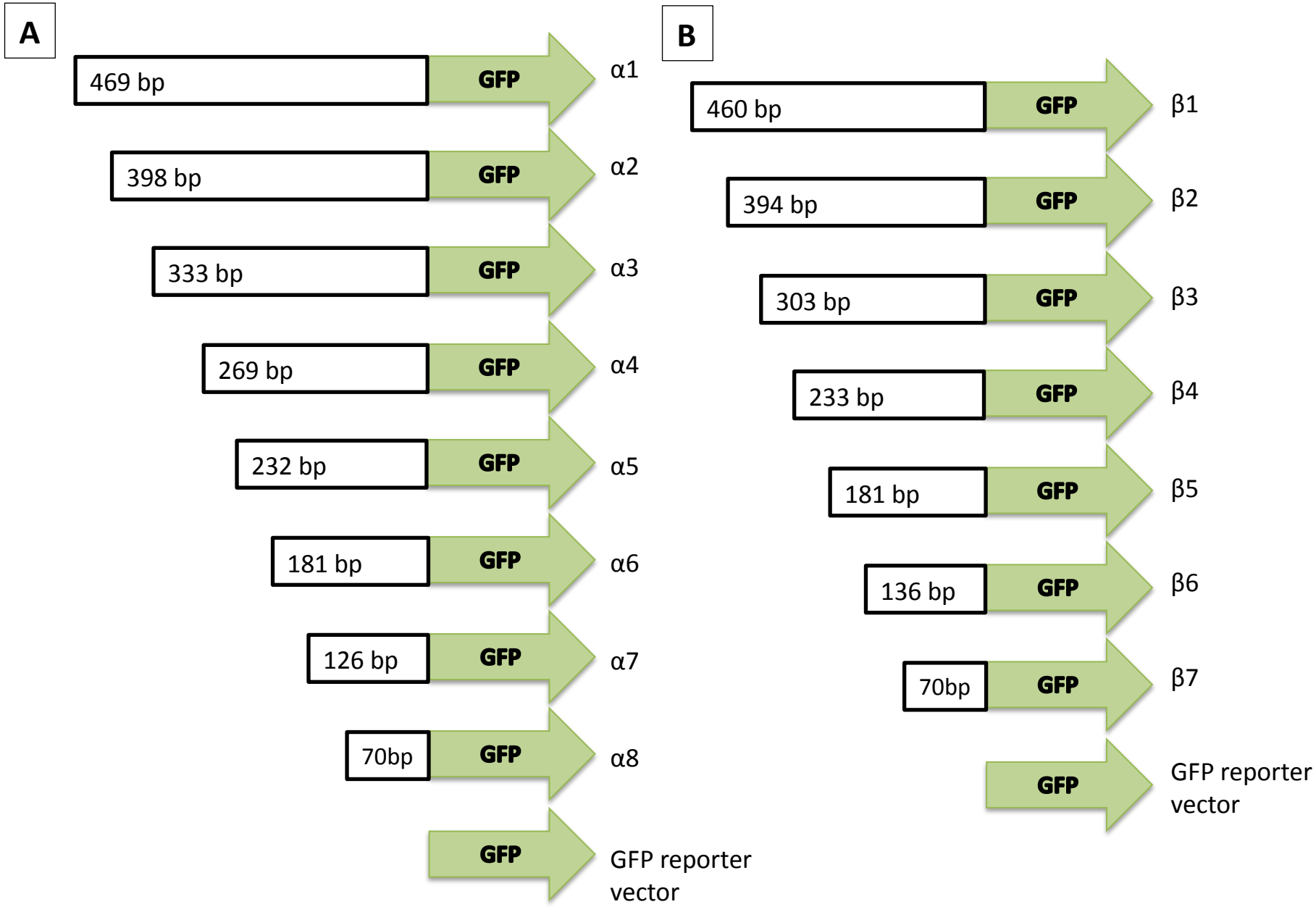

Figure 5.1: Construction of α-GFP and β-GFP fusion constructs. Truncated promoter regions of *ihfα* (A) and *ihfβ* (B) genes were cloned into pBH6119 promoterless vector for the purpose of GFP reporter assays. Figures adapted from Pitre et al.,2013.

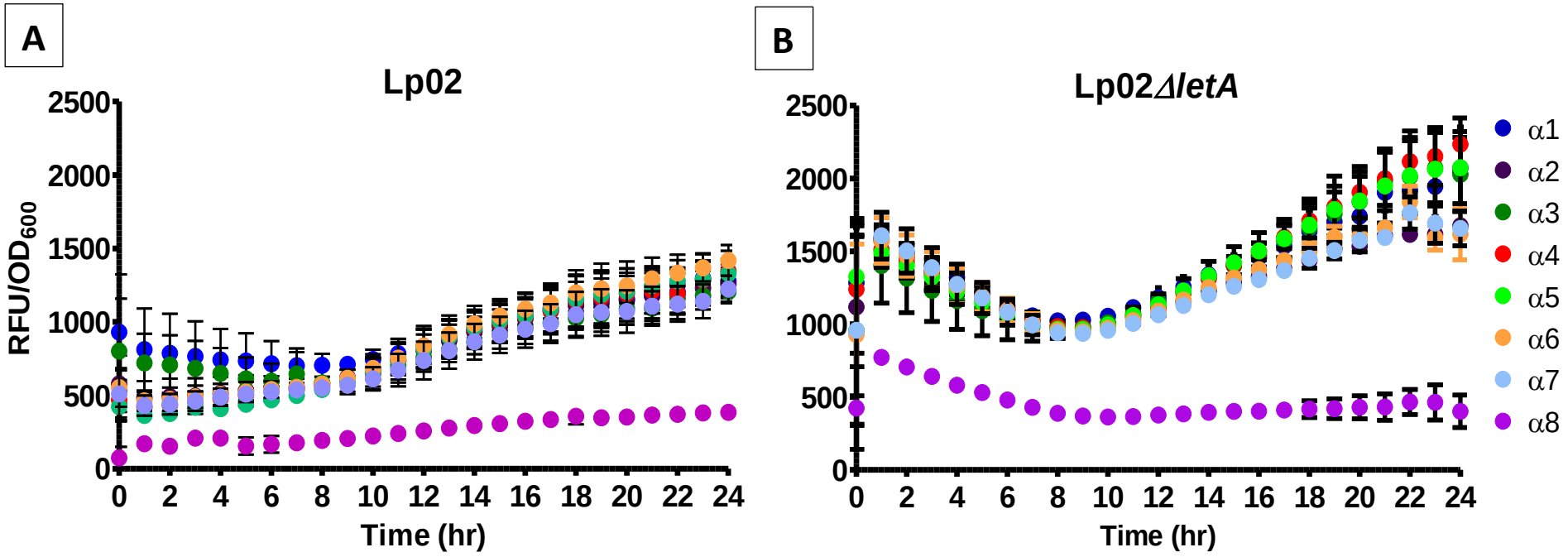

Figure 5.2: GFP expression profiles of *ihfα*. Florescence was detected from the α-GFP reporter plasmids on an hourly basis for 24 hours in Lp02 (A) and Lp02*ΔletA* (B) background. Error bars represents SEM. Data represents an average from three independent experiments. Figures adapted and modified from Pitre, C *et al.,* 2013.

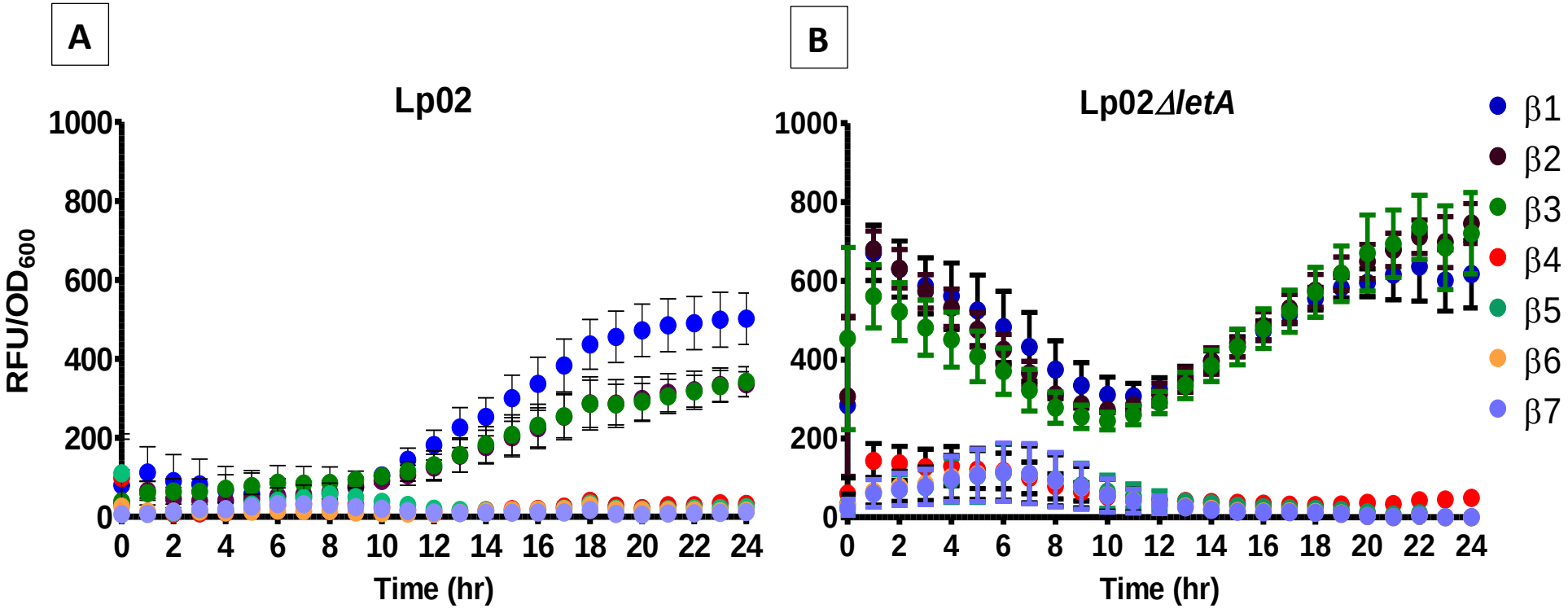

Figure 5.3: GFP expression profiles of *ihfB*. Florescence was detected from the β-GFP reporter plasmids on an hourly basis for 24 hours in Lp02 (A) and Lp02*ΔletA* (B) background. Error bars represents SEM. Data represents an average from three independent experiments. Figures adapted and modified from Pitre, C *et al.,* 2013.

between -460 to -303 regions of the *ihf*B promoter. There was no change in the GFP expression during first few hours and the fluorescent levels reached maximum (600 RFU/OD_{600} units) at the post-exponential growth phase (Figure 5.3A).

In Δ*letA* mutant strain background, the expression from the β1-3 constructs was significantly elevated during the lag growth phase (Figure 5.3B). Thus, the β1-3 construct expression started with 600 RFU/OD_{600} units in the Δ*letA* strain background reaching to the maximum of 700 RFU/OD_{600} units during the post-exponential growth phase (Figure 5.3B). Moreover, the β4-7 constructs had a minor peak in first few hours of the GFP assay; however, the no fluorescence was detected from β4-7 constructs during the log and post-exponential growth phase. Thus, this data show that LetA acts as a repressor of *ihfB* gene.

5.2 Double knockout (*ΔrpoSletA)* construction

As stated earlier, in *L. pneumophila* IHF is comprised of alpha subunit and beta subunit encoded by *ihfα* and *ihfβ* genes, respectively. Both of these genes are positively regulated by RpoS and negatively controlled by LetA (Pitre *et al.*, 2013). Pitre *et al*., 2013 stated that IHF could have an autoregulatory component and to further investigate this possibility *ΔrpoSletA* double mutant strain was constructed.

Similar knock out strategy was used to create *ΔrpoS* mutant as described in methods and materials. The pSR47S suicide vector (Figure 3.3) was used to clone the 5' and 3' flanking regions of *rpoS* using rpoS 5' and rpoS 3' primer set (Table 2.2). The RpoS KO vector (Table 2.3) was verified by PCR and sequencing. The plasmid was then electroporated in Lp02 strain and selection steps were followed as described in methods and materials. The same approach was used to create LetA KO (Table 2.3) vector and once the *ΔrpoS* mutant was verified by sequencing (For primers see Table 2.2), LetA KO vector

was electroporated in the Δ*rpoS* mutant strain. After selection and counter selection steps, the *ΔrpoSletA* double mutant was verified by PCR and sequencing.

5.3 IHF auto regulation

The α-GFP and β-GFP constructs were electroporated in *ΔrpoSletA* mutant strain and their expression profiles were developed. The expression data from α-GFP and β-GFP constructs in Lp02 strain has been described earlier. Interestingly, the expression profile in *ΔrpoSletA* background was very similar to the one seen in the Lp02 background (Figure 5.4). Thus it seems that LetA and RpoS are not essential for the expression of *ihfA* gene and the expression is either a result of IHF auto regulation or from unknown regulator. The β-GFP expression profile in Lp02 has been described previously and interestingly, β1-3 had expression levels that were a little lower during the exponential and post exponential phase compare to wildtype Lp02 (Figure 5.5). The expression from the other construct was very low in *ΔrpoSletA* as expected from Lp02. Thus, these data confirm that IHF positively regulates the expression of *ihfA* and *ihfB* genes. Moreover, all these experiments were done with an assumption that IHF is regulated by RpoS and LetA.

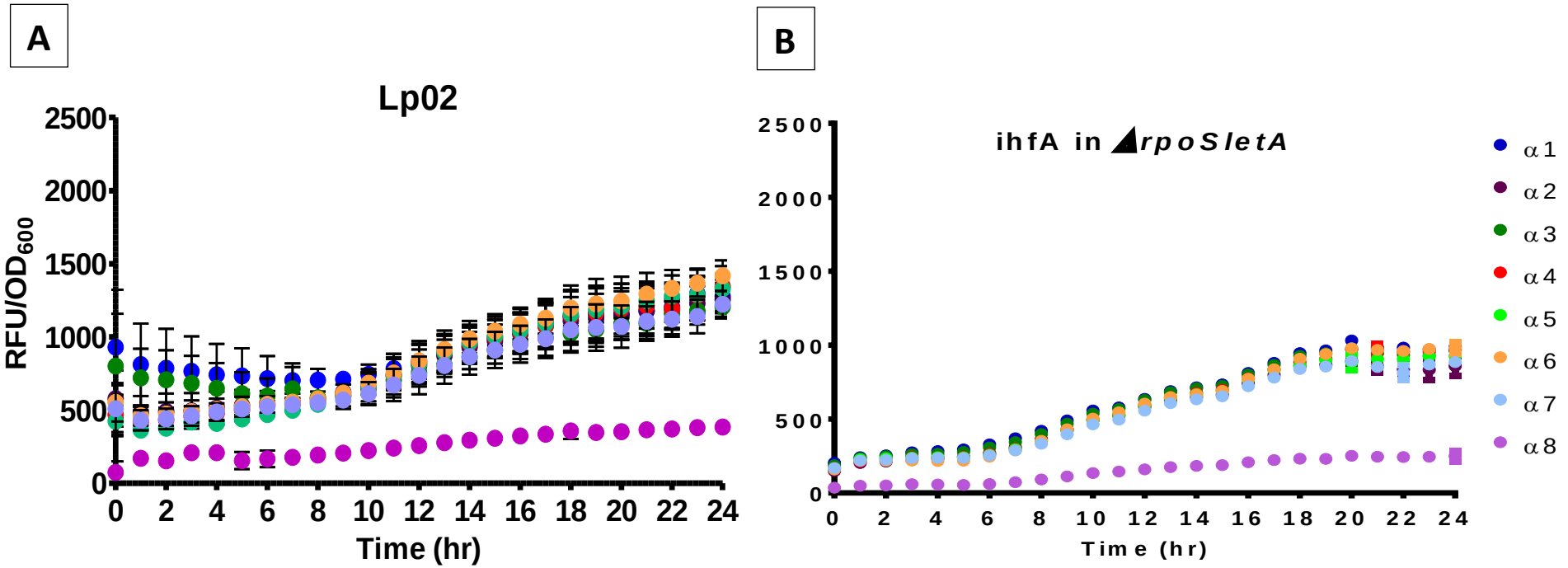

Figure 5.4: GFP expression profiles of *ihfA*. Florescence was detected from the α-GFP reporter plasmids on an hourly basis for 24 hours in Lp02 (A) and Lp02Δ*rpoS*Δ*letA* (B) background. Error bars represents SEM. Data represents an average from three independent experiments. Figures adapted and modified from Pitre, C *et al.,* 2013.

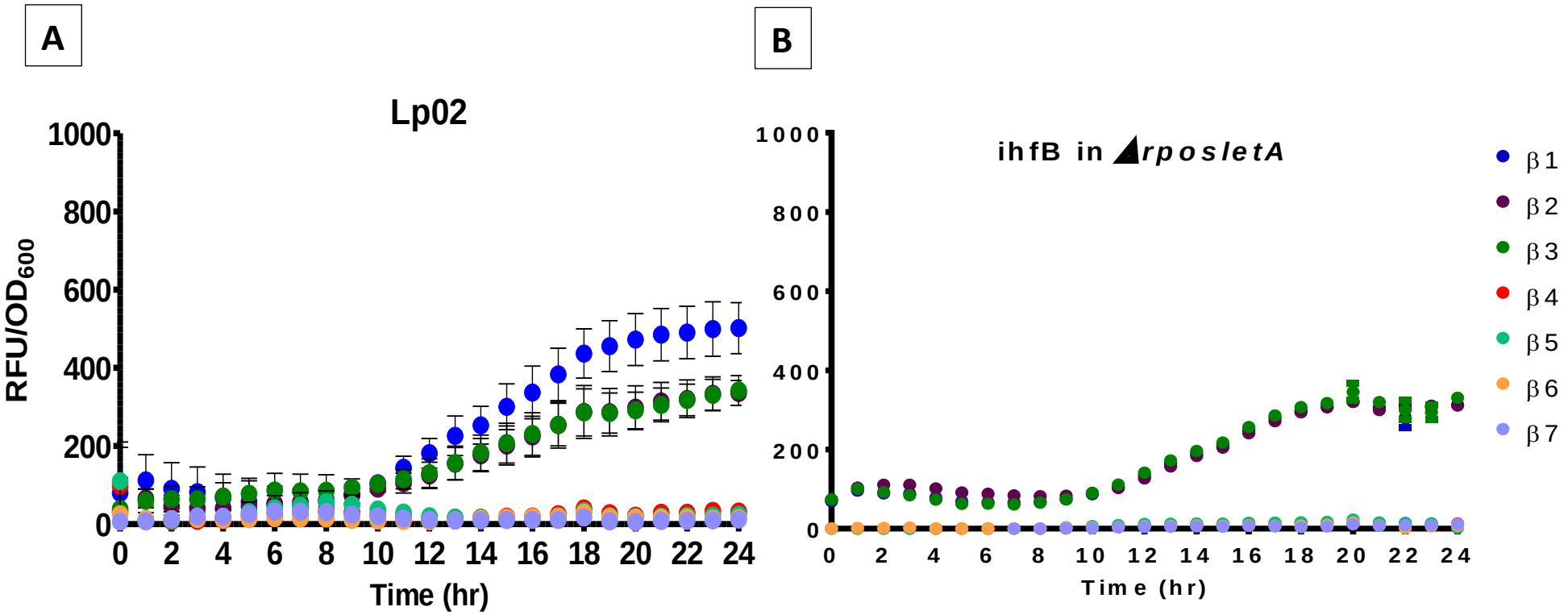

Figure 5.5: GFP expression profiles of *ihfB*. Florescence was detected from the β-GFP reporter plasmids on an hourly basis for 24 hours in Lp02 (A) and Δ*rpoS*Δ*letA* (B) background. Error bars represents SEM. Data represents an average from three independent experiments. Figures adapted and modified from Pitre, C *et al.,* 2013.

COLLABORATIONS

The following projects were collaborated with Miss Jennifer Tanner.

1. GFP reporter assays to assess the role of PsrA in the regulation of the Dot/Icm system
2. PsrA EMSAs and DNaseI footprinting studies on the *icmR* and *oxyR* promoter regions
3. GFP reporter assays to investigate the PsrA and CpxR role in *ihfA,* and *ihfB* regulation
4. PsrA, CpxR and OxyR EMSAs and DNaseI footprinting studies to study the binding sites on *icmR, oxyR,* and RsmZ promoters
5. Dideoxy-sequencing reactions for the following genes were prepared: *icmR, oxyR,* RsmZ, and RsmY
6. EMSA studies on the *rpoS* promoter regions were also performed with PsrA
7. Moreover, PsrA and CpxR functional role was characterised with respect to the motility (*flaA).*
8. PsrA and *oxyR* regulation was also studied.

REFERENCES

Altman, E., and Segal, G. (2008) The response regulator CpxR directly regulates expression of several *Legionella pneumophila* icm/dot components as well as new translocated substrates. *J Bacteriol* **190**: 1985–96

Altschul, S.F., Madden, T.L., Schäffer, a a, Zhang, J., Zhang, Z., Miller, W., and Lipman, D.J. (1997) Gapped BLAST and PSI-BLAST: a new generation of protein database search programs. *Nucleic Acids Res* **25**: 3389–402

Arvizu-Gómez, J.L., Hernández-Morales, A., Pastor-Palacios, G., Brieba, L.G., and Álvarez-Morales, A. (2011) Integration Host Factor (IHF) binds to the promoter region of the phtD operon involved in phaseolotoxin synthesis in *P. syringae* pv. phaseolicola NPS3121. *BMC Microbiol* **11**: 90

Aviv, M., and Giladi, H. (1994) Expression of the genes coding for the *Escherichia coli* integration host factor are controlled by growth phase, rpoS, ppGpp and by autoregulation. *Mol Microbiol* **14**: 1021–1031

Bachman, M. a, and Swanson, M.S. (2001) RpoS co-operates with other factors to induce *Legionella pneumophila* virulence in the stationary phase. *Mol Microbiol* **40**: 1201–14

Bachman, M.A., and Swanson, M.S. (2004b) Genetic evidence that *Legionella pneumophila* RpoS modulates expression of the transmission phenotype in both the exponential phase and the stationary phase. *Infect Immun* **72**: 2468–76

Bandyopadhyay, P., Xiao, H., Coleman, H.A., Price-Whelan, A., and Steinman, H.M. (2004) Icm/dot-independent entry of *Legionella pneumophila* into amoeba and macrophage hosts. *Infect Immun* **72**: 4541–51

Banerji, S., Bewersdorff, M., Hermes, B., Cianciotto, N.P., and Flieger, A. (2005) Characterization of the Major Secreted Zinc Metalloprotease- Dependent Glycerophospholipid : Cholesterol Acyltransferase , PlaC , of *Legionella* Characterization of the Major Secreted Zinc Metalloprotease- Dependent Glycerophospholipid : Cholesterol Acyltr. *Infect Immun* **73**: 2899–2909.

Battesti, A., Majdalani, N., and Gottesman, S. (2011) The RpoS-mediated general stress response in *Escherichia coli*. *Annu Rev Microbiol* **65**: 189–213

Berger, K.H., and Isberg, R.R. (1993) Two distinct defects in intracellular growth complemented by a single genetic locus in *Legionella pneumophila*. *Mol Microbiol* **7**: 7–19

Broich, M., Rydzewski, K., Mcnealy, T.L., Marre, R., and Flieger, A. (2006) The Global Regulatory Proteins LetA and Lysophospholipase A , Acyltransferase , and Other Hydrolytic

Activities of *Legionella pneumophila* JR32 The Global Regulatory Proteins LetA and RpoS Control Phospholipase A , Lysophospholipase A , Acyltransferase , a. *J Bacteriol* **188**: 1218.

Browning, D.F., and Busby, S.J. (2004) The regulation of bacterial transcription initiation. *Nat Rev Microbiol* **2**: 57–65

Brüggemann, H., Hagman, A., Jules, M., Sismeiro, O., Dillies, M.-A., Gouyette, C., *et al.* (2006) Virulence strategies for infecting phagocytes deduced from the in vivo transcriptional program of *Legionella pneumophila*. *Cell Microbiol* **8**: 1228–40

Carlson, H.K., Vance, R.E., and Marletta, M. a (2010) H-NOX regulation of c-di-GMP metabolism and biofilm formation in *Legionella pneumophila*. *Mol Microbiol* **77**: 930–942

Chatterji, D., and Ojha, A.K. (2001) Revisiting the stringent response, ppGpp and starvation signaling. *Curr Opin Microbiol* **4**: 160–5

Cocotl-Yañez, M., and Sampieri, A. (2011) Roles of RpoS and PsrA in cyst formation and alkylresorcinol synthesis in *Azotobacter vinelandii*. *Microbiology* **157**: 1685–93

Coers, J., Kagan, J.C., Matthews, M., Nagai, H., Zuckman, D.M., and Roy, C.R. (2000) Identification of Icm protein complexes that play distinct roles in the biogenesis of an organelle permissive for *Legionella pneumophila* intracellular growth. *Mol Microbiol* **38**: 719–736

Consortium, T.U. (2014) Activities at the Universal Protein Resource (UniProt). *Nucleic Acids Res* **42**: D191–8

Dalebroux, Z.D., Edwards, R.L., and Swanson, M.S. (2009) SpoT governs *Legionella pneumophila* differentiation in host macrophages. *Mol Microbiol* **71**: 640–58

Edwards, R.L., Dalebroux, Z.D., and Swanson, M.S. (2009) *Legionella pneumophila* couples fatty acid flux to microbial differentiation and virulence. *Mol Microbiol* **71**: 1190–1204

Faulkner, G., and Garduno, R.A. (2002) Ultrastructural Analysis of Differentiation in *Legionella pneumophila*. *J Bacteriol* **184**: 7025–7041.

Fields, B.S., Benson, R.F., and Besser, R.E. (2002) *Legionella* and Legionnaires ' Disease : 25 Years of Investigation *Legionella* and Legionnaires ' Disease : 25 Years of Investigation. *Clin Microbiol Rev* **15**.

Flieger, a, Gongab, S., Faigle, M., Mayer, H. a, Kehrer, U., Mussotter, J., *et al.* (2000) Phospholipase A secreted by *Legionella pneumophila* destroys alveolar surfactant phospholipids. *FEMS Microbiol Lett* **188**: 129–33

Forsbach-Birk, V., McNealy, T., Shi, C., Lynch, D., and Marre, R. (2004) Reduced expression of the global regulator protein CsrA in *Legionella pneumophila* affects virulence-associated regulators and growth in *Acanthamoeba castellanii*. *Int J Med Microbiol* **294**: 15–25

Gal-Mor, O., and Segal, G. (2003) Identification of CpxR as a Positive Regulator of icm and dot Virulence Genes of *Legionella pneumophila*. *J Bacteriol* **185**: 4908–4919

Garduño, R. (2007) Life cycle, growth cycles and developmental cycle of *Legionella pneumophila*. *Legion pneumophila* 65–84

Garduño, R., Garduño, E., Margot, H., and Hoffman, P.S. (2002) Intracellular growth of *Legionella pneumophila* gives rise to a differentiated form dissimilar to stationary-phase forms. *Infect Immun* **70**: 6273

Gooderham, W.J., Bains, M., McPhee, J.B., Wiegand, I., and Hancock, R.E.W. (2008) Induction by cationic antimicrobial peptides and involvement in intrinsic polymyxin and antimicrobial peptide resistance, biofilm formation, and swarming motility of PsrA in *Pseudomonas aeruginosa*. *J Bacteriol* **190**: 5624–34

Goosen, N., and Putte, P. (1995) The regulation of transcription initiation by integration host factor. *Mol Microbiol* **16**: 1–7

Hales, L.M., and Shuman, H.A. (1999) The Legionella pneumophila rpoS Gene Is Required for Growth within *Acanthamoeba castellanii*. *J Appl Microbiol* **181**: 4879.

Hammer, B.K., and Swanson, M.S. (1999) Co-ordination of *Legionella pneumophila* virulence with entry into stationary phase by ppGpp. *Mol Microbiol* **33**: 721–31

Hammer, B.K., Tateda, E.S., and Swanson, M.S. (2002) A two-component regulator induces the transmission phenotype of stationary-phase *Legionella pneumophila*. *Mol Microbiol* **44**: 107–18

Hengge-Aronis, R. (2002) Signal Transduction and Regulatory Mechanisms Involved in Control of the S (RpoS) Subunit of RNA Polymerase. *Microbiol Mol Biol Rev* **66**: 373–395

Heuner, K., Bender-Beck, L., Brand, B.C., Lück, P.C., Mann, K.H., Marre, R., *et al.* (1995) Cloning and genetic characterization of the flagellum subunit gene (flaA) of *Legionella pneumophila* serogroup 1. *Infect Immun* **63**: 2499–507

Heuner, K., and Steinert, M. (2003) The flagellum of *Legionella pneumophila* and its link to the expression of the virulent phenotype. *Int J Med Microbiol* **293**: 133–143

Hoffman, P., Friedman, H., and Bendinelli, M. (2007) *Legionella pneumophila: Pathogenesis and Immunity*. Springer US, Boston, MA. http://link.springer.com/10.1007/978-0-387-70896-6.

Hovel-Miner, G., Pampou, S., Faucher, S.P., Clarke, M., Morozova, I., Morozov, P., *et al.* (2009) SigmaS controls multiple pathways associated with intracellular multiplication of *Legionella pneumophila*. *J Bacteriol* **191**: 2461–73.

Humair, B., Wackwitz, B., and Haas, D. (2010a) GacA-controlled activation of promoters for small RNA genes in *Pseudomonas fluorescens*. *Appl Environ Microbiol* **76**: 1497–506

Humair, B., Wackwitz, B., and Haas, D. (2010b) GacA-controlled activation of promoters for small RNA genes in *Pseudomonas fluorescens*. *Appl Environ Microbiol* **76**: 1497–506

Isberg, R.R., O'Connor, T.J., and Heidtman, M. (2009) The *Legionella pneumophila* replication vacuole: making a cosy niche inside host cells. *Nat Rev Microbiol* **7**: 13–24

Jesús, D.A. De, Connor, T.J.O., and Isberg, R.R. (2013) *Legionella*. **954**: 251–264 http://link.springer.com/10.1007/978-1-62703-161-5. Accessed March 15, 2013.

Jones, P., Binns, D., Chang, H.-Y., Fraser, M., Li, W., McAnulla, C., *et al.* (2014) InterProScan 5: genome-scale protein function classification. *Bioinformatics* **30**: 1236–40

Jules, M., and Buchrieser, C. (2007) *Legionella pneumophila* adaptation to intracellular life and the host response: clues from genomics and transcriptomics. *FEBS Lett* **581**: 2829–38

Kang, Y., Lunin, V. V, Skarina, T., Savchenko, A., Schurr, M.J., and Hoang, T.T. (2009) The long-chain fatty acid sensor, PsrA, modulates the expression of rpoS and the type III secretion exsCEBA operon in *Pseudomonas aeruginosa*. *Mol Microbiol* **73**: 120–36

Kang, Y., Nguyen, D.T., Son, M.S., and Hoang, T.T. (2008) The *Pseudomonas aeruginosa* PsrA responds to long-chain fatty acid signals to regulate the fadBA5 beta-oxidation operon. *Microbiology* **154**: 1584–98

Kojic, M., Aguilar, C., and Venturi, V. (2002) TetR Family Member PsrA Directly Binds the *Pseudomonas* rpoS and psrA Promoters. *J Bacteriol* **184**: 2324–2330.

Kojic, M., Jovcic, B., Vindigni, A., Odreman, F., and Venturi, V. (2005) Novel target genes of PsrA transcriptional regulator of *Pseudomonas aeruginosa*. *FEMS Microbiol Lett* **246**: 175–81

Kojic, M., and Venturi, V. (2001) Regulation of rpoS gene expression in *Pseudomonas*: involvement of a TetR family regulator. *J Bacteriol* **183**: 3712–20

Kozak, N.A., Buss, M., Lucas, C.E., Frace, M., Govil, D., Travis, T., *et al.* (2010) Virulence factors encoded by *Legionella longbeachae* identified on the basis of the genome sequence analysis of clinical isolate D-4968. *J Bacteriol* **192**: 1030–44

LeBlanc, J.J., Brassinga, A.K.C., Ewann, F., Davidson, R.J., and Hoffman, P.S. (2008) An ortholog of OxyR in *Legionella pneumophila* is expressed postexponentially and negatively regulates the alkyl hydroperoxide reductase (ahpC2D) operon. *J Bacteriol* **190**: 3444–55

Lunin, V.V., Skarina, T., Onopriyenko, O., Kim, Y., Joachimiak, A., Edwards, A.M., Savchenko, A. (2005) The crystal structure of transcriptional regulator PA3006. *RCSB Protein Data Bank* http://www.rcsb.org/pdb/explore/explore.do?structureId=2FBQ. Accessed May 5, 2014.

Lynch, D., Fieser, N., Gloggler, K., Forsbach-Birk, V., and Marre, R. (2003) The response regulator LetA regulates the stationary-phase stress response in *Legionella pneumophila* and is required for efficient infection of *Acanthamoeba castellanii*. *FEMS Microbiol Lett* **219**: 241–248

Magnusson, L.U., Farewell, A., and Nyström, T. (2005a) ppGpp: a global regulator in Escherichia coli. *Trends Microbiol* **13**: 236–42

Magnusson, L.U., Farewell, A., and Nyström, T. (2005b) ppGpp: a global regulator in Escherichia coli. *Trends Microbiol* **13**: 236–42

Mangan, M.W., Lucchini, S., Danino, V., Cróinín, T.O., Hinton, J.C.D., and Dorman, C.J. (2006) The integration host factor (IHF) integrates stationary-phase and virulence gene expression in *Salmonella enterica* serovar Typhimurium. *Mol Microbiol* **59**: 1831–47

McNealy, T.L., Forsbach-Birk, V., Shi, C., and Marre, R. (2005) The Hfq homolog in *Legionella pneumophila* demonstrates regulation by LetA and RpoS and interacts with the global regulator CsrA. *J Bacteriol* **187**: 1527–32

Merriam, J., Mathur, R., Maxfield-Boumil, R., and Isberg, R. (1997) Analysis of the Legi*onella pneumophila* fliI gene: intracellular growth of a defined mutant defective for flagellum biosynthesis. *Infect Immun* **65**: 2497–2501

Michalska, K., Li, H., Gu, M., Joachimiak, A. (2013) Crystal structure of TetR transcriptional regulator from *Legionella pneumophila*. *RCSB Protein Data Bank* http://www.rcsb.org/pdb/explore.do?structureId=3ON4. Accessed May 4, 2014.

Molmeret, M. (2002) icmT Is Essential for Pore Formation-Mediated Egress of *Legionella pneumophila* from Mammalian and Protozoan Cells. *Infect Immun* **70**: 69–78

Molmeret, M., Santic', M., Asare, R., Carabeo, R. a, and Abu Kwaik, Y. (2007) Rapid escape of the dot/icm mutants of *Legionella pneumophila* into the cytosol of mammalian and protozoan cells. *Infect Immun* **75**: 3290–304

Molofsky, A.B., and Swanson, M.S. (2003) *Legionella pneumophila* CsrA is a pivotal repressor of transmission traits and activator of replication. *Mol Microbiol* **50**: 445–461

Molofsky, A.B., and Swanson, M.S. (2004) Differentiate to thrive: lessons from the *Legionella pneumophila* life cycle. *Mol Microbiol* **53**: 29–40

Morash, M.G., Brassinga, A.K.C., Warthan, M., Gourabathini, P., Garduño, R. a, Goodman, S.D., and Hoffman, P.S. (2009) Reciprocal expression of integration host factor and HU in the developmental cycle and infectivity of *Legionella pneumophila*. *Appl Environ Microbiol* **75**: 1826–37

Newton, H.J., Ang, D.K.Y., Driel, I.R. van, and Hartland, E.L. (2010) Molecular pathogenesis of infections caused by *Legionella pneumophila*. *Clin Microbiol Rev* **23**: 274–98

Nickerson, C., and Curtiss, R. 3rd (1997) Role of sigma factor RpoS in initial stages of *Salmonella typhimurium* infection. *Infect Immun* **65**: 1814–1823

Overhage, J., Lewenza, S., Marr, A.K., and Hancock, R.E.W. (2007) Identification of genes involved in swarming motility using a *Pseudomonas aeruginosa* PAO1 mini-Tn5-lux mutant library. *J Bacteriol* **189**: 2164–9

Papavinasasundaram, K.G., Colston, M.J., and Davis, E.O. (1998) Construction and complementation of a recA deletion mutant of Mycobacterium smegmatis reveals that the intein in *Mycobacterium tuberculosis* recA does not affect RecA function. *Mol Microbiol* **30**: 525–534

Pitre, C. a J., Tanner, J.R., Patel, P., and Brassinga, A.K.C. (2013) Regulatory control of temporally expressed integration host factor (IHF) in *Legionella pneumophila*. *Microbiology* **159**: 475–92

Ramos, J.L., Martínez-Bueno, M., Molina-Henares, A.J., Terán, W., Watanabe, K., Zhang, X., *et al.* (2005) The TetR family of transcriptional repressors. *Microbiol Mol Biol Rev* **69**: 326–56

Rasis, M., and Segal, G. (2009) The LetA-RsmYZ-CsrA regulatory cascade, together with RpoS and PmrA, post-transcriptionally regulates stationary phase activation of *Legionella pneumophila* Icm/Dot effectors. *Mol Microbiol* **72**: 995–1010

Roy, C.R., Berger, K.H., and Isberg, R.R. (1998) *Legionella pneumophila* DotA protein is required for early phagosome trafficking decisions that occur within minutes of bacterial uptake. *Mol Microbiol* **28**: 663–674

Sahr, T., Brüggemann, H., Jules, M., Lomma, M., Albert-Weissenberger, C., Cazalet, C., and Buchrieser, C. (2009a) Two small ncRNAs jointly govern virulence and transmission in *Legionella pneumophila*. *Mol Microbiol* **72**: 741–62

Sahr, T., Brüggemann, H., Jules, M., Lomma, M., Albert-Weissenberger, C., Cazalet, C., and Buchrieser, C. (2009b) Two small ncRNAs jointly govern virulence and transmission in *Legionella pneumophila*. *Mol Microbiol* **72**: 741–62

Sauer, J.-D., Bachman, M. a, and Swanson, M.S. (2005) The phagosomal transporter A couples threonine acquisition to differentiation and replication of *Legionella pneumophila* in macrophages. *Proc Natl Acad Sci U S A* **102**: 9924–9

Segal, G., Feldman, M., and Zusman, T. (2005) The Icm/Dot type-IV secretion systems of *Legionella pneumophila* and *Coxiella burnetii*. *FEMS Microbiol Rev* **29**: 65–81

Sexton, J.A., Pinkner, J.S., Roth, R., Heuser, J.E., Hultgren, S.J., and Vogel, J.P. (2004) The *Legionella pneumophila* PilT homologue DotB exhibits ATPase activity that is critical for intracellular growth. *J Bacteriol* **186**: 1658–66

Shen, D.K., Filopon, D., Kuhn, L., Polack, B., and Toussaint, B. (2006) PsrA Is a Positive Transcriptional Regulator of the Type III Secretion System in *Pseudomonas aeruginosa*. *Infect Immun* **74**: 1121.

Simossis, V. a, and Heringa, J. (2005) PRALINE: a multiple sequence alignment toolbox that integrates homology-extended and secondary structure information. *Nucleic Acids Res* **33**: W289–94

Solovyev V, S.A. (2011) Automatic Annotation of Microbial Genomes and Metagenomic Sequences. In *Handbook of Molecular Microbial Ecology I: Metagenomics and Complementary Approaches*. John Wiley & Sons, p. 800

Srivatsan, A., and Wang, J.D. (2008) Control of bacterial transcription, translation and replication by (p)ppGpp. *Curr Opin Microbiol* **11**: 100–5

Stonehouse, E., Kovacikova, G., Taylor, R.K., and Skorupski, K. (2008) Integration host factor positively regulates virulence gene expression in *Vibrio cholerae*. *J Bacteriol* **190**: 4736–48

Suh, S.-J., Silo-Suh, L., Woods, D.E., Hassett, D.J., West, S.E.H., and Ohman, D.E. (1999) Effect of rpoS Mutation on the Stress Response and Expression of Virulence Factors in *Pseudomonas aeruginosa*. *J Bacteriol* **181**: 3890–3897

Swanson, M.S., and Hammer, B.K. (2000) *Legionella pneumophila* pathogesesis: a fateful journey from amoebae to macrophages. *Annu Rev Microbiol* **54**: 567–613

Whistler, C.A., Corbell, N.A., Sarniguet, A., Ream, W., and Loper, J.E. (1998) The Two-Component Regulators GacS and GacA Influence Accumulation of the Stationary-Phase Sigma Factor ς S and the Stress Response in *Pseudomonas*. *J Bacteriol* **180**: 6635.

Yerushalmi, G., Zusman, T., and Segal, G. (2005) Additive effect on intracellular growth by *Legionella pneumophila* Icm/Dot proteins containing a lipobox motif. *Infect Immun* **73**: 7578–87

Yildiz, F.H., and Schoolnik, G.K. (1998) Role of rpoS in Stress Survival and Virulence of *Vibrio cholerae*. *J Bacteriol* **180**: 773–784

Zusman, T., Aloni, G., Halperin, E., Kotzer, H., Degtyar, E., Feldman, M., and Segal, G. (2007) The response regulator PmrA is a major regulator of the icm/dot type IV secretion system in *Legionella pneumophila* and *Coxiella burnetii*. *Mol Microbiol* **63**: 1508–23

Zusman, T., Gal-mor, O., and Segal, G. (2002) Characterization of a Legionella pneumophila relA Insertion Mutant and Roles of RelA and RpoS in Virulence Gene Expression Characterization of a *Legionella pneumophila* relA Insertion Mutant and Roles of RelA and RpoS in Virulence Gene Expression. *J Bacteriol* **184**: 67.